DIVERGENT EFFECTS OF ANGIOTENSIN II RECEPTOR TYPES 1A AND 2 ON VASCULAR FUNCTIONS INVOLVE NADPH OXIDASE-DEPENDENT OXIDATIVE STRESS AND NO-DEPENDENT GUANYLYL CYCLASE

A thesis submitted in a partial fulfilment of the requirements for the Doctor degree in Human Biology (Dr. biol. hom.)
Faculty of Medicine, Justus-Liebig-University Giessen-Germany

Submitted by

Ashraf Mohamed Abouelwafa Taye
from
Egypt

Giessen, 2004

From Rudolf-Buchheim-Institute for Pharmacology

Director: Prof. Dr. Harald H.H.W. Schmidt
Faculty of Medicine
Justus- Liebig-University Giessen-Germany

1. Advisor: Prof. Dr. Harald H.H.W. Schmidt

2. Advisor: Hochschuldozent Dr. Nobert Weissmann

Day of Disputation: 14.01.2005

AFFIDAVIT

Hereby, I declare on oath, that the thesis «DIVERGENT EFFECTS OF ANGIOTENSIN II RECEPTOR TYPES 1A AND 2 ON VASCULAR FUNCTIONS INVOLVE NADPH OXIDASE-DEPENDENT OXIDATIVE STRESS AND NO-DEPENDENT GUANYLYL CYCLASE» is the product of my original research, and I did not use other sources or methods than those I have cited.

In addition, I declare that this thesis is not submitted to any another evaluation, neither in this form nor in another.

I have not acquired or tried to acquire any other academic degree than that documented in the application.

Giessen, 01-10-2004 Ashraf M. A.Taye

Acknowledgements

I would like to thank:

Prof. Dr. Montaser Khalifa for his supporting me in Egypt as well as in Germany to achieve this work. Trustfully, I am grateful for his kind assistance.

Prof. Dr. Harald H.H.W. Schmidt for having given me on opportunity to perform this interesting study under his scientific supervision and support;

My wife for her continuous help and encouraging me to do my best, and this made me more motivated and I am happy that finally her wait is over;

My colleague, Sven Wind for his good disposition to discuss everything related to our project and also for his friendship;

Dr. Arun Kumar H.S for his kind help in correction of my paper and my thesis;

Dr. Knut Beuerlein for his support in the correction of my thesis;

Dr. Nobert Weissmann for his help in the isolted lung experiments;

Dr. Pavel Nedvetsky for his continuous help for Western blotting technique in the beginning;

Mr. Helmut Müller and Ms$_s$. Petra Kronich and Bärbel Füher for their technical assistance, and friendly support to me;

Finally, for all members of the Rudolf-Buchheim-Institute for their kind and friendly help.

To the memory of my parents and to my wife and daughter

Content

1. Abbreviations

µM	Micromolar
3NT	3-Nitrotyrosine
AA-Bis	Acrylamide Bisacryamide
ACE	Angiotensin-converting enzyme
ACEIs	Angiotensin-converting enzyme inhibitors
ACh	Acetylcholine
Ang II	Angiotensin II
ANOVA	Analysis of variance
APS	Ammonium persulfate
AT_1	Angiotensin II type 1 receptor
AT_{1A} and AT_{1B}	Angiotensin II receptor subtypes 1A and 1B
$AT_{1A}^{-/-}$ mice	Angiotensin type 1A receptor-deficient mice
$AT_{1B}^{-/-}$ mice	Angiotensin type 1B receptor-deficient mice
AT_2	Angiotensin II type 2 receptor
$AT_2^{-/Y}$ mice	Angiotensin type 2 receptor-deficient mice
BSA	Bovine serum albumin
Ca Cl_2	Calcium Chloride
cGMP	Cyclic guanisine-3’, 5’-monophosphate
DMSO	Dimethylsulfoxide
DNA	Deoxyribonucleic acid
dNTP	deoxy-nucleoside triphosphate
DOCA	Deoxycortecosterone acetate
DPI	Diphenylen-Iodonium
DTT	Dithiothreitol
EC_{50}	The concentration that produces half of the maximal respons
ECL	Enhanced chemiluminescence
EDRF	Endothelium derived relaxing factor
EDTA	Ethylendiamintetracetate
EGYTA	Etylen-Glycol-bis (2-aminoethylether)-N,N,N,N-Tetraacetat

E_{max}	Maximal efficacy
eNOS	Endothelial nitric oxide synthase
eNOS	Endothelial nitric oxide synthase
FAD	Flavin adenine dinucleotide
GTP	Guansinotriphosphate
HEPES	N-(2-hydroxyethyl) piperazin –N’-2(ethansulfonic acid)
KCl	Ptassium chloride
kDa	Kilodalton (as expression for the protein molecular weight)
ko	Knockout
L-NAME	N^G-nitro-L-arginine methyl ester
M	Molar (mol/L)
$MgCl_2$	Magnisium chloride
Min	Minute
mM	Milimolar
NaCl	Sodium chloride
NADPH	Nicotinamide adenine dinucleotide phosphate reduced form
NO	Nitric oxide
NOS	Nitric oxide synthase
Nox	NADPH oxidase
Nox1	NADPH oxidase isoform type 1
Nox2	NADPH oxidase isoform type 2
Nox4	NADPH oxidase isoform type 4
$O_2^{-\cdot}$	Superoxide anion
$ONOO^-$	Peroxynitrite
PAGE	Polyacryliamide gel electrophoresis
PBS	Phosphate-buffer saline
PCR	Polymerase chain reaction
pD2	$-logEC_{50}$
PE	Phenylephrine
PKC	Protein Kinase C
PMSF	Phenylmethylsulphonylflouride
RAS	Renin-angiotensin system
RLU	Relative light unit

ROS	Reactive oxygen species
SDS	Sodium dodecyl sulfate
SEM	Standard error of the mean
sGC	Soluble guanylyl cyclase
SHR	Spontaneous hypertensive rats
SLB	Special lysis buffer
SOD	Superoxide dimutase
Spermine NONOate	(Z)-1-{N-[3-Aminopropyl]-N-[4-(aminopropylammonio) butyl]-amino}diazen-1ium-1,2-dioate
TEA	Triethanolamine
TEMED	N,N,N’,N’-Tetramethyl-1,3-propandiol
Tris	2-Amino—2-hydroxymethyl-1,3-propanediol
TNF-μ	Tumour necrosis factor-μ
T-TBS	Tris-buffered saline with0.1 % Tween 20
U	unit
VSMC	Vascular smooth muscle cell
wt	Wild type

2. Introduction

2.1. Angiotensin II (Ang II) Receptors

Ang II is a potent octapeptide of the renin-angiotensin system (RAS) and plays an important role in structural and functional regulation of cardiovascular system [1, 2]. The physiological actions of Ang II in cardiovascular system are mediated via its binding to two main receptors, AT_1 and AT_2. Among the AT_1 receptors, two subtypes, AT_{1A} and AT_{1B}, have been identified in rat and mouse [3]. It is widely accepted that the AT_1 receptors account for majority of cardiovascular effects evoked by Ang II [4, 5]. Stimulation of AT_1 receptors leads to cellular growth, hypertrophy, angiogenesis, vasoconstriction and cardiac remodeling. In contrast, AT_2 receptor stimulation results in antiproliferation including decreased neointimal formation and apoptosis, antiangiogenesis, vasodilatation, and inhibition of cardiac remodeling [6-9]. Nevertheless, it has been shown that AT_2 receptor activation not only counteracts the Ang II-mediated vasoconstriction, but also actively induces vasodilatation [10-12]. Wherein, range of signaling pathways, including nitric oxide (NO) and bradykinin production may be involved [12, 13]. An Increasing amount of literature demonstrates that AT_2 receptors-mediated relaxation in a range of isolated arteries including rabbit renal arterioles [14] and rabbit cerebral arteries [15], which is not only endothelium-dependent [14] but it is also endothelium-independent [11]. This depends on the techniques employed, and appears to involve a range of signaling pathways, including NO-bradykinin production [12] and modulation of K^+ channel activity [14]. A functional interaction has been demonstrated between AT_1 and AT_2 receptors concerning vascular tone modulation *in vitro* [16, 17]. Under basal conditions, an elevated blood pressure was reported for AT_2 receptor knockout mice [18], and mice overexpressing the AT_2 receptor showed a blunted pressure response to chronic Ang II infusion [19].

The subcellular mechanisms and signaling pathways whereby Ang II mediates its physiological and pathophysiological vascular effects are complex [20]. Emerging evidence indicates that production of reactive oxygen species (ROS) and activation of reduction-oxidation (redox)-dependent signaling cascades are critically involved in Ang II-induced pathophysiology [21, 22]. It is well established that AT_1 receptor activation stimulates non-phagocytic NADPH oxidases (Nox) and generation of ROS in various vascular cell types, including vascular smooth muscle cells (VSMCs) [23], endothelial cells [24] and fibroblast [25].

2.1.1. Functional interplay between AT_1 receptor subtypes

In rodents, AT_{1A} and AT_{1B} receptors show a sequence homology of 94 % and are pharmacologically indistinguishable. The AT_{1A} receptor is the major Ang II receptor subtype expressed in the cardiovascular system of adult mice, suggesting that this receptor is mainly involved in regulating blood pressure homeostasis. Indeed, arterial pressure in mice was affected differently by gene targeting of either the AT_{1A} or AT_{1B} receptor [26-28]. Deletion of the AT_{1A} receptor gene, but not the AT_{1B} receptor gene leads to a decrease in resting arterial pressure. Blood pressure increase following Ang II infusion is greatly attenuated but not abolished in Angiotensin type 1A receptor-deficient mice ($AT_{1A}^{-/-}$) [26, 27]. The attenuated pressor effect of Ang II in $AT_{1A}^{-/-}$ mice might be due to a deficient vasoconstrictor response, because the vasoconstriction of isolated arteries is also weakened in $AT_{1A}^{-/-}$ mice [29]. In contrast, the elevated pressor effect of Ang II in AT_{1A} receptor-deficient mice ($AT_{1B}^{-/-}$) was not different from that in wt control mice [30].

2.1.2. Interaction between Ang II and NO

Since both Ang II and NO affect vascular tone, fluid volume and remodeling, they may be protective or deleterious to target organs such as endothelium, vascular smooth muscle cells (VSMCs) and mesangial cells. Abnormal vascular tone and vascular remodeling are key features in cardiovascular pathophysiology. Both, NO and Ang II are important factors in these pathological mechanisms. Imbalance between Ang II and NO, therefore, leads to development and progression of many cardiovascular diseases. For example, endothelium-dependent vascular relaxation is impaired in transgenic mice overexpressing renin or angiotensinogen [31]. Gene transfer of eNOS effectively restored the vasomotor function in Ang II-infused rabbits [32]. The vascular response to Ang II is enhanced in eNOS-deficient mice [33]. Furthermore, long-term blockade of NO synthesis with L-NAME caused systemic arterial hypertension, which could be prevented by AT_1 receptor antagonists [33, 34].

Ang II/NO imbalance often results from loss of NO bioavailability due to endothelial dysfunction and oxidative stress and/or enhancement of the local tissue actions of Ang II [35] (Fig.2.1.).

Additionally, NO seems to be a physiological antagonist of Ang II, because it decreases the level of angiotensin-converting enzyme (ACE) mRNA in endothelium, downregulates the expression of AT_1 receptors in VSMCs and inhibits the production of endothelin [36-38].

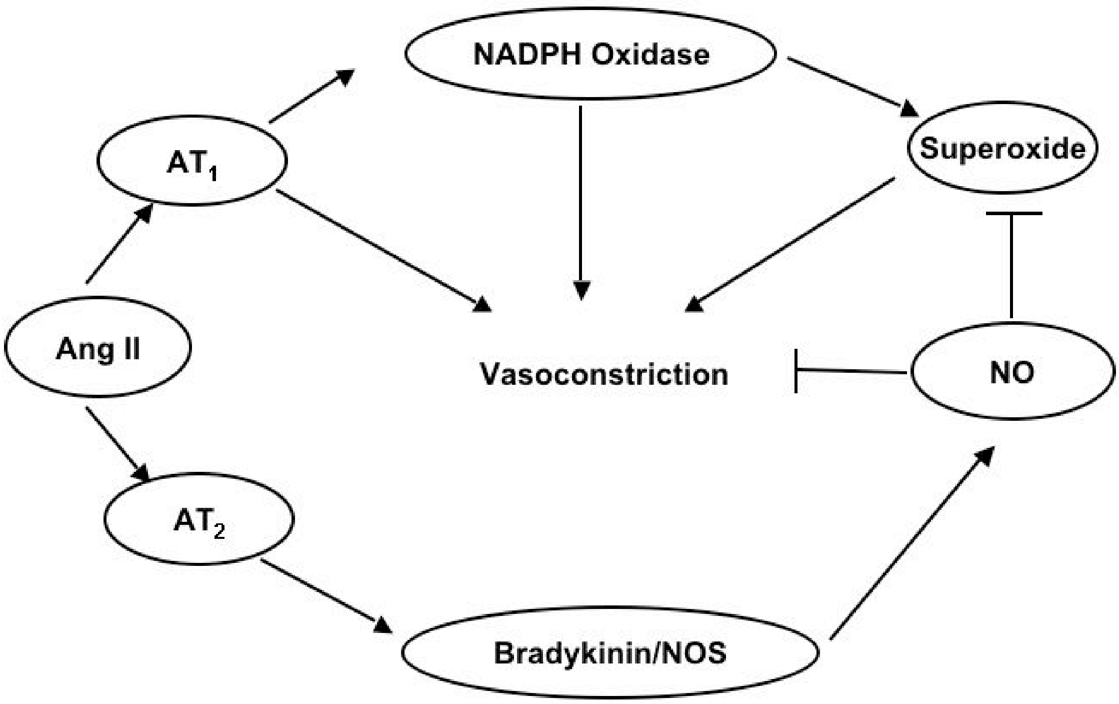

Fig. 2.1. Functional interaction between Ang II and NO: The AT_1 and AT_2 receptors have contrasting effects (modified after de Gasparo *et al.*[39]).

2.2. Endothelium and NO

The endothelium plays a key role in maintaining normal vascular function and structure [40]. Hence, endothelial dysfunction impairs vascular tone, platelet aggregation and monocyte adhesion, and seems to be associated with an increased predisposition to cardiovascular abnormalities. The strategic location of the endothelium allows discerning changes in hemodynamic forces and blood-borne signals as well as to respond to these changes by releasing numbers of autocrine and paracrine substances. Endothelium-derived NO is a physiological mediator of numerous cellular and organ functions. The formation of NO is catalyzed by NO synthease (NOS) from L-arginine. Three isoenzymes have been identified, referred to here as neuronal NOS (nNOS), inducible NOS (iNOS), and endothelial NOS (eNOS). The cellular effect of NO can be cyclic guanosinmonophosphate (cGMP)-dependent or cGMP-independent [41]. For the cGMP dependent mechanism, NO activates soluble guanylyl cyclase (sGC), stimulating production of cGMP. Increased intracellular cGMP facilitates the extrusion of intracellular calcium and leads to vascular relaxation. NO has several critical role in the maintenance of vascular homeostasis. In vasculature, NO not only functions as a vasodilator but also inhibits VSMCs proliferation and migration, adhesion of leukocytes to the endothelium, and platelet aggregation [42]. An impairment of the NO signalling pathway, i.e. endothelial dysfunction, is one of the earliest events in vascular disease [43].

2.3. Role of ROS in vascular pathophysiology

ROS are a family of highly reactive molecules formed enzymatically in mammalian cells by reduction of molecular oxygen, producing superoxide anions ($O_2^{\cdot-}$). Under normal conditions, superoxide dismutase (SOD) rapidly reduces $O_2^{\cdot-}$ to hydrogen peroxide (H_2O_2), followed by its metabolism by other anti-oxidant enzymes, such as catalase and glutathione peroxidase. Oxidative stress is caused by the oxidation of macromolecules resulting from the increased formation of ROS and/or the decrease in the antioxidant reserve. Superoxide anions are critically involved in the breakdown of NO [44], and the reaction of $O_2^{\cdot-}$ with NO leads to production of the potent oxidant peroxynitrite [45]. Thus, peroxynitrite induces the oxidation of proteins, DNA and lipids in vascular cells [46].

Investigations during the past decade provide evidence that ROS contribute to the pathogenesis of numerous cardiovascular diseases, including hypertension, atherosclerosis, cardiac hypertrophy and heart failure [47]. Of the many factors implicated in remodeling of vessels in hypertension, Ang II seems to be one of the most important. This is supported by *in vivo* studies examining the relationship between ROS and hypertension, demonstrating that Ang II-but not noradrenaline-induced hypertension is associated increased oxidative stress [48]. The significance of ROS and Ang II in hypertension is further confirmed by clinical studies, where a recent report suggests that AT_1 receptor antagonists significantly reduce oxidative stress and improve endothelial function in hypertensive patients [49]. Involvement of oxidative stress in the pathology of hypertension was reported in humans with essential hypertension [50-52], as well as in animal models like spontaneous hypertensive rat (SHR) [53] and the Dahl salt-sensitive rats [54]. Moreover, Vaziri *et al*. (2000) [55] demonstrated that *in vivo* glutathione depletion results in increased oxidative stress followed by elevated blood pressure in normotensive rats. Similarly, elevation in vascular $O_2^{\cdot-}$ production was not only observed after Ang II infusion [56, 57], but also in other models of hypertension, like the two-kidney/one-clip [58], the one-kidney/one-clip [59] and the renin transgenic model [60]. Pathophysiological mechanisms underlying oxidative stress in these animal models is unclear, but mechanical factors, such as blood pressure, may play a role, because the elevated blood pressure itself increases NADPH oxidase generating- $O_2^{\cdot-}$ in vasculature [61]. On the other hand, it was found that *in vivo* administration of membrane–permeable SOD distinctly reduced the elevated blood pressure in SHR [62] and Ang II-infused rats [48, 63].

2.3.1. Enzymatic sources of ROS

Several enzymatic sources of ROS have been suggested. For example, NOS, the enzyme responsible for NO production can also generate $O_2^{\cdot-}$ under conditions of substrate (L-arginine) or co-factor (tetrahydrobiopterin) (BH_4) deficiency [64]. These have led to the concept of ‘‘NOS uncoupling’’, where the activity of the enzyme for NO production is decreased in association an increase in NOS-dependent $O_2^{\cdot-}$ formation. Ang II may play a crucial role in these processes in pathological conditions [57]. eNOS uncoupling has been reported in atherosclerosis [65], diabetes [66], and hypertension [67], all of which are associated with increased level of ROS. Moreover, xanthine oxidase, cytochrome P450, mitochondrial respiratory chain enzymes, and phagocyte-derived myeloperoxidase are capable to generate ROS in the vasculature

[22, 23, 68]. Nevertheless, the contribution of these enzymes to vascular generation of ROS is relatively minor compared with NADPH oxidase.

2.4. NADPH Oxidase

2.4.1. The phagocyte NADPH oxidase model

The structure and function of NADPH oxidases are well characterized initially in phagocytes where two membrane components, p22phox and gp91phox, form the cytochrome b_{558}. The catalytic subunit of this cytochrome, gp91phox, binds three prosthetic groups, one flavin adenine dinucleotide (FAD) and two heme molecules. The appropriate cytoplasmic protein complex is composed of p47phox, p67phox and p40phox, and include the small regulatory-protein Rac [69]. The function of the p40phox subunit, which is not essential for the oxidase activity, is a matter of debate [70-73]. Agonist exposure leads to the assembly of cytoplasmic components followed by their activation, which depends on the production of phosphotadic acid by phospholipase D. In addition, protein kinase C (PKC)-dependent phosphorylation of p47phox leads to conformational rearrangement and translocation of the cytosolic subunits to the membrane. The activation process of the protein complex also includes guanine nucleotide exchange of Rac-GDP to form Rac-GTP [70]. This activated cytoplasmic complex then associates with the cytochrome in the membrane to form a functional enzyme. The reduced substrate nicotinamide dinucleotide phosphate (NADPH) binds to gp91phox on the intracellular side of the membrane and releases two electrons, which are passed in turn to FAD, followed by transition to the first and second heme group. Finally, the electrons are successively transferred to molecular oxygen on the extracellular side of the membrane producing two superoxide radicals. Once $O_2^{\bullet-}$ is generated, it is metabolized enzymatically or non-enzymatically into various ROS *viz*. H_2O_2, OH^- and hypochloric acid. The phagocyte NADPH oxidases produce a large quantity of $O_2^{\bullet-}$, and this contributes to the host defence mechanism [69].

2.4.2. Vascular NADPH oxidases

The biochemical characteristics of the vascular NADPH oxidases are considerably different from those of the NADPH oxidase in neutrophils. It has been demonstrated that the capacity of the vascular enzymes for $O_2^{\bullet-}$ production is about one-third that of the neutrophil [74]. It has been also verified that the catalytic subunit gp91phox is only one member of a new family of homologous proteins termed Nox [75-78]. Hence, it is very likely that all Nox family members transfer electrons from a reduced substrate to molecular oxygen in a similar way (Fig.2.2.). As Compared to the Nox enzymes, the Duox family is characterized by N-terminal extracellular domains and an additional transmembrane domain and twice of size of the Nox proteins [77]. Thus, the name Duox stands for dual oxidase (NADPH oxidase + peroxidase). Two human Duox enzymes (Duox1 and 2) have been identified. Duox1 is found mainly in thyroid gland therefore, it is also called thyroid oxidase 1. However, the RNA of Duox1 could be detected in lung, placenta, testis and prostate [79]. Duox2 is expressed, beside the thyroid gland in colon and small intestine [80].

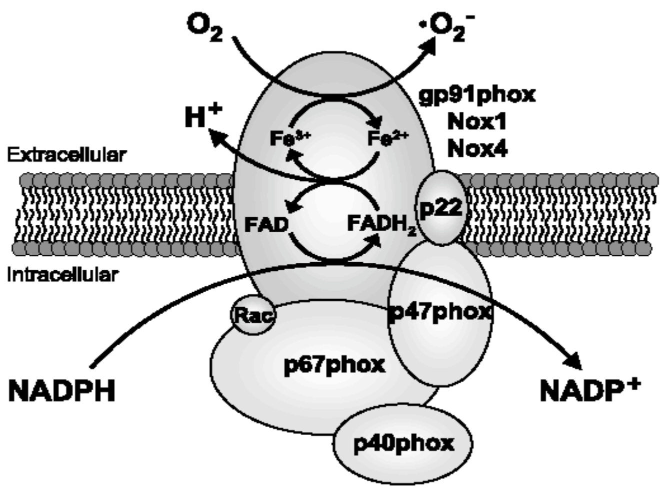

Fig. 2.2. Schematic diagram shows the biochemistry and the generalized molecular structure of NADPH oxidases. Electron flow (indicated by arrows) proceeds from reduced NADPH to FAD, to heme (Fe) and finally to molecular oxygen (O_2) yielding $O_2^{\bullet-}$ (adapted from Bengtsson *et al.* (2003) [81]).

2.4.2.1. The Nox proteins

The Nox family consists of close homologues of gp91phox, sharing their presumed six transmembrane domains and their long intracellular C-terminus. Five of the Nox family are known in human. Nox1 refers to the enzyme originally described as Mox1 [78]. The main site of expression is the colon epithelium [82]; minor sites of expression include prostate, uterus and VSMCs [75, 78]. Surprisingly, Nox1 was not expressed in VSMCs from resistance arteries [23]. So far, there is only one report of Nox1 mRNA expression in human endothelial cells and cardiac fibroblasts [83]. The term Nox2 is used as a synonym for gp91phox is predominantly expressed in granulocytes and monocytes/macrophages; minor sites of expression include B-lymphocytes [84], mesangial cells [85], and endothelial cells. Nox3 is solely found in the fetal kidney [82]. Nox4, initially termed as Renox (renal oxidase), is mainly expressed in the kidney cortex [86]. The Nox4 subunit was abundantly expressed in all vascular cells as mRNA [83] as well as protein in aortic lysate [87]. Finally, Nox5 is distinguished from the other family members by its longer N-terminus. It is found in testis and B and T-lymphocyte rich area of spleen and lymph nodes [88]. Nox isoforms are summarized in table 2.1.

Table 2.1: Nox isoforms

Isoform	Vascular	Non-vascular
Nox1	VSMCs [87, 89], endothelial cells [83]	Epithelial cells (colon [82] uterus and prostae [75, 78])
Nox2	Endothelial cells [56, 90],	Neutrophils, B-lymphocytes [84] and mesangial cells [85].
Nox3		Fetal tissues [82].
Nox4	All vascular cell types [83].	Kidney [86].
Nox5		Lymph nodes and spleen [88].
Duox1		Thyroid, lung, placenta, testis and prostate [79, 80].
Duox2		Thyroid, colon and small intestine [80].

2.4.2.2. Expression of vascular NADPH oxidases in cells and tissues

Previous investigations on the origin of vascular ROS demonstrated that NADPH oxidase is a major source of $O_2^{\cdot-}$ formation. The enzymatic activity was found in all layers of the vessel wall (endothelium [91], media [92], adventitia [93]) as well as in cultured VSMCs [89]. Since this enzyme shared some features with the phagocytic oxidase, researchers attempted to demonstrate the presence of phagocytic NADPH oxidase subunits in the vessel wall, particularly the major four: gp91phox, p22phox, p47phox, and p67phox [94].

Intima and Adventitia

In the endothelium, expression of the mRNA of all subunits has been demonstrated [95]. These results are confirmed by detection of all four proteins using Western blotting analysis [96] and immunohistochemistry [97]. In the adventitia, the four major phagocytic subunits were also detected by immunohistochemistry [98]. In addition, p22phox and gp91phox proteins were found in about 25-30% of intimal smooth muscle cells in non-diseased regions of human aorta [99].

Media

In the media, the situation is more complicated, because phagocytic subunits have been not found at all. The presence of p22phox subunit in VSMCs was demonstrated using molecular cloning [100] and Western blotting [23]. The other major phagocytic oxidase subunits, p67phox and gp91phox are either very low or undetectable in aortic VSMCs and media [99, 101]. In contrast to cells from large vessels, VSMCs from human resistance arteries reveal mRNA and protein of all major phagocytic NADPH oxidase subunits [23], In this context, it should be mentioned that translocation of p67phox from the cytosolic to the particulate fraction is observed following to Ang II stimulation and blocking $O_2^{\cdot-}$ production by gp91phox antisense oligonucleotides [23]. Also, the vascular NADPH oxidase may be differentially regulated in conduit and resistant arteries.

2.4.2.3.Biochemical characteristics of vascular NADPH oxidases

Low and constitutive activity

The rate of $O_2^{\cdot -}$ production in vascular cells is thought to be 1 to 10% of that in leukocytes [102]. As it might be expected from the cytotoxicity of superoxide, the phagocytic NADPH oxidase enzyme is inactive in the absence of stimuli [69, 70]. In order to observe the enzyme activity in homogenized neutrophils, it is therefore necessary to add a cytosolic fraction with p47phox and p67phox to the membrane fraction containing cytochrome. In contrast, oxidase activity was observed in isolated membrane fractions of unstimulated vascular cells [98] and moreover, enzyme activity is inhibited by addition of cytosolic fractions [103]. This constitutive activity can be explained by detection of p47phox and p67phox proteins in the particulate fraction of vascular cells [23, 98].

Induced activity

Vascular NADPH oxidases are constitutive enzymes, but they can be also regulated by humoral factors, such as Ang II [89], platelet-derived growth factor [104], thrombin [105], tumour necrosis factor-μ (TNF-μ)[106], and glucocorticoids [107]. Although the vascular enzymes are activated after few minutes of stimulation [108], their activity can also be markedly upregulated after hours of exposure to agonists. Thus, the rate of $O_2^{\cdot -}$ production was increased two to three-fold in VSMCs-exposed to Ang II for 4-8 h[103]. This effect probably results from the increased expression of NADPH oxidase [101]. Indeed, new protein synthesis was required for upregulation of oxidase subunits in VSMCs exposed to Ang II for 2 h [23].

2.4.2.4. Activation pathways of NADPH oxidases

PKC

Since phosphorylation of the p47phox subunit by PKC is required for activation of the phagocytic oxidase, several studies have investigated the role of this kinase in activation of the vascular oxidases. Accordingly, treatment of VSMCs with PKC inhibitors reduces ROS production after stimulation by platelet derived growth factor (PDGF) or Ang II [107, 108]. Furthermore, TNF-μ-induced translocation of p47phox in endothelial cells is inhibited by the PKC inhibitor chelerythrine [109]. It is noteworthy that the effect of PKC inhibition is usually partial, especially after exposure to the agonist for longer periods [108], suggesting different pathways of enzyme activation. However, PKC activation may have long-lasting effects on ROS production because upregulation of the oxidase subunits was also reported [101].

Phospholipase D

The possibility that lipid metabolites involved in signaling might activate the vascular oxidases was a subject of several investigations. Exogenous phosphatidic acid significantly increased oxidase activity in intact VSMCs and homogenates [110]. In addition, incubation of VSMCs with sphinganine or suramin, which are non-specific inhibitors of phospholipase D, leads to Ang II-induced ROS formation [111, 112].

Phospholipase A_2

In vitro study, it has been has demonstrated that the phagocytic oxidase could be activated by the addition of fatty acids. Similarly, in VSMCs homogenates, exogenous arachidonic acid and linoleic acid specifically increased NADPH oxidase activity [89, 113]. Free fatty acids, together with phospholipase, are produced in cells after agonist activation of phospholipase A_2 suggesting that this enzyme might activate NADPH oxidases.

2.4.2.5. NADPH oxidases and vascular diseases

Atherosclerosis

$O_2^{\cdot-}$ is presumed to participate in atherogenesis is through the formation of oxidized lipids, particularly oxidized low-density lipoportein (LDL). The altered bioactivity of oxidized compared with unoxidized LDL was first reported by Hessler *et al.* (1983) [114]. It has been demonstrated that activated monocytes could oxidize LDL [115, 116]. This was found to be a unique activity of leukocytes, because they are the only cells which can oxidize LDL in the absence of free metal ions [117]. Macrophages-mediated LDL oxidation was shown to be dependent on the production of $O_2^{\cdot-}$ by the NAD(P)H oxidase enzyme complex [117, 118]. There is substantial evidence that elevated NAD(P)H oxidase activity is closely linked with atherogenesis and vascular remodeling after balloon angioplasty. It has been shown that NAD(P)H oxidase activity is upregulated with intimal hyperplasia induced by periarterial collars [119], hypercholestremia and arterial balloon injury [120]. Increased NAD(P)H oxidase activity is also linked to clinical risk factors concerning atherosclerosis and impaired eNOS function in patients with coronary artery disease [121]. Studies examining expression of oxidase subunits during atherogenesis consistently demonstrate that although gp91phox is upregulated, Nox4 expression remains relatively unchanged throughout lesion development [119]. In atherosclerotic lesions Nox4 was highly expressed with Nox1 and p22phox and produced $O_2^{\cdot-}$, suggesting a crucial role for Nox4 in atherosclerotic lesions [83]. NAD(P)H oxidase has been investigated for its contributions to the development of arthrosclerosis in mice. Three studies have been performed in animals with gene knockout of either of 2 components of this enzyme complex (p47phox or gp91phox) [122, 123]. All three studies indicate that NADPH oxidase has a little or no effect on the development of atherosclerosis. However, a recent study performed by Barry *et al.* (2001) [122, 124] showed that crossing genetically hypercholesterolaemic apolipoprotein E-knockout (Apo E -/-) mice with p47phox-dificient mice reduces the area of the descending aorta covered by lesions by a staggering 80%, regardless of whether the animals were fed by a standard chow or high fat diet. This demonstrates that increased NAD(P)H oxidase activity is not just a symptom of atherosclerosis, but a causative factor in pathogenesis of the disease.

Experimental hypertension

In DOCA–salt induced hypertension, an enhanced vascular $O_2^{\cdot-}$ production with impaired endothelium-dependent relaxation was observed [125]. Wu *et al.* (2001) [126] have reported that the enhanced superoxide production in the aorta of DOCA-salt hypertensive rats was associated with an increased Nox activity. Moreover, Heitzer *et al.* (1999) [58] showed that increased aortic $O_2^{\cdot-}$ generation in renal hypertension model was associated with over-activity of NADPH oxidase.

Genetic hypertension

An early study performed by Suzuki *et al.* (1995) [53] described an increase in $O_2^{\cdot-}$ generation in venules and arterioles of spontaneous hypertensive rats (SHR). Recently, it has been shown that enhanced NADPH oxidase–mediated $O_2^{\cdot-}$ production is associated with upregulation of p22phox mRNA expression and development of endothelial dysfunction in the aorta of adult SHR [127]. In contrast, in norepinephrine-induced hypertension, neither $O_2^{\cdot-}$ production nor NADPH activity is enhanced [128]. Interestingly, p22phox mRNA expression and Nox activity was normalized after treatment with AT_1 receptor antagonist irbesartan, indicating a critical role of Ang II in the upregulation of Nox in adult SHR [127]. Additionally, an enhanced expression of AT_1 receptor and ACE has been reported in vessels of adult SHR [129]. In addition it was demonstrated that apocynin, a specific inhibitor of NADPH oxidase subunit assembly, decreases the enhanced $O_2^{\cdot -}$production in the aortic wall of 9 to 12 month-old SHR stroke prone, suggesting a potential role of NADPH oxidase in vascular generation of $O_2^{\cdot -}$ in this model of hypertension [130].

2.4.2.5. Activation of vascular NADPH oxidases by Ang II

A growing body of evidence indicates that NADPH oxidases are activated by mechanical forces (shear stress), hormones and cytokines [22, 47]. Ang II is widely accepted as an important activating stimulus for vascular NADPH oxidases. Griendling et al. (1994) [89] showed that pathophysiologically relevant concentrations of Ang II increased NADPH oxidase activity in rat VSMCs. In VSMCs, Ang II stimulates formation of ROS primarily via activation of the multisubunits enzyme NADPH oxidase [70]. ROS seems to play a crucial role in Ang II signaling in vasculature. Supporting this hypothesis, Ang II is related to produce ROS in vascular cells, while antioxidants and inhibitors of ROS-generating system abolish agonist-mediated signaling pathways. Transcription factors [131], protein tyrosine phosphatases [132], protein tyrosine kinases [131], mitogen-activated protein (MAP) kinases and ion channels [133](56) have been demonstrated to be regulated by ROS produced by Ang II (Fig. 2.3.).

Although mechanisms linking Ang II to the enzyme as well as upstream signaling molecules modulating NADPH oxidase in vasculature have not been fully elucidated, phospholipase D and PKC are suggested to be involved [111, 112]. In this context, it has been demonstrated that the upstream activator of epidermal growth factor (EGF) receptor transactivation, c-Src, plays an important role in the sustained Ang II-mediated activation of NADPH oxidase in VSMCs [108]. Furthermore, c-Src has been found to regulate NADPH oxidase-derived $O_2^{\cdot -}$ generation by stimulating phosphorylation of p47phox in Ang II-treated VSMCs [134].

Activation of NADPH oxidase by Ang II have been shown in several clinically relevant animal models of disease. Ang II-induced hypertension in rats is associated with a distinct increase in vascular $O_2^{\cdot-}$ production [48, 135, 136]. These responses seem to be mediated by activation of the AT_1 receptor, because they could be normalized by administration of losartan [136]. Moreover, Ang II-induced hypertrophy was abrogated by DPI [89]. In addition, catalase overexpression attenuated the Ang II-induced effects on growth [137]. Finally, in cardiac myocyte, Ang II- and TNF-μ-induced hypertrophy was associated with an intracellular release of ROS [138, 139].

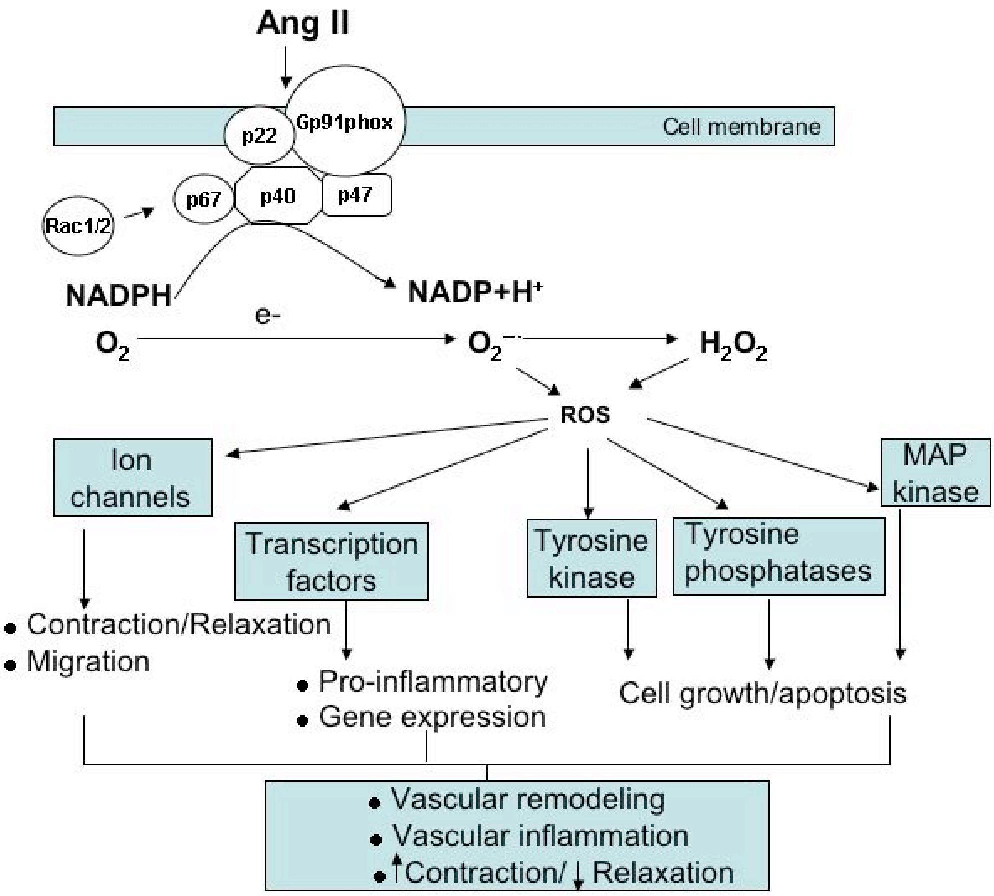

Fig. 2.3. Signaling pathways by Ang II in VSMCs. Ang II stimulates formation of ROS primarily via activation of the multisubunits enzyme NADPH oxidase. Intracellular ROS modulate the activity of tyrosine kinases and activate MAP kinases. ROS also influence gene and protein expression by activating transcription factors. ROS stimulate ion channels, such as plasma membrane Ca^{+2} and K^{+}, producing changes in cation concentrations. Activation of these redox-sensitive pathways results in several cellular responses (adapted from [140]).

2.4.2.6. Regulation of the vascular NADPH oxidase subunits by Ang II *in vitro* and *in vivo*

P22phox

Numerous studies have shown that the oxidase subunits are frequently upregulated after Ang II treatments leading to increased ROS production. For example, a recent study by Rueckschloss *et al.* (2002) [141] showed that the p22phox mRNA was elevated in endothelial cells-exposed to Ang II. Antisense RNA of p22phox, inhibits its expression as well as decreased Ang II-induced $O_2^{\cdot -}$ production, indicating that p22phox is a required component of the vascular oxidase [142]. Moreover, it has been demonstrated that the mRNA level of p22phox was upregulated in the aorta of rat chronically infused with Ang II [57, 143]. Besides, a simultaneous decrease in blood pressure, vascular oxidase activity and expression of p22phox mRNA has been observed by treatment of Ang II-infused rats with the PKC inhibitor chelerythrine [57] or with AT_1 receptor antagonists [143, 144].

P67phox, p40phox and p47phox

In vitro studies, it have been shown that Ang II upregulates p67phox mRNA expression and the oxidase activity in endothelial cells [141] and adventitial fibrocytes [145]. Immunodepletion of p67phox, blocks the oxidase activity in fibrocytes [98]. However, this effect can be reversed by addition of recombinant protein [98] indicating that p67phox is a functional part of the fibrocytic enzyme. In VSMCs from resistance arteries, Ang II upregulated proteins of all phagocytic oxidase subunits [23]. This is the first report that points to a functional role of p40phox in vascular cells. In VSMCs and endothelial cells of p47phox-deficient mice, Ang II-mediated signaling and ROS production was significantly reduced [146]. Additionally, electroporation of p47phox antibodies inhibits Ang II-induced ROS production in VSMCs [147]. Cifuentes *et al.* (2000) [56] have demonstrated that the p67phox protein is upregulated in aortic adventitia of mice after Ang II infusion for 7 days. In this context, a cell-permeable decoy peptide has been designed to using the p47phox sequence necessary for binding to gp91phox [148]. In the following rudimentary tests using aortic rings, this peptide abolished Ang II-induced $O_2^{\cdot -}$ production. Apart from blocking the peptide vascular $O_2^{\cdot -}$ production, it has also inhibited the increase in blood pressure induced by a 7-day Ang II infusion [148]. It has also been reported that disruption of the p47phox gene abolishes the elevation of vascular superoxide and markedly reduces the increase in blood pressure in mice infused with Ang II for 7 days [146]. These findings together with the results described by Wang *et al* [90], indicate that p47phox is an essential component of the vascular NADPH oxidase controlling the development of Ang II-induced hypertension.

gp91phox (Nox2)

Recent studies show that Ang II increases $O_2^{\cdot-}$ production and gp91phox mRNA levels in endothelial cells [141, 149, 150] as well as in rat aorta [57]. Furthermore, both gp91phox mRNA and protein were increased in the aortic adventitia of mice after Ang II infusion [56, 90]. Blocking of AT_1 receptors decreased gp91phox mRNA expression in endothelial cells [57, 141] and in internal mammary artery of patients with coronary heart disease [141]. In rat, administration of chelerythrine, which inhibited Ang II-induced hypertension, also prevented gp91phox upregulation [57].

Although basal blood pressure is diminished in gp91phox-deficient mice-infused by Ang II, absence of gp91phox does not reduce the hypertensive effect of the agonist [90]. In addition, deletion of the gp91phox gene does not inhibit Ang II-induced adventitial nitrotyrosine accumulation and aortic media thickening [135, 151]. Recently, it has been shown that cardiac hypertrophy caused by subpressor infusion of Ang II is attenuated in mice deficient in gp91phox, suggesting involvement of this isoform in myocardial hypertrophy [152]. However, contrasting roles of NADPH oxidase isoforms in pressure overload and to Ang II-induced cardiac hypertrophy have been reported [153].

Nox1 and Nox4

It has been shown that antisense to Nox1 mRNA completely inhibited Ang II-induced $O_2^{\cdot-}$ production in VSMCs, supporting the role of Nox1 in redox signaling in VSMCs. [101]. This study also reported that Ang II upregulates the Nox1 mRNA expression levels in these cells. In contrast, treatment with atrovastatin decreased both, ROS production and Nox1 mRNA expression [154]. Since VSMCs from large arteries express little or no gp91phox, Nox1 therefore, seems to be an essential part of the oxidase as well as functional substitute for gp91phox in VSMCs. However, contrary results probably due to different cell lines and respective exposure to serum before starting experiments have been observed [87, 101]. Nox4 has recently been reported to be the major catalytic component in endothelial cells [155]. In rats made hypertensive by the renin gene overexpression or infusion of Ang II for 7 days, Nox1 mRNA expression was markedly upregulated [57, 87], and the Nox4 mRNA and protein was also increased to a lesser extent in aorta and kidney [87]. After *in vivo* administration of chelerythine, the increase in Nox1 mRNA expression levels and blood pressure due to Ang II infusion is markedly reduced [57].

However, to date, nothing is known about the *in vivo* regulation of Nox1 and Nox4 via Ang II receptors (AT_{1A} or AT_2) during normal physiology.

3. Aims of the Study

Several studies suggest that AT_2 receptors might oppose the actions of the AT_1 receptors with respect to blood pressure, vascular tone and cellular proliferation under pathological condition. Whether Ang II receptors are also counter-regulatory in regulation of NADPH oxidase and vascular tone under physiological conditions is not known. Considering the increasing use of AT_1 receptor blockers clinically, it would be interesting and therapeutically important to understand the regulation of NADPH oxidase isoforms particularly Nox1 and Nox4 and vascular tone by Ang II under physiological conditions. Therefore, in the present study, we took advantages of mice with gene-targeted mutations in the AT_{1A} or AT_2 receptors ($AT_{1A}^{-/-}$ or $AT_2^{-/Y}$ mice, respectively) as powerful tools to examine:

1. The expressional regulation of Nox1 and Nox4 by AT_{1A} and AT_2 receptors under physiological levels of Ang II.
2. The relative contribution of these receptors to NADPH oxidase activity or vascular functions.
3. The interplay between Ang II receptors (AT_{1A} and AT_2) and NO signaling pathways involving eNOS and sGC protein expression and its functional relevance by the way of endothelium dependent and independent vascular relaxation in isolated aortic rings from mice- deficient in AT_{1A} or AT_2 receptors.

4.Materials

4.1. Antibodies

Primary antibody	Dilution	Secondary antibody	Dilution
Nox1 (rabbit): Peptides-antibodies, polyclonal antibody.	1: 25000 (Advanced ECL)	Goat anti-rabbit conjugated to horseradish peroxidase (DAKO, Denmark).	1: 20000
Nox2 (rabbit): polyclonal conjugated, synthetic peptide corresponding to amino acids 548-560 of human gp91phox.	1: 2000 (Advanced ECL)	Goat anti-rabbit conjugated to horseradish peroxidase (DAKO, Denmark).	1: 20000
Nox4 (rabbit) Peptides-antibodies, polyclonal aantibody.	1: 10000 (Advanced ECL)	Goat anti-rabbit conjugated to horseradish peroxidase (DAKO, Denmark).	1: 20000
sGC□$_1$ (rabbit) Polyclonal human sGC□$_1$ affinity-purified against the sGC□$_1$peptide (residues 634-647).	1: 6000 (Normal ECL)	Goat anti-rabbit conjugated to horseradish peroxidase (DAKO, Denmark).	1: 2000
sGC□$_1$(rabbit) Polyclonal human sGC□$_1$ affinity-purified against the sGC□$_1$peptides (residues 593-614).	1: 4000 (Normal ECL)	Goat anti-rabbit conjugated to horseradish peroxidase (DAKO, Denmark).	1: 2000
anti-nitrotyrosine (rabbit) polyclonal antibody.	1: 1000 (Normal ECL)	Goat anti-rabbit conjugated to horseradish peroxidase (DAKO, Denmark).	1: 2000
eNOS (mouse) anti-eNOS monoclonal antibody.	1: 2500 (Normal ECL)	Anti-mouse: peroxidase conjugated from goat (DAKO, Glostrup, Denmark).	1: 2000

4.2. Chemicals

Chemical	**Producer**
β-Mercaptoethanol	Carl Roth Gmbh (Karlsruhe)
Acetylcholine	Sigma (Deisenhofen)
Acrylamide (30%) with 0.8% Bisacriamid	Carl Roth Gmbh (Karlsruhe)
Apocynin	CALBIOCHEMA
APS	Merck (Dramstadt)
Bovine serum albumin (BSA)	Sigma (Deisenhofen)
$CaCl_2$	Merck (Dramstadt)
Complete EDTA free (protease inhibitor set)	Roche Molecular Biochemicals (Mannheim)
DPI	Kingeston, Ontario,Canada
EDTA	Sigma (Deisenhofen)
EGTA	Sigma (Deisenhofen)
Ethanol	Merck (Dramstadt)
Folin-Chiocateu's phenol reagent	Merck (Dramstadt)
Glucose	Carl Roth Gmbh (Karlsruhe)
Glycine	Carl Roth Gmbh (Karlsruhe)
HEPES	Sigma (Deisenhofen)
HPR-Immunoglobulin (ant-rabbit)	DAKO (Hamburg)
KCl	Carl Roth Gmbh (Karlsruhe)
KH_2PO_4	Carl Roth Gmbh (Karlsruhe)
L-NAME	Sigma (Deisenhofen)
Methanol	Merck (Dramstadt)
$MgSO_4.7H_2O$	Merck (Dramstadt)
NaCl	Merck (Dramstadt)
$NaHCO_3$	Merck (Dramstadt)
$NaNO_2$	Merck (Dramstadt)

NaOH	Carl Roth Gmbh (Karlsruhe)
Oxypurinol	Sigma (Deisenhofen)
Phenylehrine	Sigma (Deisenhofen)
SDS	Carl Roth Gmbh (Karlsruhe)
sGC□$_1$	Produced in our lab
sGC□$_1$	Produced in our lab
SOD	Sigma (Deisenhofen)
Sodium Pyrophosphate	Sigma (Deisenhofen)
Spermine NONOate	Alexis cooperation (Lausen, Switzerland)
Sucrose	Sigma (Deisenhofen
TEMED	Sigma (Deisenhofen)
Tris	Carl Roth Gmbh (Karlsruhe)
Triton X-100	Serva Feinbiochemica (Heidelberg, Germany

Water was deionised to 18 M□ cm (Milli-Q;Millipore, Eschborn)

4.3. Software

Software	**Version**	**Producer**
Adobe Acrobat	4.0	Adobe system (San Jose, CA, USA)
Adobe Photoshop	7.0	Adobe system (San Jose, CA, USA)
EndNote	6.0	ISI research software (Berkeley ,CA USA)
IBJ-BeMon 32		PowerLab, Germany
Kodak ID Image analysis software		Eastman Kodak company (New Haven, USA)
Microsoft office Mac	2002	Microsoft Coperation (Remond, WA, USA)
Graph Pad Prism	3.0/4.0	Graph Pad Software (San Diego, Ca, USA)

5. Methods

5.1. Tail cuts and earmarks

In our present study, potential transgenic mice are screened for the presence of gene by performing polymerase chain reaction (PCR) with a DNA sample extracted from the tail biopsy. When the tail biopsy was performed, the sample was assigned with identification number and the mouse is marked with that number. In Fig. 5.1., we show how to mark a mouse by ear punching. This scheme allows mice to be numbered from 1 to 99 and is sufficient for most purposes when combined with cage card identification including also sex and age.

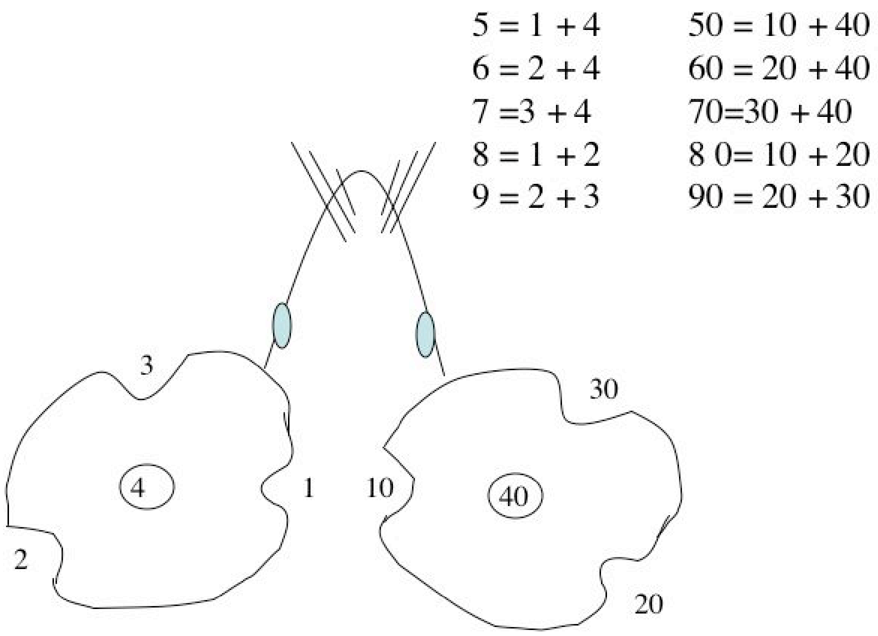

Fig. 5.1. A scheme for marking a mouse by ear punching, using a continuous number system from 1 to 99.

5.2. Isolation of mouse genomic DNA from tail biopsies

Isolation of genomic DNA was performed by two methods.

5.2.1. Using DNeasy tissue kits (Qiagen, Germany)

1. We cut up to 0.4 - 0.6 cm length of tail into a 1.5 ml microcentrifuge tube and 180 µl of buffer ATL were added.
2. We added 20 µl of proteinase K, mixed well by vortexing, and incubated at 55°C over night for complete lysis.
3. After a short vortex (15 second), 400 µl of buffer AL-ethanol mixture was added to the sample, and mixed vigorously by vortexing.
4. Then, this mixture was pipeted into the DNeasy spin column and placed in a new 2 ml collection tube and centrifuged at 8000 rpm for 1 min.
5. After, the DNeasy mini spin column was placed in a new 2 ml collection tube, 500 µl of buffer AW1 was added and centrifuged at 10000 x g for 1 min.
6. Next, we placed the DNA spin column in a new 2 ml collection tube, and 500 µl of buffer AW2 was added, which was followed by centrifugation for 3 min at full speed (14000 rpm) to dry the DNeasy membrane.
7. Finally, the DNeasy mini spin column was placed in a clean 1.5 ml or 2 ml micro-centrifuge tube and 200 µl of buffer AE was directly added into the DNeasy membrane for the elution of DNA. Then, this was incubated at room temperature for 1 min, and centrifuged for 1 min at 10000 x g to elute.

5.2.2. Using special lysis buffer

50 mM	KCl
1.5 mM	$MgCl_2$
10 mM	Tris-Hcl, pH 8.3
0.45%	Nonidet P 40
0.45%	Tween 20
100 µg /ml	Proteinase K

<u>Procedure</u>

Add about 400 µl of this lysis buffer (mentioned above) to a tail cut and lyse at 55°C for overnight with continuous shaking. Then, we heated to inactivate the proteinase K at 94°C for 20 min. After spin down the condensation, samples were briefly centrifuged (3 min, 8000 x g), and the supernatant was separated in sterile eppendorf tube.

5.3. Determination of DNA yield

The DNA yield was determined by measuring the concentration of DNA in the elute by its absorbance at 260 nm (A_{260}) using spectrophotometer (Pharmacica LKB. Biochrom 4060). Absorbance readings at 260 nm should fall between 0.15 and 1.0 to be accurate. An A_{260} of 1 (with a 1 cm detection path) corresponds to 50 µg DNA/1 ml water. Distilled water should be used as diluents when measuring DNA concentration since the relationship between absorbance and concentration is based on extinction coefficient calculated for nucleic acids in water [156]. Using a 0.1 ml cuvette, the absorbance of the diluted sample was measured.

An example of calculations involved in DNA quantification is shown below:

Volume of DNA sample = 100 µl

Dilution = 10 µl of DNA sample + 90 µl of distilled water

Concentration of DNA = 50 µg / ml x A_{260} x dilution factor

= 50 µg / ml x A_{260} x 10

5.4. Generation and genotyping of AT_{1A} receptor-deficient mice

5.4.1. Generation of $AT_{1A}^{-/-}$ mice

Male and female heterozygous $AT_{1A}^{+/-}$ mice were produced by Jackson laboratories (USA) and mated to get homozygous mice. The founder strains were developed by Coffman *et al.* (1995)[26]. Mice of F_2 progeny were derived from mating between 129X and C57Bl/6j from the F_1 AT_{1A} heterozygous parents. The F_2 generation of $AT_{1A}^{+/+}$ and $AT_{1A}^{-/-}$ had similar random assortment of background genes, making them appropriate matches for our study. Animals were bred and maintained Animals were bred and maintained in isolated ventilated cages under specificed pathogen-free conditions according to the recommendations of Federation of European Laboratory Animals Science Association (FELASA) in isolated ventilated cages under specified pathogen-free conditions.

5.4.2. Genotyping of $AT_{1A}^{-/-}$ mice

The genotyping of mice in the present study was performed by PCR. PCR technique is designed for amplification of specific regions of DNA using *Taq* DNA polymerase. *Taq* polymerase is a thermostable enzyme isolated from *Thermus aquaticus*.

Materials:

DNA-agarose gel loading buffer

0.25% (w/v)	Bromophenolblue
0.25% (w/v)	Xylencyanol
30%	glycerol in water

TAE-buffer

40 mM	Tris-HCl
2 mM	EDTA
0.1% (v/v)	CH_3COOH (Eissig).

Markers

1kb-DNA (Eurogenetic, Seraing, Belgium)

Primers

Upstream (5`-ACCAACTCAACCCAGAAAAGC-3`)

Downstream (5`-CCAGGATGTTCTTGGTTAGG-3`)

Protocol

Buffer S (10x) (PeQlab)	5 µl
dNTPs (10mM)	1 µl
Upstream primer (50 pmol/ µl)	1 µl
Downstream primer (50 pmol/ µl)	1 µl
Taq-polymerase (5 U/ µl)	0.25 µl
DNA template (100-200 ng)	X µl (depend on amount of DNA)
H_2O (sterile and distilled) to	50 µl

PCR Profile

Activation	Amplification 30 cycles			Termination	
	Denaturation	Annealing	Elongation		
5 min	1 min	1 min	1.2 min	7 min	∞
95°C	95°C	55°C	72°C	72°C	4°C

Procedure

To perform several parallel reactions, we recommended the preparation of a master mix. In the master mix, all ingredients including buffer, dNTPs, primers and *Taq* DNA polymerase were combined in a single tube. Then, the mixture was aliquoted into individual thin-walled PCR tubes containing templates of DNA, on ice. The master mix of setting reactions minimizes the possibility of pipeting errors and saves time by reducing the number of reagent transfers. After tubes were gently vortexed, we made a brief centrifugation (1000 x g for 2 min, 4°C). Then, tubes are placed in the PCR thermo-cycler machine. The DNA products were amplified using PCR profile (mentioned above) with appropriate number of cycles to be clearly visible on an agarose gel. After amplification process, a 6-8 µl of DNA- agarose loading buffer was added to each 50 µl of PCR product. Subsequently, the PCR products (20 µl) were loaded onto ethidium bromide-stained 1.2% agarose gel, at 100 volt for 50 min using 1-kb marker. Bands were visualized using a UV lamp (UV Transilluminator, Micro Bio Tech Brand, Germany) and imaging system (Kodak EDAS 290, USA). The wt band (+) is detected at 620-bp, and the mutant band (-) is detected at 1.2-kb sequences (Fig. 5.2.).

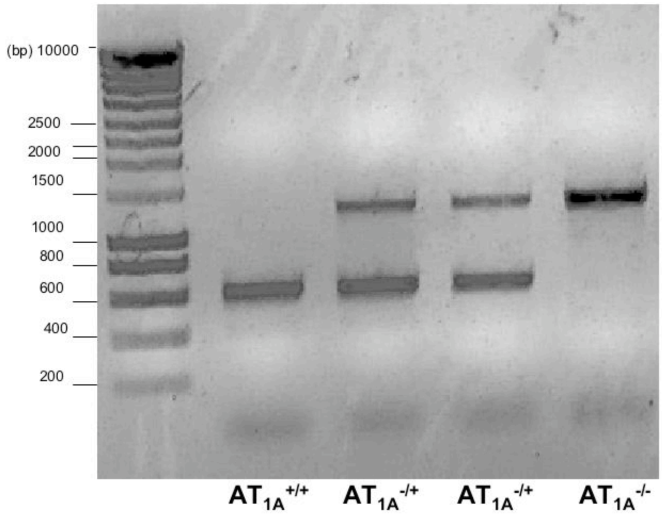

Fig. 5.2. PCR analysis for AT_{1A} receptor-deficient mice using 1-kb marker, showing the mutant band could be detected at 1.2-kb and wt band at 620-bp.

5.5. Generation and genotyping of AT_2 receptor-deficient mice

5.5.1. Generation of $AT_2^{-/Y}$ mice

Mice lacking AT_2 receptors were originally produced by Hein *et al.* (1995) [157]. Germline-transmitting chimeric mice were crossed back into an FVB/N background for 8 generation. The Ang II AT_2 receptor gene is located on the X chromosome. Therefore, only wt ($AT_2^{+/Y}$) and hemizygous ($AT_2^{-/Y}$) male littermates (3-4 months-old) derived from crossing of male wt FVB/N and heterozygous mice were used in our present study. Animals were bred and maintained in isolated ventilated cages under specificed pathogen-free conditions according to Federation of European Laboratory Animals Science Association (FELASA) requirements.

5.5.2. Genotyping of $AT_2^{-/Y}$ mice

Primer-Sequences (in 5`to 3`direction)

wt "+" Primer: 5`-CCT TGG CTG ACT TAC TCC TT-3`

AT_2 "-" Primer: 5`-GAA CTA CAT AAG ATG CTT GCC-3`

AT_2-ko "-" Primer: 5`-TAG TTG CCA GCC ATC TGT TG-3`

Protocol

10x Buffer (Eppendorf)	5 µl
AT_2-wt"+" Primer (50 pmol/µl)	1 µl

AT_2 "-" Primer (50 pmol/µl)	1 µl
AT_2-ko "-" Primer ((50 pmol/µl)	1 µl
dNTP (10 mM)	0.5 µl
Taq-Polymerase 5 U/ µl	0.25 µl
DNA template (100-200 ng)	X µl (depend on amount of DNA)
H_2O (sterile and distilled) to	50 µ

PCR-profile

Activation	Amplification 35 cycles			Termination	
	Denaturation	Annealing	Elongation		
5 min	30 sec	30 sec	40 sec	7 min	∞
95°C	95°C	55°C	72°C	72°C	4°C

Procedure

All ingredients (water, buffer, dNTPs, primers and *Taq* DNA polymerase) were combined to make master mix. Then, the mixture is aliquoted into individual thin-walled PCR tubes containing templates of DNA, on ice. After tubes were gently vortexed, we made a brief centrifugation (1000 x g for 2 min, 4°C). After a brief centrifugation (15 sec), tubes were placed in the PCR thermo-cycler machine. The DNA products were amplified using PCR profile mentioned above with appropriate number of cycles to be clearly visible on an agarose gel. After amplification process, a 6-8 µl of DNA- agarose loading buffer was added to each 50 µl of PCR products. The PCR products (20 µl) were loaded onto ethidium bromide-stained 2% agarose gel, at 100 volt for 50 min using 1-kb marker. Finally, bands were detected using a UV lamp (UV Transilluminator, Micro). The expected-PCR-Products were detected at 234-bp for the wt allel and 383-bp for the mutant allel (Fig. 5.3.).

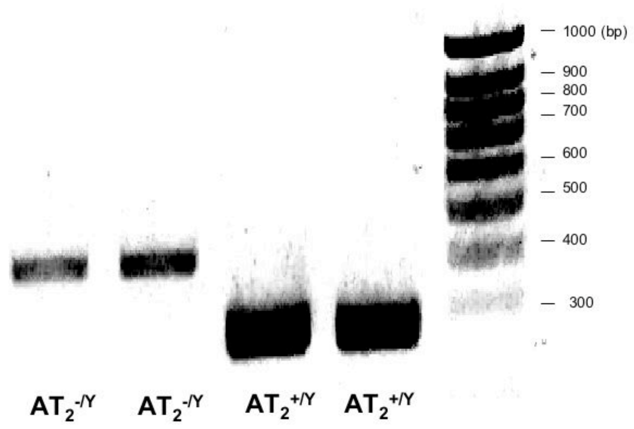

Fig. 5.3. PCR analysis of AT_2-receptor-deficient mice using a 100 bp marker. As shown, the mutant ($AT_2^{-/Y}$) band could be detected at 383-bp and wt ($AT_2^{+/Y}$) band at 234-bp.

Marker

100-bp-DNA (Eurogenetic, Seraing, Belgium)

5.6. Protein analysis

5.6.1. Tissues lysis for Western blots

Materials:

2x SLB (Special-Lysis- Buffer)

40 mM	Tris-HCl pH 7.4
150 mM	NaCl
2% (w/v)	Na-deoxycholat
2% (v/v)	Triton X-100
0.1 (w/v)	SDS
50 mM	EDTA
50 mM	EGTA
50 mM	Na-pyrophosphate
2 mM	Vanadat
2x	Protease inhibitor complete EDTA free (Roche)

Rotiload buffer

62.5 mM	Phosphate buffer (pH 6.8)
10% (v/v)	Glycerol
2% (w/v)	SDS
0.01% (w/v)	Bromophenol blue
5% (v/v)	2-Mercaptoethanol

Procedure

For Western blotting analysis, mice were sacrificed by cervical dislocation. Aorta and other organs were excised rapidly, and the fat or connective tissues were manually removed under a binocular microscope. Tissues were washed with normal saline and immediately frozen in liquid nitrogen, and stored in –80°C. The frozen tissues were powdered and an amount of 40 - 45 mg of the powdered tissue was transferred to a 1.5 ml eppendorf tube. For tissue lysis, about 350 µl of 2x SLB lysis buffer (mentioned above) was added to the powdered tissue. Because liver contains more proteins compared to other organs, we added about 400 µl of lysis buffer to 40 – 45 mg powdered tissue from liver. The mixture was vortexed, and further mixed for 10 min using an eppendorf mixer. Following which, the same volume of 2x rotiload buffer was added and boiled for 15 min at 95°C in eppendorf thermo-mixer. The mixture was centrifuged at 8000 x g for 10 min, and the supernatant was transferred to fresh eppendorf tubes without touching the pellets. After protein precipitation with trichloroacetic acid, protein concentrations were determined by the Lowry method [158].

5.6.2. Protein determination

Materials:

Folin I reagents for Lowry-protein determination

Folin I reagent is a mixture of A to D in ratio 1: 1: 28: 10, respectively.

Solution A

1% (w/v) $CuSO_4$

Solution B

2% (w/v) Na-Tartrate

Solution C

3.4% (w/v) $NaCO_3$ in 0.2 M NaOH

Solution D

10% (w/v) SDS

In samples with rotiload buffer for SDS-PAGE, protein was determined according to Lowry method after precipitation of protein by trichloroacetic acid [158]. Different concentrations of BSA (0.0 mg, 0.1 mg, 0.2 mg, 0.4 mg, 0.8 mg 1.6 mg 2.4 mg and 3.2 mg / ml distilled water) were prepared. 50 µl volume of BSA- standards, and 10 µl of protein extract were diluted with 1 ml of distilled water and 100 µl of 0.15% deoxycholic acid was added. After 10 min incubation at room temperature on eppendorf shaker, 100 µl of 72% trichloroacetic acid was added, and incubate for 15 min with shaking at room temperature. Then, samples and standards were centrifuged at 16000 x g for 10 min. After aspiration of the supernatant, pellets were resuspended in 300 µl water and 300 µl of Folin 1 reagent (see above) was added, and incubated for 10 min with shaking at room temperature. Subsequently, 150 µl of 25% (v/v) Folin-Ciocalteus-Phenol reagent (diluted to 1: 3 with water) was added to samples as well as standards and incubated for 30 min with shaking. Finally, a volume of 300 µl was twice pipeted into a 96-well plate. The protein concentration was measured at 595 nm using a spectraMax 340 (Molecular Devices). BSA protein standards were used to calculate the concentration of protein from its optical density.

5.6.3. SDS-Polyacrylamid-gelelectrphoresis (SDS-PAGE)

Materials:

Electrophoresis buffer

25 mM	Tris.HCl
120 mM	Glycin
0.1%	SDS

SDS-gel (9%)

Separation gel	Collection gel
9% (v/v) AA-Bis	5 % (v/v) AA-Bis
750 mM Tris/Hcl, pH 8.8	625 mM Tris/Hcl,pH 6.8
0.1% (v/v) SDS	0.1% (v/v) SDS
0.05% (v/v) TEMED	0.1% (v/v) TEMED
0.07% (w/v) APS	0.05% (w/v) APS

Protein markers

BOA-protein marker (Biomol, Hamburg).

Equal amounts of protein (50µg) were run on 9% polyacrylamide gels with 1 mm thickness in electrophoresis chambers, according to the method described by Laemmli [159]. We used a lysate from Caco-2 (colon carcinoma cell line) as a standard reference for Nox1 and a lysate of A7r5 (VSMC line) cell for Nox4. Then, these chambers were supplied with constant current 15 mA / gel.

5.6.4. Western blotting

Materials:

Blotting buffer (pH10.0)

48 mM	Tris, HCl
39 mM	Glycin
0.1% (w/v)	SDS
20% (v/v)	Methanol

T-TBS (pH 7.5)

20 mM	Tris, HCl
150 mM	NaCl
0.1 % (v/v)	Tween 20

Procedure

Anti-Nox1 and anti-Nox4 rabbit polyclonal antibodies were raised against the following peptides: Nox1 (aa545561)= RYSSLDPRKVQFYC; Nox4 (aa84101)=RGSQKVPSRRTRRLLDKS; Anti-Nox2 from (Upstate, biotechnology, Biomol, Hamburg)).

Equal amounts of protein (50 µg) were electrophoretically size separated on 9% SDS-polyacrylamide gel according to the method described by Laemmli *et al.* (1970) [159]. Proteins were transferred into nitrocellulose membranes by semidry blotting at 1.2 mA/cm^{-2} for 1 h by using blotting buffer as decided by Darley *et al.* (1992) [160]. Equal rates of transfer were confirmed by reversible staining with Ponceau-S (0.1%

(w/v). Non-specific binding was blocked by incubation in 2% non-fat dry milk powder in T-TBS (see above) at room temperature for 3h.
For Nox1, Nox2 and Nox4 detection in tissue homogenates, anti-Nox1, anti-Nox2 and anti-Nox4 antibodies were diluted in 2% milk with T-TBS and incubated with nitrocellulose membrane at 4°C overnight. Membranes were washed in T-TBS 4 times for 10 min each. Subsequently, these membranes were incubated for 1 h at room temperature in dark with the horseradish peroxidase–conjugated secondary antibody that was diluted in 2% milk. After washing blots with T-TBS 4 times 10 min each. Finally, they were incubated for 1 min at room temprature with ECL (enhanced chemiluminescence Amersham Pharmacia Biotech, Germany) or for 5 min with ECL-advanced (Amersham Pharmacia Biotech).

<u>Signal Quantification</u>

Protein content was analysed by densitometry using Image Station 440CF (Kodak Digital Science), and light signals were quantified using the Kodak ID image analysis software (Scientific Imaging System, Eastman Kodak Company, New Haven, USA).

5.6.5. Determination of 3-nitrotyrosine (3NT) immunoreactivity

3NT immunoreactivity in mouse aortic tissue was determined by Western blot analysis as previously described for Nox1 and Nox4. The anti-nitrotyrosine antibody employed was polyclonal generated by Uttenthal *et al.* (1998) [161] in rabbit. A secondary antibody (horseradish peroxidase–conjugated antirabbit), diluted in 3% milk in T-TBS was used. After incubation with the secondary antibody for 1h, membranes were washed 4 times with T-TBS (each for 15 min). Immunodetections were visualized using enhanced chemiluminescence kits as previously described.

5.6.6. Determination of sGC protein expression

<u>Lysis buffer of sGC (Marletta buffer)</u>

25 mM	TEA-HCL pH7.0
1 mM	EDTA pH 8.0
5 mM	DTT
50 mM	NaCl
10% (g/v)	Glycerin

Protease inhibitor (complete EDTA free tablet)

Procedure

The homogenized tissues (25% w/v) were subjected to lysis using the lysis buffer (see above) at 4°C and with the aid of a tissue girder fitted with a motor-driven ground-glass pestle. Homogenates were centrifuged at 12000 x g for 5 min at 4°C to remove nuclear fragments, and the supernatant was used for determination of protein concentrations. Equal amounts of protein were separated by SDS-PAGE (9%), and were determined by Western blot analysis as described previously [162]. For sGCα_1 and sGCβ_1 protein detection in tissue homogenates, polyclonal anti-sGCα_1 and sGCβ_1, as previously described were used [163]. These antibodies were diluted with 3 % milk in T-TBS and incubated with nitrocellulose membrane at 4°C overnight. After 3 washing steps with T-TBS (each 15 min), the membranes were incubated with the secondary antibody. A secondary antibody, diluted with 3% milk in T-TBS was used. After incubation with the secondary antibody for 1h at room temprature, membranes were washed for 4 times with T-TBS (each for 15 min). Incubation with the secondary antibody and washing occurred at room temperature. Immunocomplexes were visualized using enhanced chemiluminescence kits as described above for Nox1 and Nox4.

5.6.7. Determination of eNOS protein expression

Homogenization buffer, pH 7.4

10 mM	HEPES buffer
250 mM	Sucrose
3 mM	EDTA
1 mM	PMSF

Procedure

To determine the eNOS protein expression, the tissue pieces were homogenized in buffer mentioned above [164] at 4 °C with the aid of a tissue girder fitted with a motor-driven ground-glass pestle. Equal volume of denaturing buffer (rotiload buffer), was added and heated to 80°C for 15 min, following which, the mixture was centrifuged at 5600 g for 3 min. Equal amounts (50 µg) of proteins were separated by SDS-PAGE (9%), and subjected to Western blotting analysis as previously described. For immunodetection of eNOS protein expression, anti-eNOS monoclonal antibody (Transduction Laboratories) diluted (1: 2500) with 3% milk in T-TBS as described by Vaziri *et al.* (2001)[165] was used. Anti-mouse antibody conjugated to horseradish peroxidase in 3% milk in T-TBS was used as secondary antibody. Incubation with the secondary antibody and washing was performed at room temperature. Immunocomplexes were visualized using an enhanced chemiluminescence kit as described before.

5.6.8. Stripping of blots

Materials:

Stripping-Buffer (pH 6.8)

2%	SDS
62.5 mM	Tris
100 mM	β-Mercaptoethanol

This is a method used for immunodetection of the same blot by another primary antibody. The primary and secondary antibodies were removed from the membrane after incubation with 10 ml stripping buffer and warmed in water bath at 60-70°C for 30 min. Then, the stripping was washed out with T-BST at least 4 times (each time for 15 min). Thus, these blots are ready to be used for further immunodetection.

5.7. Measurement of NADPH–oxidase activity using lucigenin-enhanced chemiluminescence method

Materials:

Krebs Buffer (pH 7.4)

118 mM	NaCl,
4.7 mM	KCl,
2.5 mM	$CaCl_2$. $2H_2O$
1.18 mM	$MgSO_4.7H_2O$
1.18 mM	KH_2PO_4
24.9 mM	$NaHCO_3$
11 mM	Glucose
0.03 mM	EDTA

NADPH-dependent $O_2^{\cdot-}$ production was measured in membrane fractions of mouse aortic homogenates using lucigenin-enhanced chemiluminescence in concentration of (5 μM) as previously validated [166] to avoid redox cycling. Firstly, the thoracic aorta was excised, freed from loose connective tissue, minced under liquid nitrogen and collected in 0.5 ml of 50 mM Tris buffer containing protease inhibitor cocktail tablets (Roche, Germany) and DTT (10 mM). Membrane fractions were obtained by differential centrifugation at 500 x g (5 min, 4 °C) and 68000 x g (90 min, 4°C). The pellet containing mainly membranes and microsomes, was resuspended in 200 μl of Krebs-buffer, (mentioned above) containing 20 mM HEPES and the protein content was determined. The assay reaction mixture (100 μl) containing lucigenin (5 μM) and 50 μg of protein was kept in dark at 37°C for 20 min for equilibration. Using a 96-well plate, the NADPH oxidase activity, was measured in the presence of NADPH (100 μM) as substrate. Chemiluminescence signals were measured using the luminescence reader (Fluoroskan Ascent FL) at intervals of I min over a period of 5 min and the results expressed as Relative Light Unit (RLU). All measurements were performed in triplicates. The signals were tested in the absence and presence of different inhibitors such as the NO synthase inhibitor N^G-nitro-L-arginine methyl ester (L-NAME, 100 μM), NADPH oxidase inhibitor apocynin (100 μM), a flavoprotein inhibitor DPI (10 μM), xanthine oxidase inhibitor oxypurinol (1 mM) and the $O_2^{\bullet-}$ scavenger SOD (250 U/ml), respectively.

5.8. Isolated vascular studies

Procedure

Mice were sacrificed by cervical dislocation and the thoracic aorta was rapidly isolated as described by Russell and Watts [167]. Vessels were stored at 4°C (for up to 15 min) before being placed in isolated organ baths (IOA 5306 Isolated Organ Apparatus, (FMI Föhr Medical Instrument, Seeheim, Germany). Before mounting, each aorta was freed from excess connective tissue and cut into 3 rings of 2-3 mm in length. Changes in isometric tension were detected by a force transducer and recorded via a 6 channels transducer data acquisition system (FMI Föhr Medical Instrument, Seeheim, Germany). Aortic rings from $AT_{1A}^{-/-}$, $AT_{1A}^{+/+}$, $AT_2^{-/Y}$ and $AT_2^{+/Y}$ mice were mounted in individual organ baths containing 5 ml of Krebs buffer maintained at 37°C and bubbled continuously with 5% carbogen. Vessels were progressively stretched to the optimal resting tension (0.5 g), and then allowed to equilibrate for 40 min before addition of drugs. Krebs buffer was changed once every 15 min throughout the experiment, except during the generation of concentration-response curves. After 40-60 min of equilibration, aortic rings were challenged with a high–potassium solution (120 mM KCl) to determine whether they were viable. Subsequently, vessels that demonstrated a contraction response to the high potassium solution were used for further studies. Then, aortic rings were precontracted submaximally (60-80 %) with100 nM phenylephrine (PE). Then, concentration-response curves were generated for the endothelium-dependent dilator acetylcholine (ACh) (1 nM-10 µM). In separate experiments, concentration-response curves of ACh were generated in the absence and presence of SOD (250 U/ml) and apocynin (0.1 mM). The concentration-response curves were also determined for the NO donor spermine NONOate (1 nM-10 µM).

5.9. Lung isolation perfusion and ventilation

Procedure

For perfusion and ventilation an open chest mouse lung preparation was used [168]. A water jacketed chamber (type 839, Hugo Sachs ElektroniK, March-Hugstetten, Germany) served as an artificial thorax, which allowed for control of system temperature. Mice were deeply anesthetized intraperitoneally with pentobarbital sodium heparin (1000 U/kg) by intravenous injection. Animals were then intubated via a tracheostoma and ventilated with room air (positive pressure ventilation, 250 tidal volume, 90 breath/min and 2 cm H_2O positive end-expiratory pressure). Midsternal thoracotomy was followed by insertion of catheters into the pulmonary artery and left atrium. Using a peristaltic pump (ISM834A V2.10, Ismatec, Glattbrugg, Switzerland), buffer perfusion via the pulmonary artery was initiated at 4°C and a flow of 0.2 ml/min. For perfusion, a variety of buffer solutions were investigated. In parallel with the onset of artificial perfusion, ventilation was changed from room air to a pre-mixed gas (21% O_2 5.3% CO_2, balanced with N_2). After rinsing the lungs with ≥ 20 ml buffer, the perfusion circuit was closed for recirculation (total system volume 13 ml) and left arterial pressure was set at 2.0 mmHg. Meanwhile the flow was slowly increased from 0.2 to 1 ml/min and the entire system heated to 37°C. Pressure in the pulmonary artery was registered via a small diameter catheter. During surgery, the lungs were ventilated with positive pressure. After placing the catheter, the artificial thorax was closed and the lungs were ventilated with negative pressure. For inspiration, negative pressure was adjusted to result in a tidal volume of ~ 250 μl. End-expiratory pressure was held constant at –2 cm H_2O.

Statistical analysis

All experiments were performed in parallel on preparations from knockout and wild-type mice. Results are expressed as mean ± SEM. Statistical evaluation of the data was performed by unpaired Student´s t test for simple comparison between 2 values when appropriate. For multiple comparisons, results were analyzed by ANOVA and tested with Bonferonni multiple range tests. EC_{50} values were calculated with a non-linear regression analysis with algorithm. A value of $P < 0.05$ was considered significant. All statistical evaluations were performed using Graphpad prism software (San Diego, CA, USA).

6. Results

6.1. Effect of the targeted deletion of AT_{1A} or AT_2 receptors on expressions of Nox1 and Nox4

In the present study, it was of interest to recognize the effect of Ang II receptors (AT_{1A} and AT_2) on the expressional regulation of Nox1, Nox2 and Nox4 under physiological conditions using animals that are genetically deficient in Ang II receptors (AT_{1A} or AT_2). Western blotting revealed that the expression of NADPH oxidase subunits (Nox1 and Nox4) was significantly reduced in aortic tissues of $AT_{1A}^{-/-}$ mice when compared with $AT_{1A}^{+/+}$ mice. As shown in Fig. 6.1., Nox1 expression level was dramatically decreased to the one-fifth of that in $AT_{1A}^{+/+}$ mice (20.6 ± 9.3% of $AT_{1A}^{+/+}$ mice, ** $P < 0.01$), and Nox4 level was diminished to the one-half of that in $AT_{1A}^{+/+}$ mice (49.6 ± 6.8% of $AT_{1A}^{+/+}$ mice, * $P < 0.05$) (Fig. 6.2.).

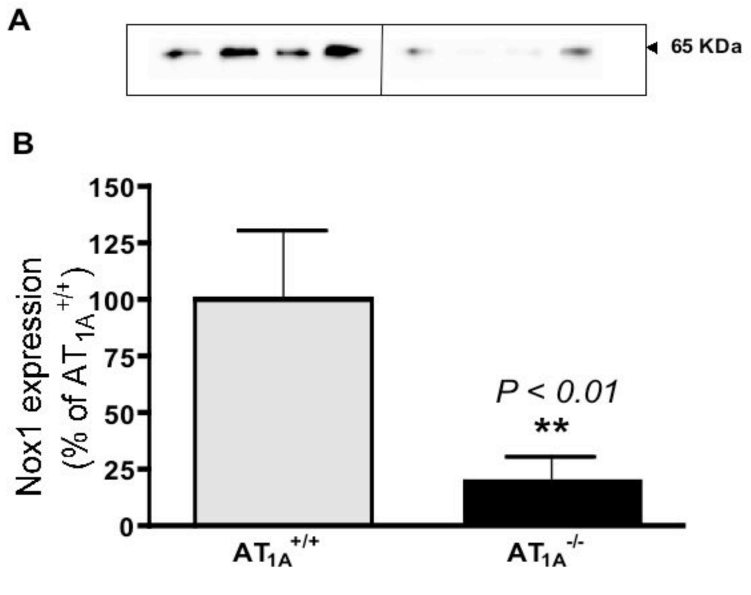

Fig. 6.1. Nox1 expression in aortic homogenates of $AT_{1A}^{-/-}$ and $AT_{1A}^{+/+}$ mice. A. Representative immunoblot of Nox1 expression in aortic homogenates of $AT_{1A}^{-/-}$ and $AT_{1A}^{+/+}$ mice. B. Densitometric analysis of Nox1 immunoblot in aorta of $AT_{1A}^{-/-}$ mice. Values are normalized to the level seen in $AT_{1A}^{+/+}$ mice (100%). In $AT_{1A}^{-/-}$ mice, the aortic Nox1 expression level was significantly downregulated compared to that in $AT_{1A}^{+/+}$ mice. Values represent means ± SEM of n = 6 experiments. Asterisks indicate statistically significant differences (*P* < 0.01; Student 's unpaired t-test).**

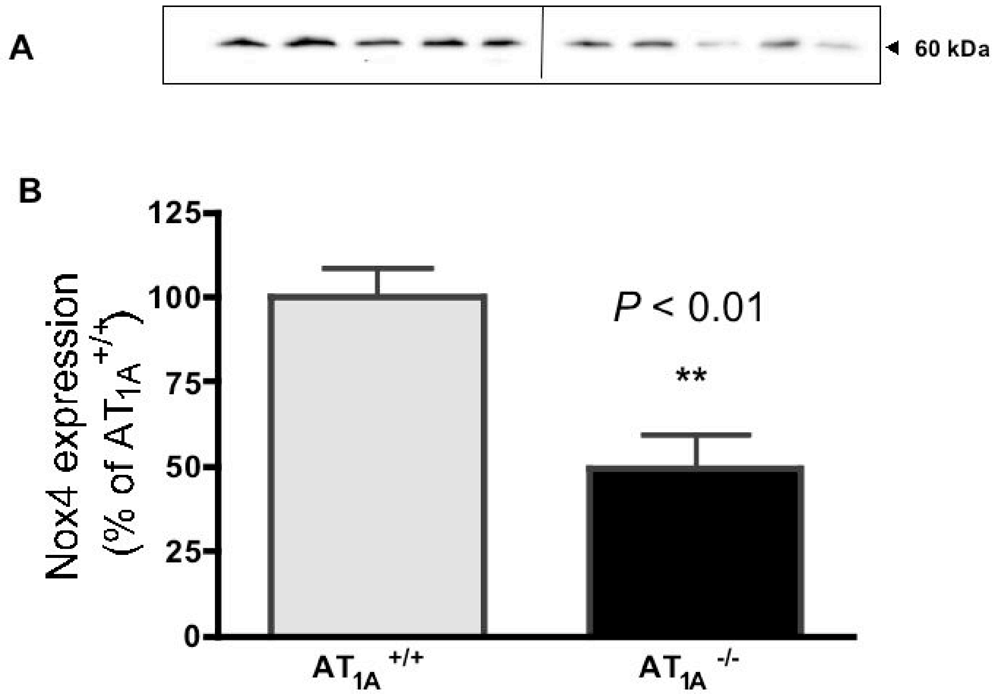

Fig. 6.2. Nox4 protein expression in aortic tissues of $AT_{1A}^{+/+}$ and $AT_{1A}^{-/-}$ mice. A. Representative immunoblot of Nox4 expression in aortic homogenates of $AT_{1A}^{-/-}$ and $AT_{1A}^{+/+}$ mice. B. Densitometric analysis of Nox4 immunoblot in aorta from $AT_{1A}^{-/-}$ mice. Values are expressed as % of $AT_{1A}^{+/+}$ mice. Data show a significant decrease in Nox4 expression in aortic tissues from $AT_{1A}^{-/-}$ mice *versus* that in $AT_{1A}^{+/+}$ mice. Values represent means ± SEM of n=6 experiments (*P* < 0.01; Student 's unpaired t-test).**

Although *in vitro* regulation of NADPH oxidase subunits by AT_2 receptor has been recently reported [141], there is a lack of information regarding *in vivo* regulation of this oxidase by AT_2 receptor. In the present work, we tried to evaluate the regulatory role of AT_2 receptor on the protein expression of Nox1 and Nox4 under physiological conditions using AT_2 receptor-deficient mice. Surprisingly, targeted disruption of the AT_2 receptor did not significantly alter the aortic Nox4 expression level *versus* that in $AT_2^{+/Y}$ mice (Fig. 6.3.). However, in the aorta from $AT_2^{-/Y}$ mice, Nox1 expression level was downregulated to the two-third of that in $AT_2^{+/Y}$ mice (68.4 ± 4.1 % of $AT_2^{+/Y}$ mice, * $P < 0.05$). On the other hand, Nox2 protein expression exhibit no significant difference in aortic tissues of either $AT_{1A}^{-/-}$ or $AT_2^{-/Y}$ mice in comparison to their respective wt.

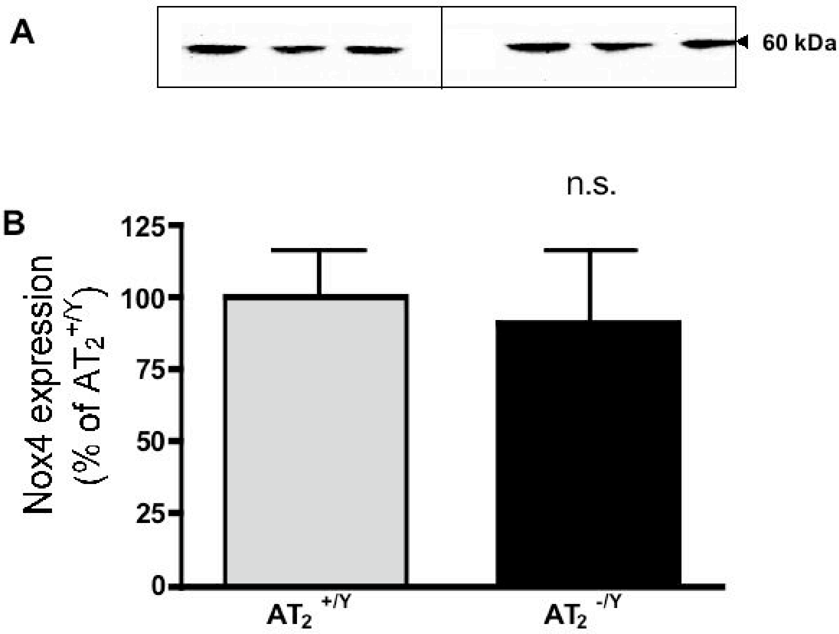

Fig. 6.3. Nox4 protein expression in aortic tissues of $AT_2^{-/Y}$ and $AT_2^{+/Y}$ mice. A. Representative immunoblot of Nox4 expression in aortic homogenates of $AT_2^{-/Y}$ and $AT_2^{+/Y}$ mice. B. Densitometric analysis of Nox4 immunoblot in aortic homogenates of $AT_2^{-/Y}$, expressed as % of $AT_2^{+/Y}$ mice. Values represent means ± SEM of n = 6 experiments. Data show no significant differences in Nox4 expression levels between aortic tissues from $AT_2^{-/Y}$ and $AT_2^{+/Y}$ mice.

Due to the importance of NADPH oxidase-derived ROS in the lung function and signaling events in the pulmonary artery [92, 169], regulation of Nox1 and Nox4 expression in lung homogenates of $AT_{1A}^{-/-}$ and $AT_2^{-/Y}$ mice was investigated. In the lung of $AT_{1A}^{-/-}$ mice, Nox1 expression was mildly decreased compared to that in $AT_{1A}^{+/+}$ mice (61.1 ± 6.2% of $AT_{1A}^{+/+}$ mice, $P < 0.05$), Nox4 expression level remained unchanged. In the lung of $AT_2^{-/Y}$ mice, Nox1 expression level was significantly upregulated (129.4 ± 14,2% of $AT_2^{+/Y}$ mice, * $P < 0.05$)(data not shown). In addition, the lung of $AT_2^{-/Y}$ mice revealed a dramatic increase in the Nox4 expression with respect to that of $AT_2^{+/Y}$ mice. We found that Nox4 expression level was approximately 4.7-fold higher (476 ± 85.8% of $AT_2^{+/Y}$ mice. ** $P < 0.001$) than that in $AT_2^{+/Y}$ mice (Fig. 6.4.).

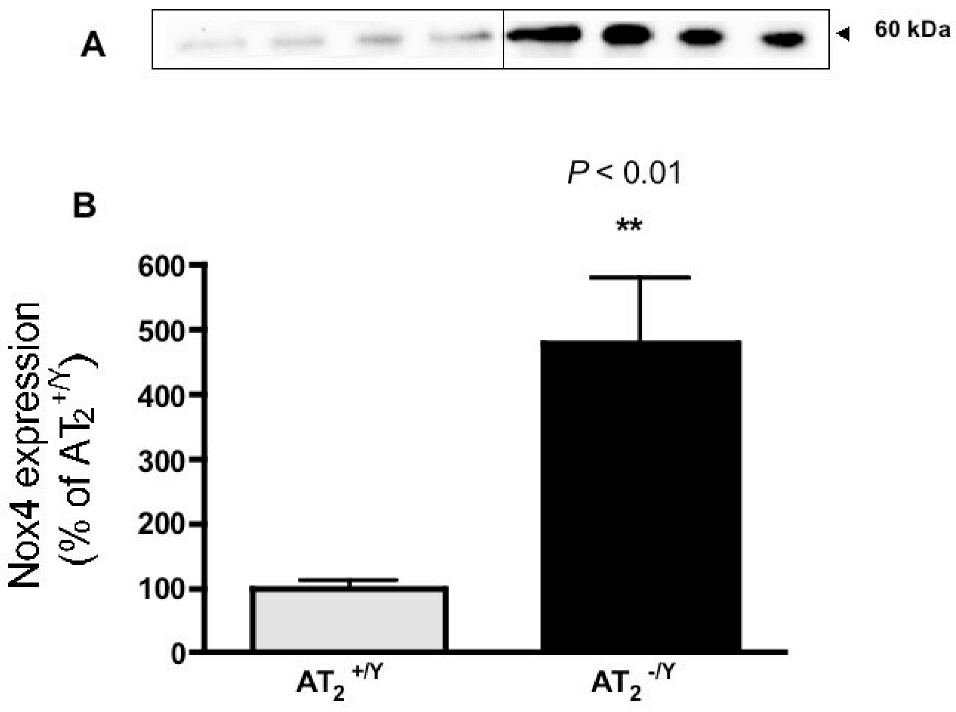

Fig. 6.4. Nox4 expression in the lung homogenates of $AT_2^{+/Y}$ and $AT_2^{-/Y}$ mice. A. Representative immunoblot of Nox4 expression in the lung homogenates of $AT_2^{-/Y}$ and $AT_2^{+/Y}$ mice. B. Densitometric analysis of Nox4 immunoblot in the lung of $AT_2^{-/Y}$ mice, expressed as % of the $AT_2^{+/Y}$ mice. Nox4 expression level was 4.7-fold greater than that in $AT_2^{+/Y}$ mice. Data represent means ± SEM of n = 5 experiments (*P* < 0.01; Student 's unpaired t-test).**

6.2. Effect of the targeted deletion of AT_{1A} or AT_2 receptors on NADPH oxidase activity

In order to examine the NADPH oxidase expression-functional correlation, NADPH oxidase activity was measured in aortic membrane fractions from $AT_{1A}^{-/-}$ and $AT_{1A}^{+/+}$ mice using lucigenin-enhanced chemiluminescence method [166]. As shown in Fig. 6.5., addition of NADPH (100 μM) as a substrate resulted in a substantially stimulation of $O_2^{\cdot-}$ production in aortic homogenates of $AT_{1A}^{-/-}$ and $AT_{1A}^{+/+}$ mice. However, addition of 100 μM of NADH had no stimulatory effect, suggesting an NADPH oxidase and no non-specific NADH oxidoreductase component was involved.

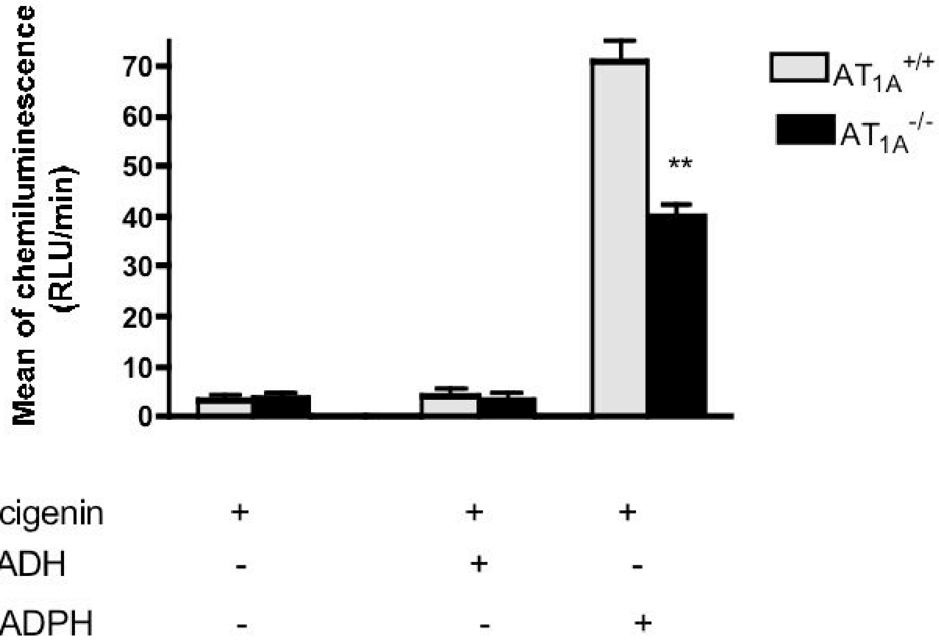

Fig. 6.5. Basal NADPH-dependent $O_2^{\cdot-}$ generation in aortic homogenates of $AT_{1A}^{-/-}$ and $AT_{1A}^{+/+}$ mice in the absence and presence of NADPH and NADH as a substrate, estimated using lucigenin-enhanced chemiluminescence method. NADPH rather than NADH oxidase is mainly involved in the lucigenin-enhanced chemiluminescence. In the aorta of $AT_{1A}^{-/-}$ mice, the level of lucigenin chemiluminescence was markedly decreased compared to that in $AT_{1A}^{+/+}$ mice. ROS levels are expressed as relative light units (RLU). Data represent means ± SEM of 7 independent experiments (*P* < 0.01, $AT_{1A}^{+/+}$ *versus* that in $AT_{1A}^{-/-}$ mice; ANOVA-test).**

In addition, in aortic homogenates of $AT_1^{-/-}$ mice, we have found that NADPH-dependent $O_2^{\cdot-}$ production was significantly lower than that in $AT_{1A}^{+/+}$ mice (39.8 ± 4 in $AT_{1A}^{-/-}$ mice *versus* 70.8 ± 6 in $AT_{1A}^{+/+}$ mice; ***P* < 0.01 RLU/min). To distinguish the NADPH-dependent $O_2^{\cdot-}$ formation from other $O_2^{\cdot-}$-generating enzymes such as xanthine oxidase and uncoupled eNOS, the basal $O_2^{\cdot-}$ formation was measured in the absence and presence of respective inhibitors of these enzymes. Neither the xanthine oxidase inhibitor (oxypurinol) nor the NOS inhibitor (L-NAME) was able to produce significant effects on basal $O_2^{\cdot-}$ formation. However, the enhanced chemiluminescence signals were abolished by the flavoprotein inhibitor DPI (10 μM), and inhibited to 50% by apocynin. The specificity of the specificity of lucigenin chemiluminescence for $O_2^{\bullet -}$ quantification was examined by the effect of SOD ($O_2^{\bullet -}$ scavenger) that was additionally determined. We observed that SOD inhibited approximately about 64% of the lucigenin chemiluminescence level (Fig. 6.6.).

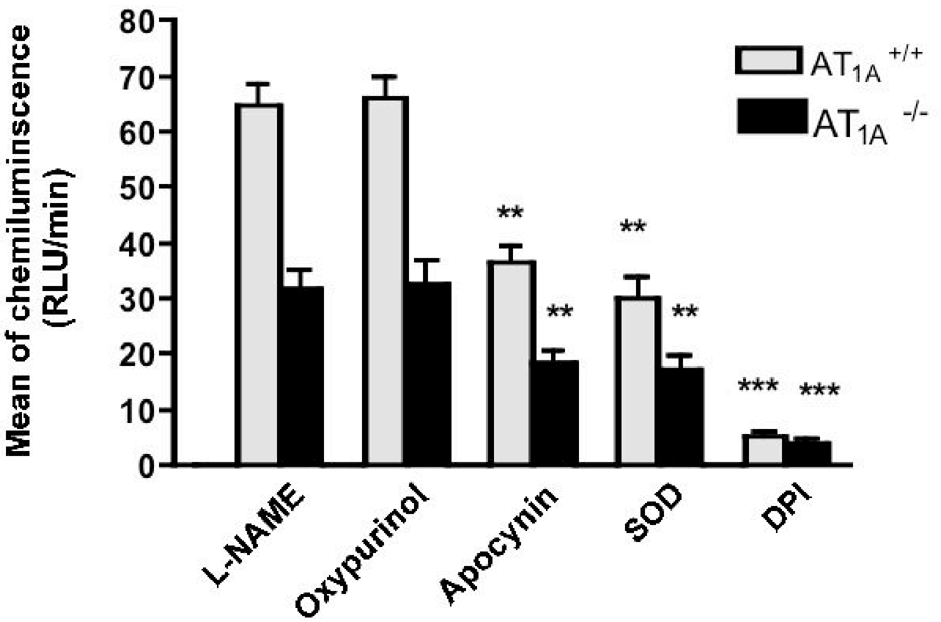

Fig. 6.6. Effect of different inhibitors of $O_2^{\bullet -}$-generating enzymes on the NADPH-dependent $O_2^{\bullet -}$ production in aortic homogenates of $AT_{1A}^{-/-}$ and $AT_{1A}^{+/+}$ mice. The level of lucigenin chemiluminescence signals in aortic homogenates of $AT_{1A}^{-/-}$ and $AT_{1A}^{+/+}$ mice were measured in the absence and presence of different inhibitors to $O_2^{\bullet -}$-generating enzymes. Values represent means ± SEM of 7 independent experiments ($P < 0.01$, *** $P < 0.001$ for $AT_{1A}^{+/+}$ *versus* $AT_{1A}^{-/-}$ mice; ANOVA-test).**

Fig. 6.7. illustrates our calculation of the absolute inhibitable ROS formation for apocynin, SOD and DPI based on the data shown in Fig. 6.6. It is noteworthy that the absolute inhibitable ROS generation by apocynin and DPI in aortic tissues from $AT_{1A}^{+/+}$ mice (exclusively represent NADPH oxidase activity) were 1.4 and 1.8 -fold, respectively greater than that in $AT_{1A}^{-/-}$ mice. The inhibitable effect of ROS by SOD indicates the specificity of the chemiluminescence signals to superoxide anions.

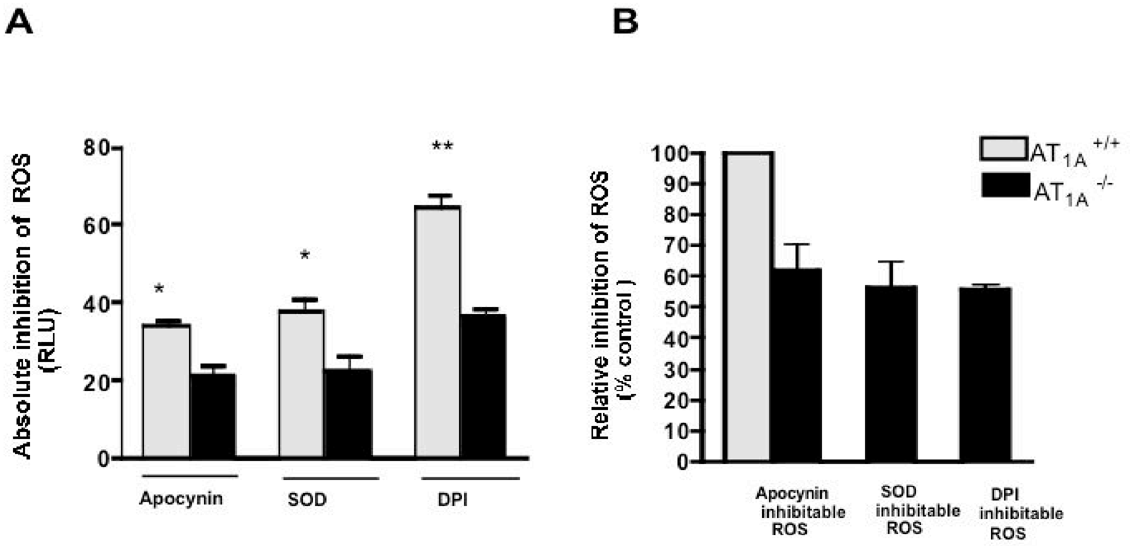

Fig. 6.7. A/B Calculation of the data from Fig. 6.6., A. Absolute values of ROS inhibitable formation for apocynin, SOD and DPI in aortic tissues of $AT_{1A}^{+/+}$ and $AT_{1A}^{-/-}$ mice. B. ROS Inhibitable formation of apocynin, SOD and DPI are expressed as % of $AT_{1A}^{+/+}$ mice. Only the apocynin-inhibitable signal is considered to represent exclusively NADPH oxidase activity.

Recently, it has been described that AT_2 receptor functions as antagonist of the AT_1 receptor-induced $O_2^{\cdot-}$ formation in endothelial cells by a tyrosine phosphatase involved pathway [170]. Nevertheless, nothing is known regarding the role of AT_2 receptors in basal $O_2^{\cdot-}$ formation. To analyse the possible role of the AT_2 receptor in basal activity of NADPH oxidase, we have studied NADPH oxidase-dependent $O_2^{\cdot-}$ production in aortic homogenates from $AT_2^{+/Y}$ and $AT_2^{-/Y}$ mice. Surprisingly, we found that aortic homogenates from $AT_2^{-/Y}$ mice showed insignificant differences in basal NADPH oxidase activity compared to that in $AT_2^{+/Y}$ mice. In addition, absolute inhibitable chemiluminescence signals for apocynin in membrane fractions from $AT_2^{+/Y}$ and $AT_2^{-/Y}$ mice were similar (Fig. 6.8.).

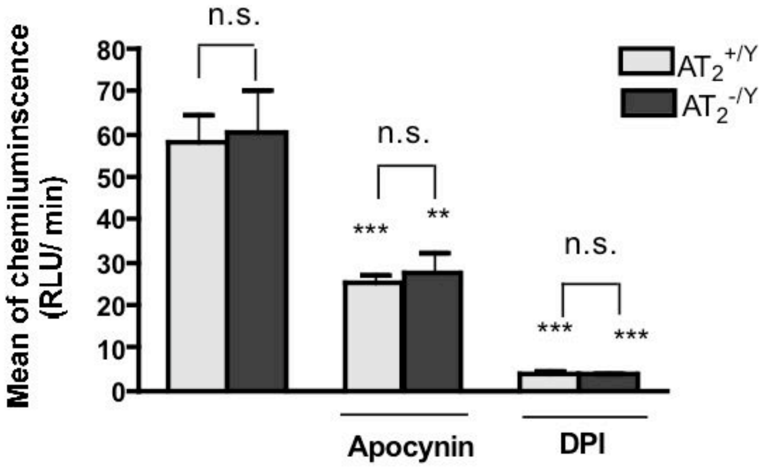

Fig. 6.8. The basal $O_2^{\cdot-}$ formation in aortic homogenates of $AT_2^{-/Y}$ and $AT_2^{+/Y}$ mice, detected by lucigenin-enhanced chemiluminescence method. ROS production was determined in the absence and presence of different inhibitors to $O_2^{\cdot-}$-generating enzymes in aortic membrane fractions of $AT_2^{-/Y}$ and $AT_2^{+/Y}$ mice. ROS levels are reported as RLU. Values represent means of RLU ± SEM of 7 experiments (*P* < 0.01, *** *P* < 0.001 indicate significant differences between $AT_2^{-/Y}$ and $AT_2^{+/Y}$ mice in the absence and presence apocynin and DPI, respectively; ANOVA-test).**

6.3. Targeted deletion of AT_{1A} receptors and nitrosative stress

The interaction between endothelium-derived NO and $O_2^{\cdot-}$ may lead to highly reactive intermediates such as peroxynitrite ($ONOO^{-}$) [171]. Protein tyrosine nitration (3NT) and increased vasoconstrictor tone are biochemical and functional indicators of the so-called endothelial dysfunction. To examine whether the alteration in Nox1 and Nox4 expression levels was reflected in the protein nitration in vascular tissues, 3NT immunoreactivity was assessed in aortic homogenates of $AT_{1A}^{-/-}$ mice with respect to their wt mice. Interestingly, in aorta of $AT_{1A}^{-/-}$ mice, the reduced expression level in Nox1 and Nox4 was associated with a subsequent decrease in 3NT contents compared to that in $AT_{1A}^{+/+}$ mice (44.5 ± 7.3% of $AT_{1A}^{+/+}$ mice, * *P* < 0.05) (Fig. 6.9.).

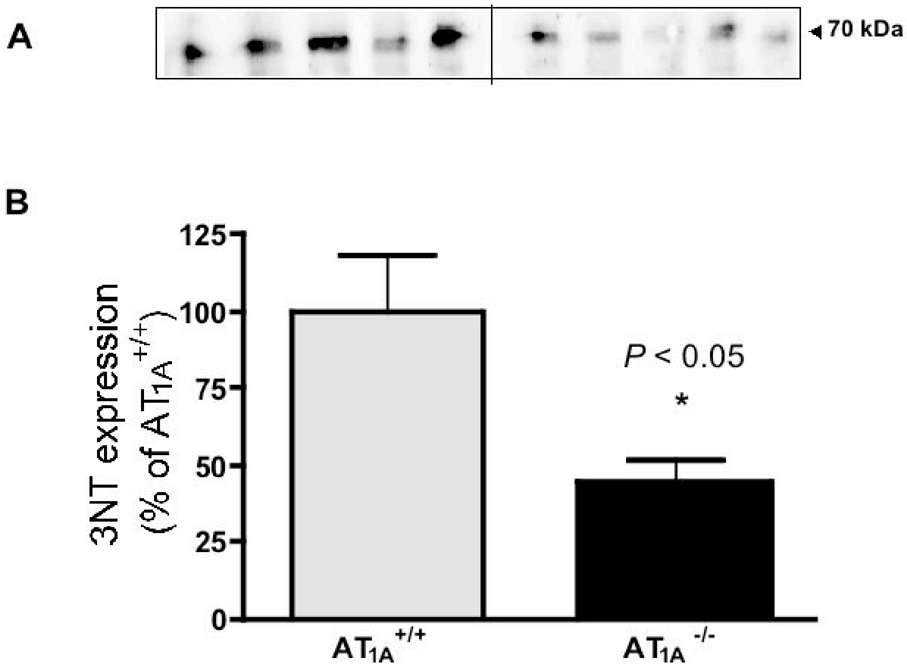

Fig. 6.9. Nitrotyrosine immunoreactivity in aortic homogenates of $AT_{1A}^{+/+}$ and $AT_{1A}^{-/-}$ mice. A single immunoreactive band was detected in protein extract from aortic homogenates of $AT_{1A}^{-/-}$ and $AT_{1A}^{+/+}$ mice. A. Representative immunoblot of the 3NT abundance in aortic homogenates of $AT_{1A}^{-/-}$ and $AT_{1A}^{+/+}$ mice. B. Densitometric analysis of 3NT immunoblot in aorta of $AT_{1A}^{-/-}$ mice, expressed as % of the $AT_{1A}^{+/+}$ mice, demonstrating that 3NT immunoreactivity was markedly reduced in aorta of $AT_{1A}^{-/-}$ mice *versus* $AT_{1A}^{+/+.}$ Data represent means ± SEM of n=5 experiments (* P < 0.05; Student 's unpaired t-test).

6.4. Effect of the targeted deletion of AT_{1A} or AT_2 receptors on the expression levels of eNOS

Several studies have demonstrated the importance of the aortic Ang II receptors-bradykinin-NO-cGMP vasodilator cascade under normal conditions [172]. Previously, Ang II has been found to stimulate an increase in cellular NO level or cGMP content in mouse aorta via activation of AT_2 receptors [19]. However, a potential contribution of AT_1 receptors to Ang II-aortic cGMP signaling has been recently suggested [172]. In the present study, we examined the specific Ang II receptor subtypes AT_{1A} and AT_2 that may contribute to regulation of eNOS expression (as a target for the NO-cGMP pathway) under physiological conditions. Western blot analysis showed that aortic homogenates of $AT_2^{-/Y}$ mice exhibited a significant decrease in the eNOS expression level to the one-half of that in $AT_2^{+/Y}$

mice (Fig. 6.10.). However, aortic tissues of $AT_{1A}^{-/-}$ mice showed insignificant changes in eNOS expression compared to that in $AT_{1A}^{+/+}$ mice (Fig. 6.11.).

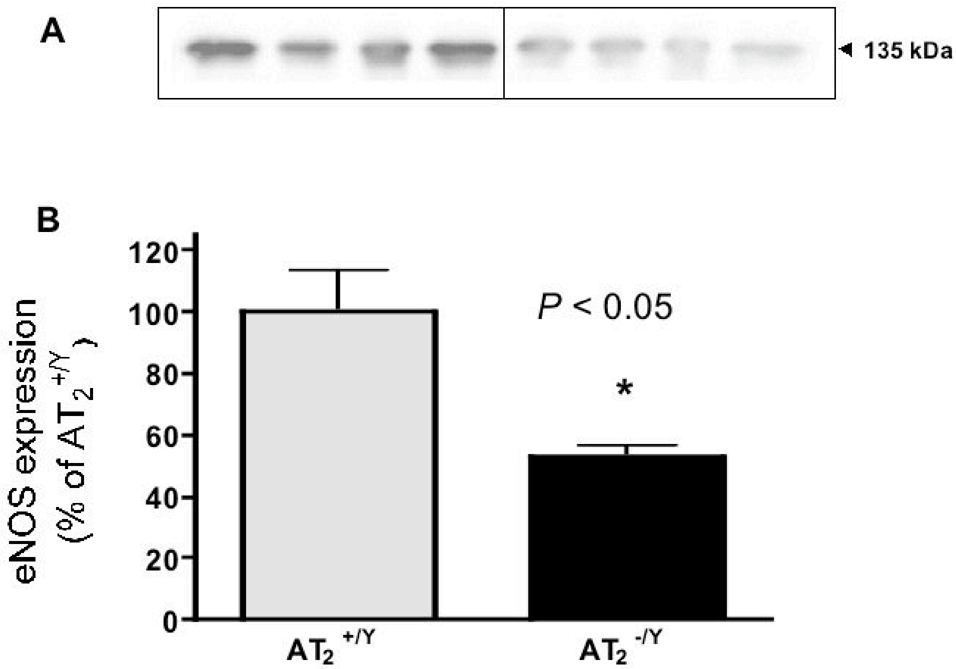

Fig. 6.10. Expression of eNOS in aortic homogenates of $AT_2^{-/Y}$ and $AT_2^{+/Y}$ mice. A. Representative immunoblot of eNOS expression in the aorta from $AT_2^{-/Y}$ and $AT_2^{+/Y}$ mice. B. Quantitative densitometry analysis of eNOS expression in aorta of $AT_2^{-/Y}$ mice, expressed as % of $AT_2^{+/Y}$ mice. As shown, in the aorta of $AT_2^{-/Y}$ mice, eNOS expression was significantly decreased to the one-half of that in $AT_2^{+/Y}$ (52.8 ± 3.2% of wt). Data represent means ± SEM of 4 experiments (* P < 0.05; Student 's unpaired t-test).

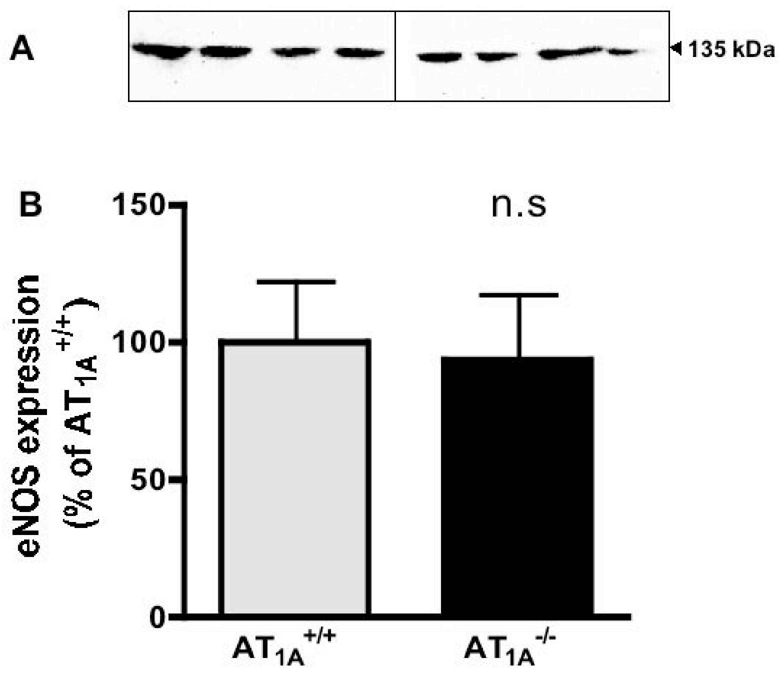

Fig. 6.11. Expression of eNOS in aortic homogenates of $AT_{1A}^{+/+}$ and $AT_{1A}^{-/-}$ mice. A. Representative immunoblot of eNOS expression in the aorta from $AT_{1A}^{-/-}$ and $AT_{1A}^{+/+}$ mice. B. Quantitative densitometry analysis of eNOS expression in the aorta of $AT_{1A}^{-/-}$ mice, expressed as % of $AT_2^{+/Y}$ mice. Data represent means ± SEM of 4 experiments. As shown, the aorta of $AT_{1A}^{-/-}$ mice exerted insignificant differences in eNOS expression compared to that in $AT_{1A}^{+/+}$ mice.

In the lung of $AT_2^{-/Y}$ mice, Western blotting analysis revealed that eNOS expression level was significantly downregulated to 50.4 ± 2.5% of that in $AT_2^{+/Y}$ mice ($P < 0.01$)(Fig. 6.12.).

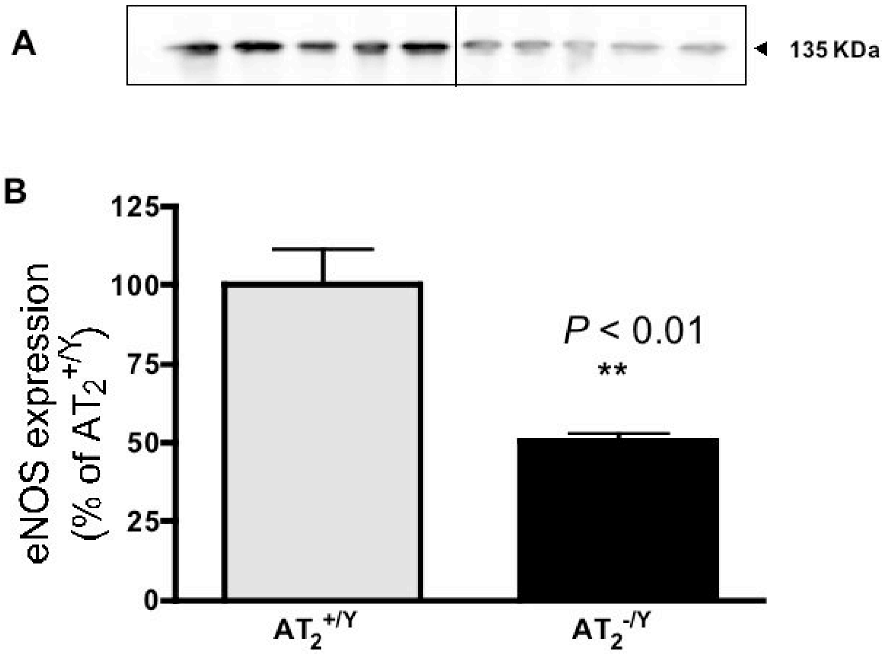

Fig. 6.12. Expression of eNOS in lung homogenates of $AT_2^{-/Y}$ and $AT_2^{+/Y}$ mice. A. Representative immunoblot of eNOS expression in the lung of $AT_2^{-/Y}$ and $AT_2^{+/Y}$ mice. B. Quantitative densitometry analysis of eNOS expression in the aorta of $AT_2^{-/Y}$ mice, expressed as % of $AT_2^{+/Y}$ mice. As shown, in the lung of $AT_2^{-/Y}$ mice, eNOS expression level was markedly decreased to the one-half of that in $AT_2^{+/Y}$mice. Data represent means ± SEM of 5 experiments (*P* < 0.01; Student 's unpaired t-test).**

6.5. Effect of the targeted disruption of AT_{1A} or AT_2 receptors on the expression of sGC subunits (α_1 and β_1)

sGC is expressed in the cytoplasm of almost all mammalian cells. This heterodimeric enzyme consists of α and β subunits, and both are required for the catalytic activity. Structural analysis of sGC in different tissues indicates multiple isotypes with different subunit compositions. In blood vessels, the most abundant subunits are α_1 and β_1.

In the present study,we tried to characterize the molecular regulation of sGC by AT_{1A} and AT_2 receptors under basal conditions using mice deficient in AT_{1A} or AT_2 receptors as appropriate approach for this. In the aorta from $AT_{1A}^{-/-}$ mice, Western blotting data revealed that gene-targeted deletion of the AT_{1A} receptors did not significantly alter the expression level of either sGCα_1 (Fig. 6.13.) or β_1 (Fig. 6.14.) subunit compared to that in $AT_{1A}^{+/+}$ mice.

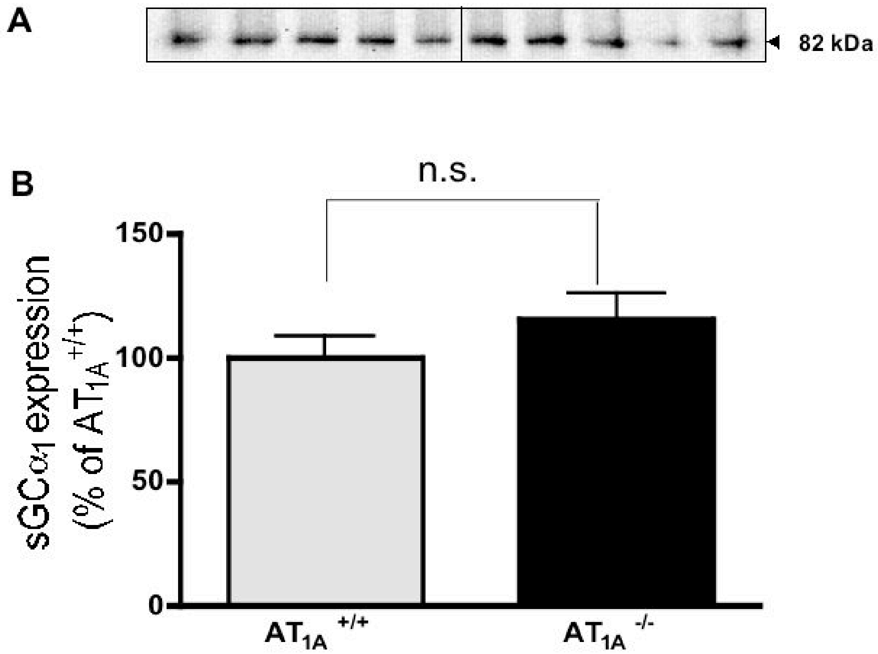

Fig. 6.13. Expression of $sGC\alpha_1$ subunit in aortic homogenates of $AT_{1A}^{-/-}$ and $AT_{1A}^{+/+}$ mice. A. Representative immunoblot of the $sGC\alpha_1$ expression in aortic homogenates of $AT_{1A}^{-/-}$ and $AT_{1A}^{+/+}$ mice. B. Densitometric analysis of $sGC\alpha_1$ immunoblot in aorta from $AT_{1A}^{-/-}$ mice, expressed as % of $AT_{1A}^{+/+}$ mice. As shown, in the aorta of $AT_{1A}^{-/-}$ mice, $sGC\alpha_1$ expression level did not significantly differ from that in $AT_{1A}^{+/+}$ mice. Data represent means ± SEM of n=5 experiments.

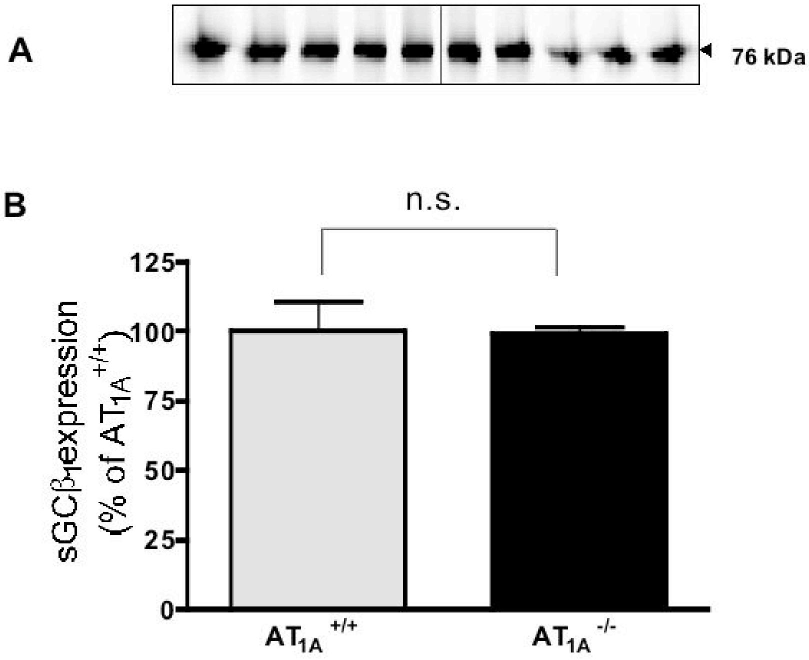

Fig. 6.14. Expression of sGCβ$_1$ subunit in aortic homogenates of $AT_{1A}^{-/-}$ and $AT_{1A}^{+/+}$ mice. A. Representative immunoblot of sGCβ$_1$ expression in aortic homogenates of $AT_{1A}^{-/-}$ and $AT_{1A}^{+/+}$ mice. B. Densitometric analysis of the sGCβ$_1$ immunoblot in aorta of $AT_{1A}^{-/-}$ mice, expressed as % of $AT_{1A}^{+/+}$ mice. As shown, the sGCβ$_1$ expression was not significantly different from that in $AT_{1A}^{+/+}$ mice. Data represent means ± SEM of n=5 experiments.

It is noteworthy that in aortic homogenates of $AT_2^{-/Y}$ mice, the expression levels of sGC (α$_1$ and β$_1$) were markedly lower than that in $AT_2^{+/Y}$ mice (60.3 ± 8.7% and 62.3 ± 4.8 % of $AT_2^{+/Y}$ mice, respectively) (Fig. 6.15.).

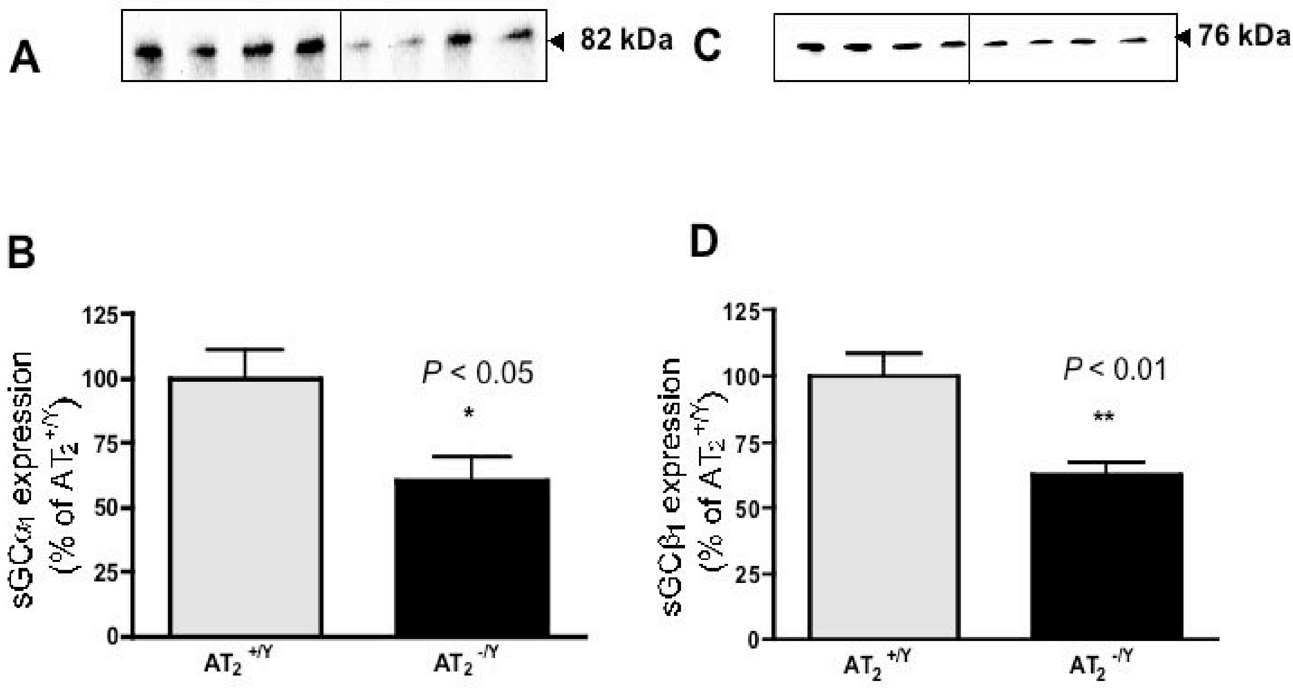

Fig. 6.15. Expression of sGC subunits (α_1 and β_1) in aortic homogenates of $AT_2^{-/Y}$ and $AT_2^{+/Y}$ mice. A. & C. Representative immunoblots of sGCα_1 and β_1 subunits, respectively in aortic homogenates of $AT_2^{-/Y}$ and $AT_2^{+/Y}$ mice. B. & D. Summarized data for quantitative densitometry analysis of sGCα_1 and β_1 expression, respectively in aortic homogenates of $AT_2^{-/Y}$ mice are expressed as % of $AT_2^{+/Y}$ mice. In the aorta from $AT_2^{-/Y}$ mice results demonstrate a significant reduction in the expression of sGCα_1 and β_1 subunits by about 40% and 38%, respectively compared to that in $AT_2^{+/Y}$ mice. Data represent means ± SEM of 5 experiments; at * P < 0.05 and ** P < 0.01 (Student 's unpaired t-test).

In addition, we have also investigated the protein expression of sGC subunits (α_1 and β_1) in the lung of $AT_2^{-/Y}$ mice. The most important observation was the dramatic reduction in the sGCβ_1 subunit expression nearly to the one-third of that in $AT_2^{+/Y}$ mice (32.8 ± 5.3% $AT_2^{+/Y}$ mice, *** $P < 0.001$)(Fig. 6.16.), whereas the sGCα_1 subunit protein expression was decreased to a lesser extent.

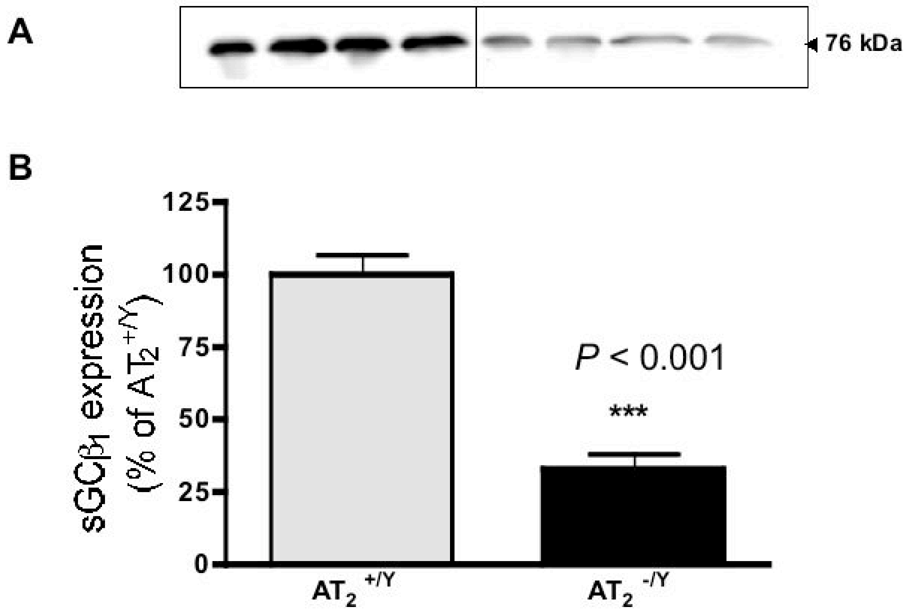

Fig. 6.16. Expression of sGCβ_1 subunit in lung homogenates of AT_2 $^{-/Y}$ and $AT_2^{+/Y}$ mice. A. Representative immunoblot of sGCβ_1 expression in lung homogenates of $AT_2^{-/Y}$ and $AT_2^{+/Y}$ mice. B. Quantitative densitometry of the sGCβ_1 expression level in the lung from $AT_2^{-/Y}$ mice, expressed as % of $AT_2^{+/Y}$ mice. Results show a significant reduction of sGC β_1 expression level in the lung from $AT_2^{-/Y}$ mice *versus* that in $AT_2^{+/Y}$ mice. Data represent means ± SEM of 4 experiments (* $P < 0.001$; Student 's unpaired t-test).**

6.6. Effect of the targeted deletion of AT_{1A} and AT_2 receptors on vascular functions

To examine the functional significance of the decreased NADPH oxidase activity in the aorta of $AT_{1A}^{-/-}$ mice, the endothelium-dependent and independent NO-mediated vasodilatory effects were studied. Using PE-preconstricted aortic rings from $AT_{1A}^{-/-}$ and $AT_{1A}^{+/+}$ mice, we could observe that the maximal response (E_{max}) of ACh-induced endothelium dependent relaxation was significantly enhanced in the aortic rings from AT_{1A} $^{-/-}$ mice *versus* that in $AT_{1A}^{+/+}$ mice (E_{max} in $AT_{1A}^{+/+}$ mice= 55.4 ± 4.1 *versus* 73.3 ± 5.9 in $AT_{1A}^{-/-}$ mice, * $P < 0.05$).

To understand the mechanism(s) behind the differential relaxation, responses to ACh were studied in the absence and presence of apocynin (NADPH oxidase inhibitor) or

SOD (superoxide anion scavenger). The difference in E_{max} of ACh-induced relaxation in aortic rings from $AT_{1A}^{-/-}$ and $AT_{1A}^{+/+}$ mice was abolished after incubation with apocynin (0.1 mM) (Fig. 6.17.), or SOD (250 U/ml) (Fig. 6.18.).

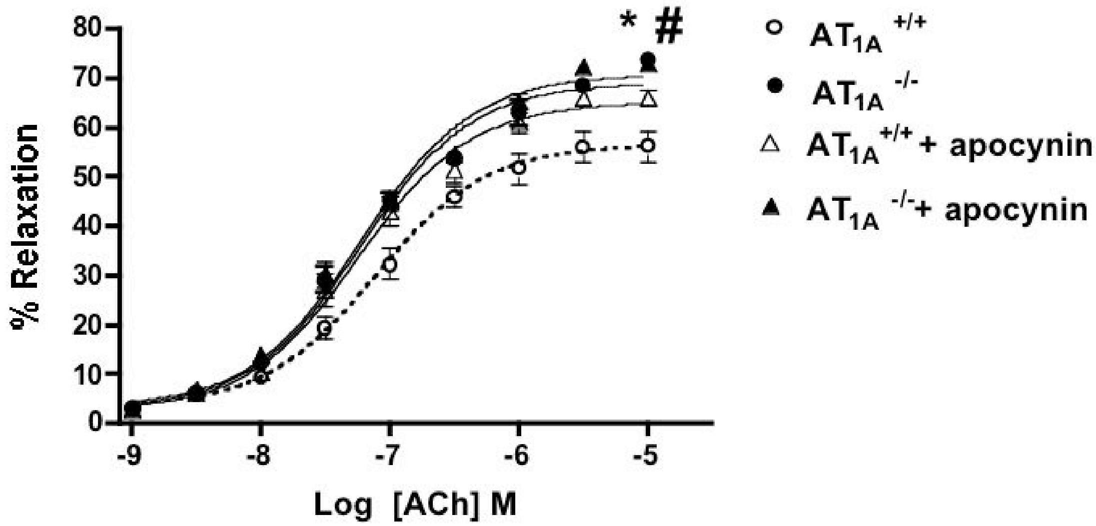

Fig. 6.17. Effect of ACh-mediated mediated endotheium-dependent relaxation on aortic rings in PE-preconstricted aortic rings from $AT_{1A}^{+/+}$ *versus* $AT_{1A}^{-/-}$ mice in the absence and presence of apocynin (0.1 mM). Concentration-response curves showing relaxation responses to ACh in PE-preconstricted aortic rings from $AT_{1A}{}^{+/+}$ *versus* $AT_{1A}{}^{-/-}$ mice as well as the effect of pretreatment with apocynin. Each point is the mean ± SEM of 7 independent experiments. * *P* < 0.05 indicates significant differences in E_{max} of ACh-induced relaxation in aortic rings from $AT_{1A}^{-/-}$ mice compared to that in $AT_{1A}^{+/+}$ mice, and # *P* < 0.05 indicates significant differences in E_{max} of ACh-induced relaxation in aortic rings from $AT_{1A}^{+/+}$ mice before and after treatment with apocynin; ANOVA and Bonferroni 's multiple comparison test.

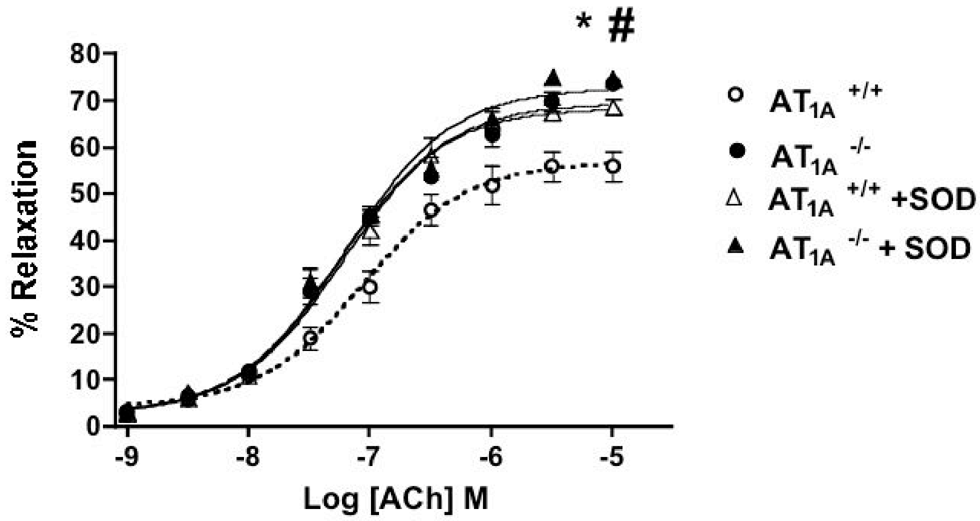

Fig. 6.18. Effect of ACh-mediated endotheium-dependent relaxation on aortic rings in PE-preconstricted aortic rings from $AT_{1A}^{+/+}$ *versus* $AT_{1A}^{-/-}$ mice in the absence and presence of SOD (250 U/ml). Concentration-response curves showing relaxation responses to ACh in PE-preconstricted aortic rings from $AT_{1A}^{+/+}$ *versus* $AT_{1A}^{-/-}$ mice as well as the effect of pretreatment with SOD. Each point is the mean ± SEM of 8 independent experiments. * $P < 0.05$ indicates significant differences in E_{max} of ACh-induced relaxation in aortic rings from $AT_{1A}^{-/-}$ mice compared to the $AT_{1A}^{+/+}$ mice, and # $P < 0.05$ indicates significant differences in E_{max} of ACh-induced relaxation in aortic rings from $AT_{1A}^{+/+}$ mice before and after treatment with SOD; ANOVA and Bonferroni 's multiple comparison test.

In aortic rings from $AT_{1A}^{-/-}$ mice, however, spermine NONOate-mediated endothelium-independent vasodilatation did not significantly differ from that of $AT_{1A}^{+/+}$ mice (Fig. 6.19.).

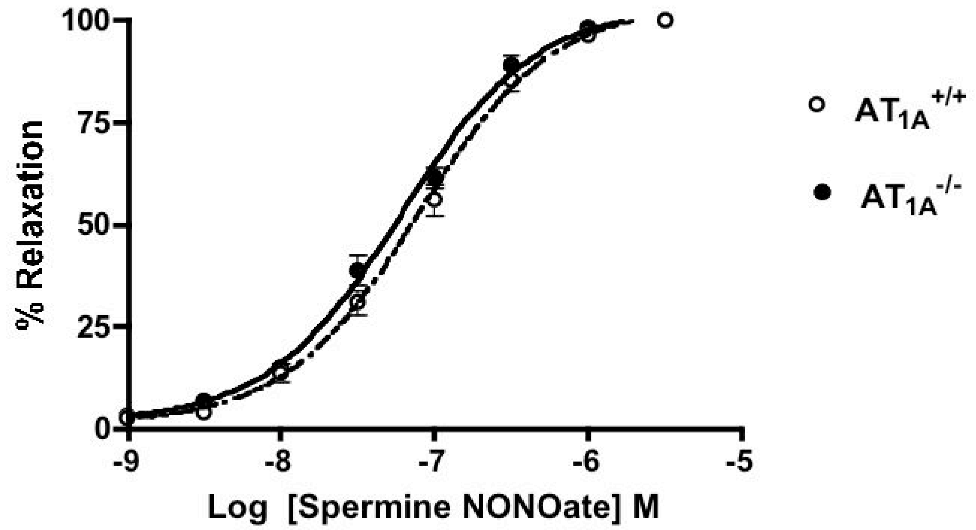

Fig. 6.19. Concentration-response curves of spermine NONOate-induced endothelium-independent relaxation in PE-preconstricted aortic rings of $AT_{1A}^{+/+}$ and $AT_{1A}^{-/-}$ mice. As shown, the relaxation responses in aortic rings of $AT_{1A}^{-/-}$ mice did not significantly differ from that of $AT_{1A}^{+/+}$ mice. Each point is the mean ± SEM of 6 independent experiments.

On the other hand, the role of AT_2 receptors in the regulation of vascular tone was analysed in several studies [14, 18, 173]. However, the underlying signaling mechanism of AT_2 receptors-mediated vasodilatation under physiological condition is not clearly defined. Accordingly, the present study was designed to investigate the relaxation responses to ACh (endothelium-dependent vasodilator) and the NO donor, sermine NONOate (endothelium-independent vasodilator) in PE-preconstricted aortic rings from $AT_2^{-/Y}$ mice. In comparison to aortic rings of $AT_2^{+/Y}$ mice, we observed a significant reduced sensitivity (affinity) to ACh as well as spermine NONOate-induced relaxations in aortic rings of $AT_2^{-/Y}$ mice. This was evidenced by a significant increase in pD2 (-log EC_{50}) value of ACh-mediated relaxation response curves pD2; 7.28 ± 0.06 in $AT_2^{-/Y}$ mice *versus* 7.68 ± 0.04 in $AT_2^{+/Y}$ mice; *** $P < 0.001$) (Fig. 6.20) and pD2 value of spermine NONOate (pD2; 6.74 ± 0.06 in $AT_2^{-/Y}$ mice *versus* 7.16 ± 0.04 in $AT_2^{+/Y}$ mice; ** $P < 0.01$)(Fig. 6.21).

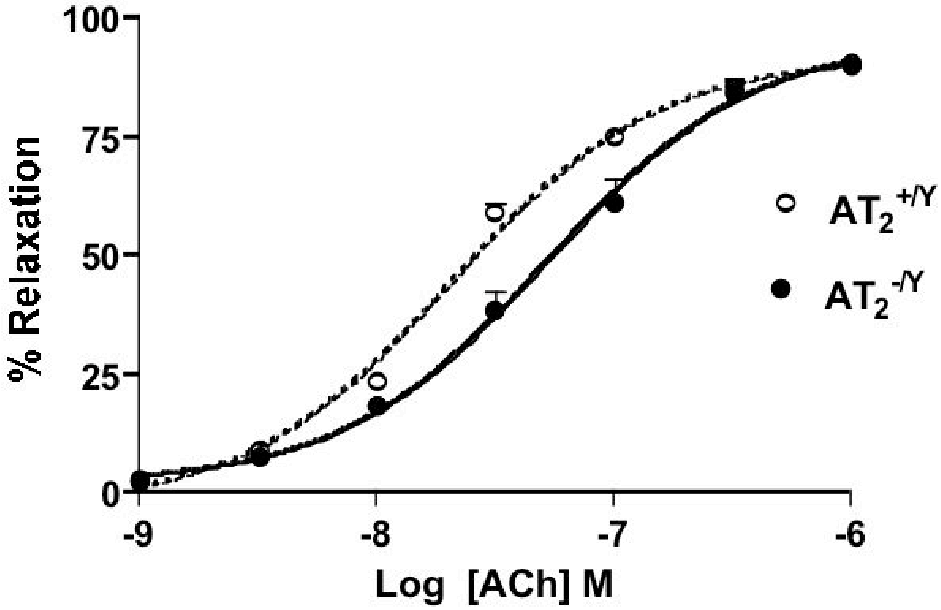

Fig. 6.20. Concentration-response curves of ACh-mediated endothelium-dependent relaxation in aortic rings of $AT_2^{+/Y}$ and $AT_2^{-/Y}$ mice. Results show a significant rightward shift of ACh concentration response curve in aortic rings from $AT_2^{-/Y}$ mice compared to that in $AT_2^{+/Y}$ mice (pD2; 7.28 ± 0.06 in $AT_2^{-/Y}$ *versus* 7.68 ± 0.04 in $AT_2^{+/Y}$ mice, *** $P < 0.001$). Each point is the mean ± SEM of 7 independent experiments.

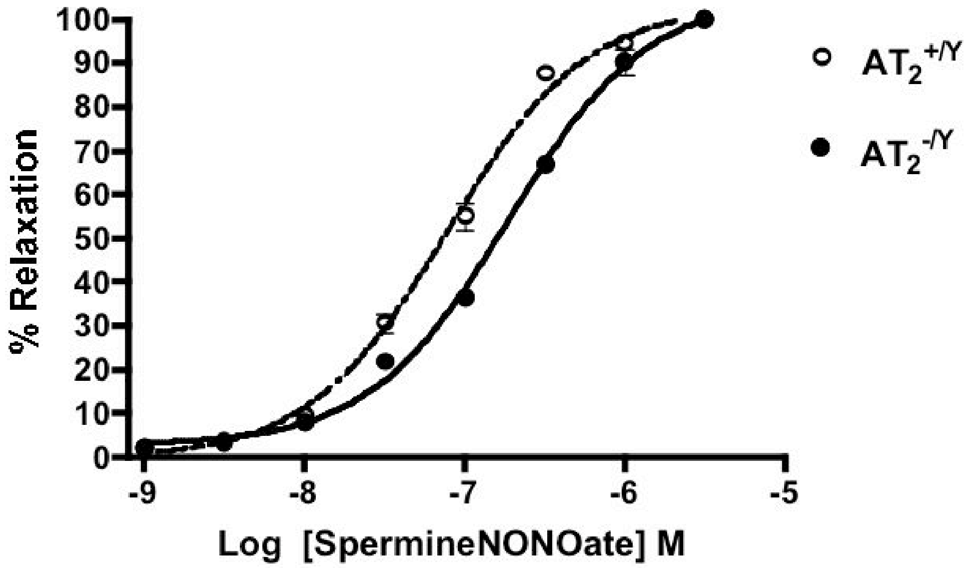

Fig. 6.21. Concentration-response curves of endothelium-independent relaxation to spermine NONOate on PE-preconstricted aortic rings from $AT_2^{+/Y}$ and $AT_2^{-/Y}$ mice. Results show a significant rightward shift of spermine NONOate concentration response curve in aortic rings of $AT_2^{-/Y}$ mice compared to that in $AT_2^{+/Y}$ mice (pD2; 6.74 ± 0.06 in $AT_2^{-/Y}$ mice *versus* 7.16 ± 0.04 in $AT_2^{+/Y}$ mice; ** *P* < 0.01). Each point is the mean ± SEM of 7 independent experiments.

Concerning the functional data in the lung of $AT_2^{-/Y}$ mice, we have found that the basal arterial pulmonary pressure was significantly higher than that of $AT_2^{+/Y}$ mice (6.7 ± 0.2 in $AT_2^{+/Y}$ mice *versus* 7.7 ± 0.13 in $AT_2^{-/Y}$ mice mmHg, $P < 0.13$, n = 4 experiments)(Fig. 6.22.).

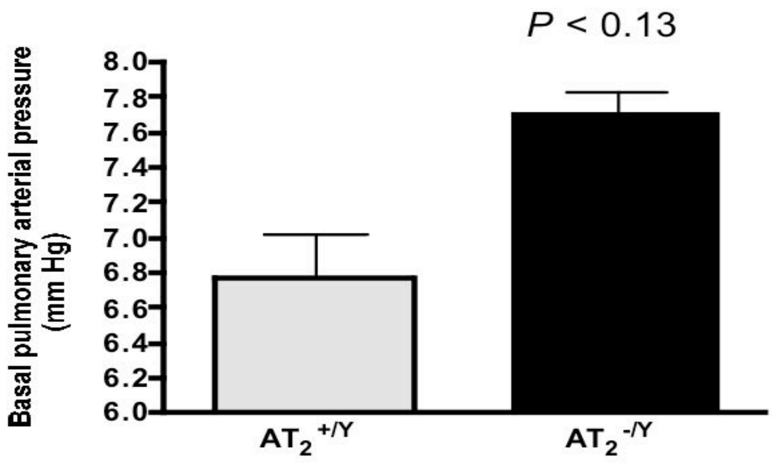

Fig. 6.22. The basal pulmonary artery pressure in the isolated buffer-perfused and ventilated lung of $AT_2^{-/Y}$ and $AT_2^{+/Y}$ mice. The baseline Pulmonary artery pressure was markedly increased in $AT_2^{-/Y}$ mice *versus* $AT_2^{+/Y}$ mice. Data represent means ± SEM of 4 independent experiments; at *P* < 0. 13 (Student 's unpaired t-test).

7. Discussion

7.1. Nox1 and Nox4 expression in $AT_{1A}^{-/-}$ and $AT_2^{-/Y}$ mice

Ang II plays an important role in regulating cardiovascular functions in health and disease. So far, most of the actions induced by Ang II are attributed to the AT_1 receptors, because AT_1 receptors expression seems to be necessary for these effects. For example, AT_1 receptors are downregulated by Ang II and growth factors diminishing the effects of Ang II on intracellular signaling [174-176]. In mouse and rat, two subtypes of the AT_1 receptor, AT_{1A} and AT_{1B} have been identified [3]. An increasing body of evidence supports the hypothesis that the AT_{1A} receptors are responsible for most of the physiological actions of Ang II. In particular, AT_{1A} receptors are much more expressed in vasculature and cardiac tissues than AT_{1B} receptors [177, 178]. The $AT_{1A}^{-/-}$ mouse model was originally developed by Coffman *et al.* (1995) [26] and has been previously used to examine putative differences in the function of AT_{1A} and AT_{1B} receptors [179]. These mice have lower blood pressure compared to that in wt littermates, and the pressor response to Ang II infusion was absent [26]. In addition, gene-targeting of the AT_{1A} receptor results in alteration in renal function and salt sensitivity [180]. In contrast, AT_{1B} receptor-deficient mice have normal basal blood pressure and only a few phenotypic changes have been observed [28]. Thus, the comparison between both knockout models supports the hypothesis that the AT_{1A} receptor plays the primary role in regulation of renal and cardiovascular functions.

It is currently well established that Ang II induces intracellular formation of ROS in the vasculature and NADPH oxidase system is a major source for Ang II induced ROS production. A number of Nox homologise including Nox1, 4, and 2, have been identified in vascular cells [87, 101, 181], with endothelial cells expressing very low levels of Nox1, intermediate levels of Nox2, and abundant Nox4 mRNA [83, 181]. In contrast, VSMCs express predominantly Nox4 [87, 99] and to a lesser extent Nox1 [87, 101], with negligible amounts of Nox2. NADPH oxidase-mediated $O_2^{\cdot -}$ production is increased in vessels of rabbits with experimental atherosclerosis [120]. These abnormalities were corrected by AT_1 receptor blockade [120]. Further, it was demonstrated that losartan treatment decreases the p22phox mRNA expression and NADPH oxidase activity in cultured VSMCs stimulated by Ang II [137, 143]. Thus, AT_1 receptor seems to predominately contribute to $O_2^{\cdot-}$ production via NADPH oxidase in vasculature. Studies examining vascular expression of NADPH oxidase subunits revealed that Ang II infusion upregulates Nox1 and Nox4 mRNA expression levels in rat aorta [57]. Previously, our group has shown that Nox4 mRNA expression was significantly increased in rats made hypertensive by overexpression of the human renin gene [87] or infusion of Ang II for 7 days [57]. Although several studies have shown that Ang II increases the generation of $O_2^{\cdot-}$ in cultured endothelial [182, 183] and VSMCs [89], there is a disagreement regarding the receptor subtypes (AT_1 or AT_2) involved in NADPH oxidase-mediated $O_2^{\cdot-}$ production *in vitro* [182, 183]. Moreover, which of the Nox isoforms functionally couple to Ang II receptors under physiological conditions is not known. Thus, identification of the protein regulation of these NADPH oxidase isoforms by Ang II receptors (AT_{1A} and AT_2) under physiological conditions is a prerequisite to target specific cellular events contributing to a pathological state. We herewith show using AT_{1A} receptor gene targeting mice, that aortic tissues of $AT_{1A}^{-/-}$ mice exhibited a marked downregulation of Nox1 and Nox4 expression *versus* that of $AT_{1A}^{+/+}$ mice. These findings support *in vivo* findings regarding the involvement of the supraphysiological levels of Ang II [87] [57] in regulation of Nox1 and Nox4. Our present data also confirm our previous *in vitro* results concerning the involvement of Ang II in regulating Nox1 and Nox4 mRNA levels in VSMCs [87].

Several studies provide evidence that Ang II receptors differentially modulate endothelial superoxide anion formation. While AT_1 receptor activates $O_2^{\cdot-}$ formation, AT_2 receptor attenuates this AT_1 receptor-induced effect [183]. Recently, Rueckschloss *et al.* (2002) [141] have shown a dose-dependent regulation of endothelial NADPH oxidase by Ang II. They have observed that induction of gp91phox expression is mediated by AT_1 receptors, whereas AT_2 receptors stimulation causes its partial inhibition [141]. In Ang II-infused rat kidney, it has been shown that AT_1 receptor antagonists decrease mRNA expression levels of both p22phox and Nox1 [184], whereas blockade of AT_2 receptors intensifies the effect of Ang II-induced increase in mRNA expression of these subunits, suggesting a countervailing effect of AT_1 and AT_2 receptors [184]. Nevertheless, the potential role of AT_2 receptor in expressional regulation of NADPH oxidase under physiological conditions remains to be clarified. To our surprise, in aorta of $AT_2^{-/Y}$ mice, although Nox1 expression exhibited a significant reduction, Nox4 expression remained unchanged compared to that in $AT_2^{+/Y}$ mice. To confirm this observation, we measured the activity of the NADPH oxidase in the aorta of these animals.

On the other hand, the importance of NADPH oxidase-derived ROS in lung function and signaling events of the pulmonary arterial smooth muscle cells has been reported in several studies [92, 169, 185]. Recently, it has been suggested that among these oxidases, Nox4 plays an important role not only in mitogenesis of these cells, but also in oxygen sensing [186]. Furthermore, it has been demonstrated that Ang II receptors (AT_1 and AT_2) have a potential role in modulation of the pulmonary vascular tone [187]. The current study provides evidence for a molecular regulation of Nox4 by AT_{1A} and AT_2 receptors. In the lung from $AT_2^{-/Y}$ mice, we observed that Nox4 expression level exhibited was dramatically upregulated compared to that in $AT_2^{+/Y}$ animals. However, the lung of $AT_{1A}^{-/-}$ mice could not show significant differences in the expression level of Nox4 compared to that in $AT_{1A}^{+/+}$ mice. These findings suggest that AT_2 receptors rather than AT_1 receptors probably contribute to regulation of Nox4 protein expression in the lung.

7.2. Effect of the targeted deletion of AT_{1A} or AT_2 receptors on the NADPH activity

Previously, it has been shown that NADPH oxidase is involved in vascular $O_2^{\cdot-}$ generation under normal conditions [92], and it is well known that Ang II activates NADPH oxidase in the vasculature [89, 136]. NADPH oxidase–mediated $O_2^{\cdot-}$ production was increased in vessels of rabbits with experimental atherosclerosis [120]. These abnormalities were corrected by AT_1 receptors blockade [120]. However, it has been recently shown that both of the Ang II receptors (AT_1 and AT_2) could induce NADPH oxidase-dependent $O_2^{\cdot-}$ formation [188]. Thus, it was necessary to identify the Ang II receptor subtypes that might predominantly contribute to the NADPH oxidase activity under physiological conditions. In addition, to examine whether the regulation of Nox1 and Nox4 by endogenous Ang II was limited to its expression or was also involved with its activity, we measured basal ROS production by lucigenin-enhanced chemiluminescence in aortic homogenates from $AT_{1A}^{-/-}$ and $AT_2^{-/Y}$ mice.

Validation of lucigenin experiments

Majority of data, regarding $O_2^{\cdot-}$ formation in vessel homogenates, are based on the measurement of the intensity of lucigenin-enhanced chemiluminescence [136, 189]. The validity of these data was recently questioned, because lucigenin at high concentrations itself increases formation of $O_2^{\cdot-}$ in the presence of flavin-containing enzymes such as NO synthase and xanthine oxidase [65, 190] that are capable of providing one-electron reduction of lucigenin. Hence, to avoid false-positive signals or redox cycling, we performed our experiments using low concentrations of lucigenin (5 μM) [191]. In our experiments, we used the particulate fractions that contain mainly membranes and microsomes [136].

Concurrent to our expression data in the aorta of $AT_{1A}^{-/-}$ mice, the basal NADPH oxidase activity was significantly lower in aorta of $AT_{1A}^{-/-}$ mice *versus* $AT_{1A}^{+/+}$, indicating that aorta of $AT_{1A}^{-/-}$ mice contains less active, membrane-associated NADPH oxidase compared to that in $AT_{1A}^{+/+}$ mice. The signal was completely blocked by DPI (non-specific flavin binding NADPH oxidase inhibitor), and partially blocked by apocynin (more specific NADPH oxidase inhibitor). Of particular interest, the absolute apocynin inhibitable signal (which exclusively represents the Nox activity) was higher in $AT_{1A}^{+/+}$ mice compared to $AT_{1A}^{-/-}$ mice. This signal was unaffected by inhibitors of other potential $O_2^{\cdot-}$-generating enzymes, such as L-NAME (uncoupled NOS) or oxypurinol (xanthine oxidase). The lack of effects of L-NAME and oxypurinol suggests that the uncoupled-eNOS or xanthine oxidase enzyme, respectively were not involved in the difference of the basal $O_2^{\cdot-}$ formation in aorta from $AT_{1A}^{+/+}$ *versus* $AT_{1A}^{-/-}$ mice. Supporting this, we did not any significant alterations in the eNOS expression levels in aorta from $AT_{1A}^{-/-}$ mice compared to that in $AT_{1A}^{+/+}$ mice. Based on these observations, we propose that NADPH oxidase enzyme is responsible for the majority of basal $O_2^{\cdot-}$ formation, which can be mediated via AT_{1A} receptor. Further, in the absence of substrate (NADPH) or when NADPH was substituted with NADH, the $O_2^{\cdot-}$ production was undetectable. The observation of enhanced $O_2^{\cdot-}$ production in mouse aortic homogenates on supplementation with NADPH and not NADH, suggests that in our hands the enzyme in aortic homogenate seems to be

NADPH oxidase and not NADH oxidase as reported by some groups [191, 192]. Together, these findings are in a good agreement with a very recent study [179], supporting the activation of AT_{1A} receptor being associated with oxidative stress in the mouse vasculature. These results support previous reports, showing that AT_1 receptor antagonists block the Ang II-induced $O_2^{\cdot-}$ formation in endothelial cells [182, 193], VSMCs [89], and intact aortic segments [120, 194]. Overall, these findings provide an important physiological relevance of AT_{1A} receptors in regulation of the expression of NADPH oxidase but also its activity.

On the other hand, the role of AT_2 receptors in the *in vitro* regulation of NADPH oxidase enzyme has been analyzed in several studies [182, 183] [89]. Furthermore, in fibroblasts and endothelial cells, concomitant application of AT_2 receptor antagonists further augmented Ang II-induced NADPH oxidase activity [98, 141]. Nevertheless, the physiological relevance of AT_2 receptor in NADPH oxidase activity *in vivo* under physiological condition is unknown. In addition, it was necessary to examine whether the reduced expression of Nox1 in aortic tissues of $AT_2^{-/Y}$ mice can affect on the activity of the oxidase enzyme. Hence, we estimated NADPH-dependent $O_2^{\cdot-}$ formation in aortic homogenates of $AT_2^{-/Y}$ and $AT_2^{+/Y}$ mice. Surprisingly, gene-targeted deletion of the AT_2 receptor resulted in insignificant alterations in NADPH oxidase activity (as evidence by apocynin inhibitable ROS formation) in aortic tissues from $AT_2^{-/Y}$ mice compared to that in $AT_2^{+/Y}$ mice. Hence, we suggest that AT_2 receptors may not be involved in the regulation of NADPH oxidase activity in aorta under physiological conditions.

7.3. Protein nitration as a biochemical marker of nitrosative stress

It has been demonstrated that the biological activities of NO are highly dependent on both anabolic and catabolic-related pathways [195]. A chemical pathway of biological importance seems to be the formation of peroxynitrite ($ONOO^-$) via the interaction of NO with $O_2^{\cdot-}$, leading to reduction of NO levels and formation of highly reactive oxidants *in vivo* [171, 196]. $ONOO^-$ and related species aggressively nitrate protein tyrosine residues, leading to the chemically stable biomarker 3NT [197]. The formation of 3NT containing proteins has been observed in some diseases such as inflammatory disorders [198], sepsis-related organ failure [199], and renal transplant rejection [200]. In addition, recent studies have shown that oxidative stress due to Ang II infusion results in an extensive tyrosine nitration of proteins in the vascular endothelium, which correlated with the extent of endothelial dysfunction and this was probably associated with increased production of $ONOO^-$ [201] [90]. Thus, 3NT immunoreactivity is considered to be a marker of concomitant formation of NO and ROS and can be detected by Western blot analysis. On the basis of these considerations, it was of interest to examine the protein nitration, which could be used as a biochemical marker to nitrosative stress. In addition, the relative contribution of AT_{1A} receptor to $ONOO^-$-induced nitrosative stress awaits elucidation.

Interestingly, and as an additional evidence for the decreased basal $O_2^{\cdot-}$ level in aortic tissues of $AT_{1A}^{-/-}$ mice, we found that 3NT contents were significantly decreased in the aorta of $AT_{1A}^{-/-}$ mice compared to that in $AT_{1A}^{+/+}$ mice. In addition, the reduced 3NT immunoreactivity was also correlated with the decrease in Nox1 and Nox4 expression levels, demonstrating a crucial role of NADPH oxidase in AT_{1A} receptors-induced nitrosative and oxidative stress. In a good agreement with this concept, Wang *et al.* (2002) [202] have demonstrated that the elevation of NADPH oxidase activity and $O_2^{\cdot-}$ production was associated with increased 3NT immunoreactivity in mouse aorta infused by Ang II.

7.4. Effect of the targeted deletion of AT_{1A} or AT_2 receptors on vascular functions

The endothelium plays a key role in the local regulation of the vasomotor tone [203]. Several studies have demonstrated the importance of endothelium-derived factor (EDRF)/NO in both basal and stimulated control of the vascular tone [203]. Several years before EDRF was identified as NO, various group reported that $O_2^{\cdot-}$ has limiting step on EDRF bioactivity [44, 204]. Hence, endothelium plays a crucial role in the regulation of vascular tone by a process catalyzed by NO synthase (NOS), NO and citrulline is formed from the substrates molecular oxygen and L-arginine. The main receptor for NO is guanylyl cyclase, its activation by NO results in formation of smooth muscle cGMP, which in turn contributes to vascular-relaxation. On the other hand, Ang II induced NADPH oxidase-mediated oxidative stress is implicated in endothelial dysfunction associated with many pathological conditions. Supporting this, systemic administration of subpressor dose of Ang II for 3 days was reported to increase peroxynitrite formation and impair the endothelial function [201], further, inhibition of AT_1 receptor activation using AT_1 receptor antagonists or ACE inhibitor improved the endothelial dysfunction [205]. Similar improvements were also observed in microvasculature [206] and in aorta isolated from rats with myocardial infarction, pretreated with AT_1 receptor antagonist [207].

Previously, Ang II was reported to increase cGMP levels, in cultured bovine aortic endothelial cell [208, 209], via an AT_2 receptor-mediated, NO (and presumably sGC)-dependent pathway [208]. However, few reports suggest that Ang II-induced activation of the cellular NO-cGMP pathway may be mediated partially [210], or in some cases, exclusively by AT_1 receptors [209, 211, 212]. To date, these studies have been performed in both, cell culture and isolated vascular preparations, suggesting that AT_1 and AT_2 receptors do not always act in a direct opposition to each other, at least, at NO–cGMP pathway. On the other hand, the specific receptor subtypes of Ang II that may contribute to NO-cGMP pathway under physiological condition remained to be addressed. In the present study, we observed that while eNOS and sGC subunits were downregulated in $AT_2^{-/Y}$ mice, they remained unaffected in $AT_{1A}^{-/-}$ mice. Our results suggest that AT_2 receptors have a direct correlation to NO synthesis and NO-cGMP signaling, while AT_{1A} receptors are devoid this effect. Supporting our findings in aorta from $AT_2^{-/Y}$mice, Tanaka *et al.* (1999) [213] have shown that the AT_2 receptor gene disruption results in a decrease in aortic cGMP content. In contrast, transgenic mice overexpressing AT_2 receptors have a high aortic cGMP content normalized by either NO-synthesis blockade or bradykinin B_2 receptor blockade [19]. Our results are also consistent with the previous reports demonstrating that AT_2 receptors blockade abolished Ang II-induced increased cGMP level in renal interstitial fluid of rats [214] as well as NOS inhibition [215, 216], thereby confirming a direct link between AT_2 receptor activation and subsequent bradykinin synthesis/release. Accordingly, our study provides an interesting fact that AT_2 receptors not only regulate the NO signaling at the eNOS level but also at the NO cyclase receptors sGα_1/β_1.

Recent studies have suggested that AT_2 receptor might oppose actions of the AT_1 receptor with respect to blood pressure and cellular proliferation [217] under pathological conditions [19, 218]. To address weather such a counter-regulatory mechanism exists under physiological conditions and functionally relevant, endothelium-dependent and independent relaxation response in thoracic aorta from AT_{1A} and AT_2 receptors gene targeting mice. Interestingly, the reduction in NADPH oxidase expression or activity in aorta of $AT_{1A}^{-/-}$ mice or the downregulation of eNOS and sGC expression levels were reflected on the increased ACh-induced endothelial-dependent NO mediated vasorelaxation in aorta of $AT_{1A}^{-/-}$ mice and reduced sensitivity to ACh-induced endothelium-dependent relaxation as well as the NO donor spermine NONOate-induced endothelium-independent relaxation aorta from $AT_2^{-/Y}$ mice, respectively. Thus, we suggest the downregulation of eNOS may account for the decreased sensitivity to ACh-induced endothelium dependent vasodilatation, whereas the decreased in sGC expression may explain the reduced sensitivity to spermine NONOate-induced endothelium independent vasodilatation. Our findings concerning spermine NONOate are in agreed with Schrammel *et al.*(1998) [219], indicating that sGC is a major physiological target of NO-donor compounds such as molsidomine. Although the molecular targets of NO are varied [41], the major function of endothelial NO is to activate a sGC in underlying VSMCs, leading to relaxation of the muscles.

Since differences observed in ACh-induced relaxation in aorta of $AT_{1A}^{-/-}$ mice were reverted by apocynin or SOD, we suggest that basal $O_2^{\cdot-}$, produced from NADPH oxidase significantly counters the relaxation process. Hence, we for the first time provide evidence to the counter-regulatory effects of AT_2 and AT_{1A} receptors on vascular tone under physiological conditions and suggest that AT_2 but not AT_{1A} receptors modulate the NO-cGMP pathway under physiological conditions. Thus, reciprocal changes in Nox/GC expression were accommodated by tyrosine nitration and apocynin-sensitive vasomotor activity.

Although we can not directly exclude the possible involvement of Nox1 and Nox2, however the facts that Nox2 is not constitutively active [220, 221], expression of Nox1 and Nox2 being low or negligible in vasculatures [181] and the report suggesting that gp91phox (Nox2) is not essential for modulating vascular tone [220], prompt us to suggest Nox4 as quantitatively the most relevant isoform for Ang II induced $O_2^{\cdot-}$ production under physiological conditions. Supporting this hypothesis, Nox2 protein expression level was not altered in the aorta of $AT_{1A}^{-/-}$ mice compared to that in $AT_{1A}^{+/+}$ mice Therefore, this may raise the possibility that Nox4 is predominantly involved in the functional consequences in aorta of $AT_{1A}^{-/-}$ mice. Supporting this hypothesis, Sorescu *et al*. (2002) [83] reported that Nox4 is abundantly expressed in cultured endothelial cells. More recently, Ago *et al.* (2004) [155] demonstrated that Nox4 is the major catalytic component of NADPH oxidases in endothelial cells. A strong correlation between p22phox / Nox4 expression and NADPH oxidase activity, with endothelial function, in arteries from patients with coronary heart diseases was reported [222]. Furthermore, Nox4 expression level was markedly higher than Nox1 in aortic VSMCs [87, 101].

Concerning the functional relevance of AT_2 receptor in the lung, we observed an elevation in arterial pulmonary pressure in the lung of $AT_2^{-/Y}$ mice compared to that in $AT_2^{+/Y}$ mice. We suggest that decreased protein expressions of sGCβ_1 subunit as well as eNOS a possible explanation for this elevated arterial pulmonary pressure. We exclude a putative role of NADPH oxidase, at least, under physiological conditions, as we could not observe any alteration in the activity of this enzyme in lung homogenates of $AT_2^{-/Y}$ mice compared to that in $AT_2^{+/Y}$ mice (data not shown). Thus, we demonstrate that the protective role of AT_2 receptor in the pulmonary vessels also is mediated via NO-cGMP vasodilator cascade, confirming the recent study from Olson *et al.* (2004) [223]. Accordingly, the AT_2 receptor is indeed linked to the increased eNOS expression as well as NO production in lung tissues. However, the functional significance of AT_2 receptor in the pulmonary vasculature requires more in-depth analysis in the future.

In conclusion, these novel findings provide evidence for the molecular regulation of NADPH oxidase isoforms (Nox1 and Nox4) *in vivo* by physiological Ang II levels. Our observations support the activation of AT_{1A} receptor being associated with oxidative stress via Nox1 and Nox4. In addition, we suggest Nox4 to be the predominant contributor to $O_2^{\cdot-}$ production under physiological Ang II concentrations. Further, this study demonstrates that the Ang II receptor subtypes (AT_{1A} and AT_2) differentially regulate NO signaling pathways and vascular tones. While AT_{1A} receptor–induced Nox4 (or Nox1) expression leading to increased oxidative stress; AT_2 receptor was found to have a protective role not only by increasing eNOS, but also via the upregulation of NO guanylyl cyclase receptors. Thus, our study while supporting the need for specific and selective Nox4 (or Nox1) inhibitors in treating a broad range of cardiovascular complications, highlights the interesting facts that an endogenous ligand (Ang II) having two distinct receptors with opposing functions under physiological conditions, which should be borne in mind while selectively modulating the undesirable physiology for therapeutic benefits.

Overall, these results showed that Ang II exerts countervailing mechanism on the vasculature by AT_{1A} receptor-dependent detrimental oxidative stress and AT_2 receptor-dependent enhanced nitrinergic signaling. Both observations provide a rational for selective interference with Ang II signaling in cardiovascular therapy.

8. Summary

Ang II is a potent vasoconstrictor agent and elicits its physiological effects on the vasculature via two distinct receptors AT_1 and AT_2. Among AT_1 receptors, two subtypes, AT_{1A} and AT_{1B} have been identified in rat and mouse. Recently, NADPH oxidase has been identified as a major enzymatic source of ROS in the vasculature. It is widely accepted that AT_1 receptors are predominantly involved in NADPH–derived ROS formation. However, there is no available information concerning the *in vivo* regulation and functional significance of Nox1 and Nox4 by Ang II under physiological conditions. Therefore, we took advantage of Ang II (AT_{1A} or AT_2) receptors-deficient mice ($AT_{1A}^{-/-}$ and $AT_2^{-/Y}$) as powerful tools to examine the expressional regulation and functional consequences of Nox1 and Nox4 by Ang II (AT_{1A} and AT_2) receptors under these conditions. Besides, we attempted to investigate the functional interplay between Ang II receptors (AT_{1A} and AT_2) and NO signalling pathway.

In the isolated aorta of mice genetically deficient in the AT_{1A} receptor, we observed that Nox1 and Nox4 levels were significantly downregulated *versus* their respective $AT_{1A}^{+/+}$ mice. Functionally, this was associated with attenuated 3NT immunoreactivity (a stable biomarker of nitrosative stress) and the basal activity of NADPH oxidase. Interestingly, this decrease in NADPH-dependent $O_2^{\cdot -}$ production was exclusively reflected in an increased efficacy of ACh-induced endothelium-dependent relaxation. Importantly, the difference in maximal relaxation-induced by ACh between $AT_{1A}^{-/-}$ and $AT_{1A}^{+/+}$ mice was inhibited by either SOD or apocynin, suggesting that indeed NADPH oxidase-derived $O_2^{\cdot -}$ formation is involved. However, Nox2 protein level remained unchanged in the aorta of $AT_{1A}^{-/-}$ and $AT_2^{-/Y}$ mice compared to their respective wt.

Collectively, these findings provide *in vivo* evidence for Nox4 and Nox1-induced oxidative stress as a pathophysiological mechanism of AT_{1A} receptors-impaired endothelium-dependent vasodilatation. Furthermore, based on the fact that Nox4 as being quantitatively the most relevant isoform under physiological conditions, we suggest that this isoform may predominantly contribute to these functional consequences.

Surprisingly, in the aorta of $AT_2^{-/Y}$ mice, there was neither alteration in Nox4 expression nor in NADPH oxidase-dependent $O_2^{\cdot-}$ production compared to that in $AT_2^{+/Y}$ mice. Of interest, the aorta of these mice exhibited a marked downregulation in NO receptor cyclase subunits sGC α_1/β_1 and eNOS protein expression compared that in $AT_2^{+/Y}$ mice. Nevertheless, in the aorta of $AT_{1A}^{-/-}$ mice, the protein expression of α_1/β_1 subunits as well as eNOS protein expression remained unchanged compared to that in $AT_{1A}^{+/+}$ mice. Functionally, the downregulation in NO solubale guanylyl cyclase receptors α_1/β_1 as well as eNOS expression levels was reflected in reduced sensitivity or affinity to ACh as well spermine NONOate–induced endothelium dependent or independent vasodilatation in the aorta of $AT_2^{-/Y}$ mice, respectively.

In conclusion, our data provide, an important evidence for the molecular mechanisms of countervailing effects of AT_{1A} (stimulatory) and AT_2 (inhibitory) receptors on vascular functions by upregulation of Nox4 (or Nox1)-mediated oxidative stress *versus* the NO-sensitive guanylyl cyclase under physiological conditions. Thus, selective AT_1 receptor blockade may be clinically advantageous by inhibiting detrimental ROS formation and simultaneously leaving the beneficial sGC signaling untouched.
A summary of our main findings in the present study is illustrated in Fig. 8.1.

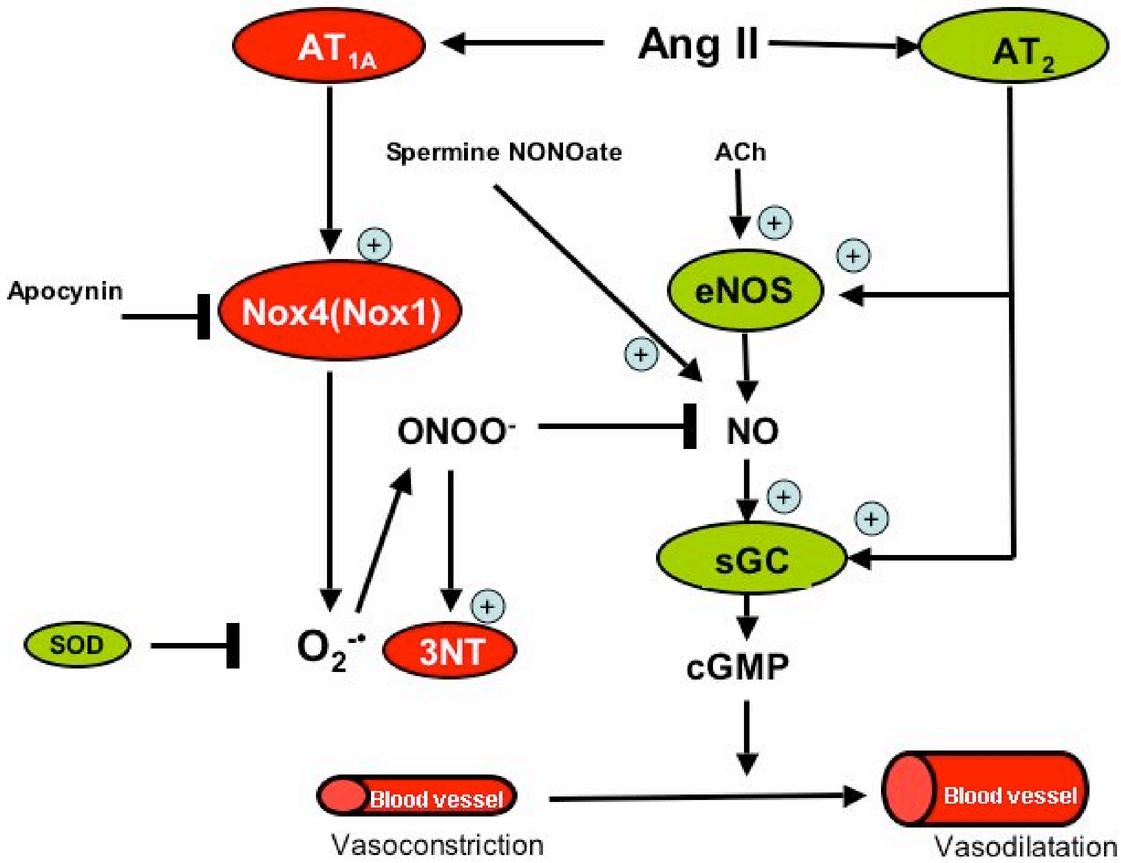

Fig. 8.1. As shown, Ang II exerts countervaing mechanisms on the vasculature by AT_{1A} and AT_2 receptors. Whereas AT_{1A} receptor mediated oxidative stress via upregulation of Nox4 (Nox1) expression, AT_2 receptor is involved in the nitrinergic signaling via increasing the expression of NO receptors soluble guanylyl cyclase as well as eNOS.

9. Zusammenfassung

Angiotensin II (Ang II) ist ein wichtiges vasokonstriktorisches Agens, welches seine physiologischen Effekte über zwei verschiedene Rezeptoren vermittelt: AT_1 und AT_2. In Ratte und Maus sind zwei Subtypen des AT_1 Rezeptors identifiziert worden, namentlich AT_{1A} und AT_{1B}. Unlängst ist die NADPH Oxidase als wichtigste enzymatische Quelle für reaktive Sauerstoffspezies (ROS) beschrieben worden. Dieses Oxidasesystem scheint durch Ang II über die AT_1 Rezeptoren aktiviert zu werden. In der vorliegenden Studie sollte geklärt werden, welche physiologische Bedeutung den Oxidase-Isoformen Nox1 und Nox4 bezüglich des AT_{1A} Rezeptors zukommt. Weiterhin wurde eine mögliche protektive Rolle von AT_2 untersucht. Zu diesem Zweck bedienten wir uns knockout Mäusen, in denen entweder das Gen für AT_{1A} ($AT_{1A}^{-/-}$) oder für AT_2 ($AT_2^{-/Y}$) deletiert wurde. Mit Hilfe dieser Modelle bestimmten wir die in vivo Regulation der Nox1 und Nox4 Proteinexpression durch AT_{1A} bzw. AT_2 Rezeptoren und deren funktionelle Signifikanz anhand von Superoxidmessungen und Vasorelaxationstudien. Außerdem untersuchten wir die Wechselwirkungen zwischen den Ang II Rezeptoren und dem Stickstoffmonoxid (NO) Signalweg.

In isolierten Aorten von $AT_{1A}^{-/-}$ Mäusen fanden wir eine signifikante Downregulation in der Nox1 und Nox4 Proteinexpression im Vergleich zu den Wildtyp-Mäusen ($AT_{1A}^{+/+}$). Funktionell wurde dies durch eine schwächere 3NT Immunoreaktivität (Biomarker für nitrosativen Stress) und einer geringeren Basalaktivität der NADPH Oxidase unterstrichen. Interessanterweise ging diese Abnahme der NADPH abhängigen Superoxidproduktion einher mit einer erhöhten Effizienz der Acetylcholin-induzierten, endothelabhängigen Gefäßrelaxation. Der Unterschied in der maximalen Gefäßrelaxation zwischen $AT_{1A}^{-/-}$ und $AT_{1A}^{+/+}$ Mäusen konnte durch SOD und Apocynin aufgehoben werden, was auf eine Beteiligung der NADPH Oxidase abhängigen Superoxidproduktion schliessen lässt. Zusammengefasst weisen diese Daten daraufhin, dass der durch Nox4 (oder Nox1) induzierte nitrosative Stress eine pathophysiologische Rationale des AT_{1A} Rezeptors darstellt, welche in einer beeinträchtigten Gefäßrelaxation resultieren kann. Da Nox4 die unter physiologischen Bedingungen quantitativ bedeutendere Isoform ist, denken

wir, dass vor allem dieses Homologe für die AT_{1A} Rezeptors vermittelte ROS-Bildung und ihre Konsequenzen verantwortlich ist.
Überraschenderweise konnten in den Aorten von $AT_2^{-/Y}$ Mäusen verglichen mit den Wildtyp-Mäusen ($AT_2^{+/Y}$) weder Veränderungen bezüglich der Nox4 Expression noch der NADPH-abhängigen Superoxidproduktion gefunden werden. Allerdings war die Proteinexpression der löslichen Guanylatcyclase (sGCα_1/β_1) und der endothelialen NO-Synthase (eNOS)in diesem Gewebe erniedrigt, im Gegensatz zu $AT_{1A}^{-/-}$ Mäusen,bei denen kein Unterschied im Vergleich zum Wildtyp detektiert werden konnte. Funktionell äusserte sich die Downregulation dieser NO pathway Enzyme in einer reduzierten Relaxationsantwort auf das Acetylcholin und Spermine NONOate.

Zusammenfassend kann man sagen, dass die vorliegenden Daten einen Einblick in die molekularen Mechanismen für die entgegengesetzten Effekte der AT_{1A} und AT_2 Rezeptoren im vaskuläresystem geben. Unter physiologischen Bedingungen wirkt dabei der AT_{1A} Rezeptor stimulierend auf die vaskuläre Funktion durch Erhöhung des Nox4 (oder Nox1) vermittelten oxidativen Stress, während der AT_2 Rezeptor diese durch Hochregulation von sGC und eNOS hemmt. In diesem Zusammenhang könnte ein selektiver AT_{1A} Rezeptorblocker klinisch von Vorteil sein, indem er die ROS Bildung hemmt, gleichzeitig aber den protektiven NO Signalweg unberührt läßt. Die Zusammenfassung der wesentlichen Erkenntnisse dieser Studie ist illustriert in Fig. 8.1.

10. References

1. de Gasparo M, Catt KJ, Inagami T, Wright JW, Unger T. International union of pharmacology. XXIII. The angiotensin II receptors. *Pharmacol Rev* **2000**;52:415-472
2. Berry C, Touyz R, Dominiczak AF, Webb RC, Johns DG. Angiotensin receptors: signaling, vascular pathophysiology, and interactions with ceramide. *Am J Physiol Heart Circ Physiol* **2001**;281:H2337-2365
3. Sasamura H, Hein L, Krieger JE, Pratt RE, Kobilka BK, Dzau VJ. Cloning, characterization, and expression of two angiotensin receptor (A_1) isoforms from the mouse genome. *Biochem Biophys Res Commun* **1992**;185:253-259
4. Timmermans PB, Wong PC, Chiu AT, et al. Angiotensin II receptors and angiotensin II receptor antagonists. *Pharmacol Rev* **1993**;45:205-251
5. Griendling KK, Lassegue B, Alexander RW. Angiotensin receptors and their therapeutic implications. *Annu Rev Pharmacol Toxicol* **1996**;36:281-306
6. de Gasparo M, Siragy HM. The AT_2 receptor: fact, fancy and fantasy. *Regul Pept* **1999**;81:11-24
7. Masaki H, Kurihara T, Yamaki A, et al. Cardiac-specific overexpression of angiotensin II AT_2 receptor causes attenuated response to AT_1 receptor-mediated pressor and chronotropic effects. *J Clin Invest* **1998**;101:527-535
8. Carey RM, Wang ZQ, Siragy HM. Update: role of the angiotensin type-2 (AT_2) receptor in blood pressure regulation. *Curr Hypertens Rep* **2000**;2:198-201
9. Horiuchi M, Akishita M, Dzau VJ. Recent progress in angiotensin II type 2 receptor research in the cardiovascular system. *Hypertension* **1999**;33:613-621
10. Barber MN, Sampey DB, Widdop RE. AT_2 receptor stimulation enhances antihypertensive effect of AT_1 receptor antagonist in hypertensive rats. *Hypertension* **1999**;34:1112-1116

11. Dimitropoulou C, White RE, Fuchs L, Zhang H, Catravas JD, Carrier GO. Angiotensin II relaxes microvessels via the AT(2) receptor and Ca^{2+}-activated K^+ (BK(Ca)) channels. *Hypertension* **2001**;37:301-307

12. Matrougui K, Loufrani L, Heymes C, Levy BI, Henrion D. Activation of AT_2 receptors by endogenous angiotensin II is involved in flow-induced dilation in rat resistance arteries. *Hypertension* **1999**;34:659-665

13. Katada J, Majima M. AT_2 receptor-dependent vasodilation is mediated by activation of vascular kinin generation under flow conditions. *Br J Pharmacol* **2002**;136:484-491

14. Arima S, Endo Y, Yaoita H, et al. Possible role of P-450 metabolite of arachidonic acid in vasodilator mechanism of angiotensin II type 2 receptor in the isolated microperfused rabbit afferent arteriole. *J Clin Invest* **1997**;100:2816-2823

15. Haberl RL. Role of angiotensin receptor subtypes in the response of rabbit brain arterioles to angiotensin. *Stroke* **1994**;25:1476-1479.

16. Zwart AS, Davis EA, Widdop RE. Modulation of AT_1 receptor-mediated contraction of rat uterine artery by AT2 receptors. *Br J Pharmacol* **1998**;125:1429-1436

17. Hannan RE, Davis EA, Widdop RE. Functional role of angiotensin II AT2 receptor in modulation of AT_1 receptor-mediated contraction in rat uterine artery: involvement of bradykinin and nitric oxide. *Br J Pharmacol* **2003**;140:987-995

18. Ichiki T, Labosky PA, Shiota C, et al. Effects on blood pressure and exploratory behaviour of mice lacking angiotensin II type-2 receptor. *Nature* **1995**;377:748-750

19. Tsutsumi Y, Matsubara H, Masaki H, et al. Angiotensin II type 2 receptor overexpression activates the vascular kinin system and causes vasodilation. *J Clin Invest* **1999**;104:925-935

20. Touyz RM, Schiffrin EL. Signal transduction mechanisms mediating the physiological and pathophysiological actions of angiotensin II in vascular smooth muscle cells. *Pharmacol Rev* **2000**;52:639-672

21. Touyz RM. Oxidative stress and vascular damage in hypertension. *Curr Hypertens Rep* **2000**;2:98-105

22. Griendling KK, Sorescu D, Ushio-Fukai M. NAD(P)H oxidase: role in cardiovascular biology and disease. *Circ Res* **2000**;86:494-501

23. Touyz RM, Chen X, Tabet F, et al. Expression of a functionally active gp91phox-containing neutrophil-type NAD(P)H oxidase in smooth muscle cells from human resistance arteries: regulation by angiotensin II. *Circ Res* **2002**;90:1205-1213

24. Ushio-Fukai M, Tang Y, Fukai T, et al. Novel role of gp91(phox)-containing NAD(P)H oxidase in vascular endothelial growth factor-induced signaling and angiogenesis. *Circ Res* **2002**;91:1160-1167

25. Rey FE, Pagano PJ. The reactive adventitia: fibroblast oxidase in vascular function. *Arterioscler Thromb Vasc Biol* **2002**;22:1962-1971

26. Ito M, Oliverio MI, Mannon PJ, et al. Regulation of blood pressure by the type 1A angiotensin II receptor gene. *Proc Natl Acad Sci U S A* **1995**;92:3521-3525

27. Sugaya T, Nishimatsu S, Tanimoto K, et al. Angiotensin II type 1a receptor-deficient mice with hypotension and hyperreninemia. *J Biol Chem* **1995**;270:18719-18722

28. Chen X, Li W, Yoshida H, et al. Targeting deletion of angiotensin type 1B receptor gene in the mouse. *Am J Physiol* **1997**;272:F299-304

29. Ruan X, Oliverio MI, Coffman TM, Arendshorst WJ. Renal vascular reactivity in mice: AngII-induced vasoconstriction in AT_{1A} receptor null mice. *J Am Soc Nephrol* **1999**;10:2620-2630

30. Oliverio MI, Kim HS, Ito M, et al. Reduced growth, abnormal kidney structure, and type 2 (AT_2) angiotensin receptor-mediated blood pressure regulation in mice lacking both AT_{1A} and AT_{1B} receptors for angiotensin II. *Proc Natl Acad Sci U S A* **1998**;95:15496-15501

31. Didion SP, Sigmund CD, Faraci FM. Impaired endothelial function in transgenic mice expressing both human renin and human angiotensinogen. *Stroke* **2000**;31:760-764; discussion 765

32. Nakane H, Miller FJ, Jr., Faraci FM, Toyoda K, Heistad DD. Gene transfer of endothelial nitric oxide synthase reduces angiotensin II-induced endothelial dysfunction. *Hypertension* **2000**;35:595-601

33. Patzak A, Mrowka R, Storch E, Hocher B, Persson PB. Interaction of angiotensin II and nitric oxide in isolated perfused afferent arterioles of mice. *J Am Soc Nephrol* **2001**;12:1122-1127

34. Pollock DM, Polakowski JS, Divish BJ, Opgenorth TJ. Angiotensin blockade reverses hypertension during long-term nitric oxide synthase inhibition. *Hypertension* **1993**;21:660-666

35. Dzau VJ. Theodore Cooper Lecture: Tissue angiotensin and pathobiology of vascular disease: a unifying hypothesis. *Hypertension* **2001**;37:1047-1052

36. Wiemer G, Itter G, Malinski T, Linz W. Decreased nitric oxide availability in normotensive and hypertensive rats with failing hearts after myocardial infarction. *Hypertension* **2001**;38:1367-1371

37. Sventek P, Li JS, Grove K, Deschepper CF, Schiffrin EL. Vascular structure and expression of endothelin-1 gene in L-NAME-treated spontaneously hypertensive rats. *Hypertension* **1996**;27:49-55

38. Takemoto M, Egashira K, Tomita H, et al. Chronic angiotensin-converting enzyme inhibition and angiotensin II type 1 receptor blockade: effects on cardiovascular remodeling in rats induced by the long-term blockade of nitric oxide synthesis. *Hypertension* **1997**;30:1621-1627

39. de Gasparo M. Angiotensin II and nitric oxide interaction. *Heart Fail Rev* **2002**;7:347-358

40. Rudic RD, Shesely EG, Maeda N, Smithies O, Segal SS, Sessa WC. Direct evidence for the importance of endothelium-derived nitric oxide in vascular remodeling. *J Clin Invest* **1998**;101:731-736

41. Denninger JW, Marletta MA. Guanylate cyclase and the NO/cGMP signaling pathway. *Biochim Biophys Acta* **1999**;1411:334-350

42. Schmidt HH, Walter U. NO at work. *Cell* **1994**;78:919-925

43. Drexler H. Nitric oxide and coronary endothelial dysfunction in humans. *Cardiovasc Res* **1999**;43:572-579

44. Gryglewski RJ, Palmer RM, Moncada S. Superoxide anion is involved in the breakdown of endothelium-derived vascular relaxing factor. *Nature* **1986**;320:454-456

45. Beckman JS, Beckman TW, Chen J, Marshall PA, Freeman BA. Apparent hydroxyl radical production by peroxynitrite: implications for endothelial injury from nitric oxide and superoxide. *Proc Natl Acad Sci U S A* **1990**;87:1620-1624

46. Ballinger SW, Patterson C, Yan CN, et al. Hydrogen peroxide- and peroxynitrite-induced mitochondrial DNA damage and dysfunction in vascular endothelial and smooth muscle cells. *Circ Res* **2000**;86:960-966

47. Cai H, Harrison DG. Endothelial dysfunction in cardiovascular diseases: the role of oxidant stress. *Circ Res* **2000**;87:840-844

48. Laursen JB, Rajagopalan S, Galis Z, Tarpey M, Freeman BA, Harrison DG. Role of superoxide in angiotensin II-induced but not catecholamine-induced hypertension. *Circulation* **1997**;95:588-593

49. Baykal Y, Yilmaz MI, Celik T, et al. Effects of antihypertensive agents, alpha receptor blockers, beta blockers, angiotensin-converting enzyme inhibitors, angiotensin receptor blockers and calcium channel blockers, on oxidative stress. *J Hypertens* **2003**;21:1207-1211

50. Vaziri ND, Oveisi F, Ding Y. Role of increased oxygen free radical activity in the pathogenesis of uremic hypertension. *Kidney Int* **1998**;53:1748-1754

51. Russo C, Olivieri O, Girelli D, et al. Anti-oxidant status and lipid peroxidation in patients with essential hypertension. *J Hypertens* **1998**;16:1267-1271

52. Sagar S, Kallo IJ, Kaul N, Ganguly NK, Sharma BK. Oxygen free radicals in essential hypertension. *Mol Cell Biochem* **1992**;111:103-108

53. Suzuki H, Swei A, Zweifach BW, Schmid-Schonbein GW. In vivo evidence for microvascular oxidative stress in spontaneously hypertensive rats. Hydroethidine microfluorography. *Hypertension* **1995**;25:1083-1089

54. Swei A, Lacy F, Delano FA, Parks DA, Schmid-Schonbein GW. A mechanism of oxygen free radical production in the Dahl hypertensive rat. *Microcirculation* **1999**;6:179-187

55. Vaziri ND, Wang XQ, Oveisi F, Rad B. Induction of oxidative stress by glutathione depletion causes severe hypertension in normal rats. *Hypertension* **2000**;36:142-146

56. Cifuentes ME, Rey FE, Carretero OA, Pagano PJ. Upregulation of p67(phox) and gp91(phox) in aortas from angiotensin II-infused mice. *Am J Physiol Heart Circ Physiol* **2000**;279:H2234-2240

57. Mollnau H, Wendt M, Szocs K, et al. Effects of angiotensin II infusion on the expression and function of NAD(P)H oxidase and components of nitric oxide/cGMP signaling. *Circ Res* **2002**;90:E58-65

58. Heitzer T, Wenzel U, Hink U, et al. Increased NAD(P)H oxidase-mediated superoxide production in renovascular hypertension: evidence for an involvement of protein kinase C. *Kidney Int* **1999**;55:252-260

59. Dobrian AD, Schriver SD, Prewitt RL. Role of angiotensin II and free radicals in blood pressure regulation in a rat model of renal hypertension. *Hypertension* **2001**;38:361-366

60. Didion SP, Ryan MJ, Baumbach GL, Sigmund CD, Faraci FM. Superoxide contributes to vascular dysfunction in mice that express human renin and angiotensinogen. *Am J Physiol Heart Circ Physiol* **2002**;283:H1569-1576

61. Ungvari Z, Csiszar A, Huang A, Kaminski PM, Wolin MS, Koller A. High pressure induces superoxide production in isolated arteries via protein kinase C-dependent activation of NAD(P)H oxidase. *Circulation* **2003**;108:1253-1258

62. Nakazono K, Watanabe N, Matsuno K, Sasaki J, Sato T, Inoue M. Does superoxide underlie the pathogenesis of hypertension? *Proc Natl Acad Sci U S A* **1991**;88:10045-10048

63. Azumi H, Inoue N, Takeshita S, et al. Expression of NADH/NADPH oxidase p22phox in human coronary arteries. *Circulation* **1999**;100:1494-1498

64. Cosentino F, Barker JE, Brand MP, et al. Reactive oxygen species mediate endothelium-dependent relaxations in tetrahydrobiopterin-deficient mice. *Arterioscler Thromb Vasc Biol* **2001**;21:496-502

65. Vasquez-Vivar J, Hogg N, Pritchard KA, Jr., Martasek P, Kalyanaraman B. Superoxide anion formation from lucigenin: an electron spin resonance spin-trapping study. *FEBS Lett* **1997**;403:127-130

66. Bagi Z, Koller A. Lack of nitric oxide mediation of flow-dependent arteriolar dilation in type I diabetes is restored by sepiapterin. *J Vasc Res* **2003**;40:47-57

67. Landmesser U, Dikalov S, Price SR, et al. Oxidation of tetrahydrobiopterin leads to uncoupling of endothelial cell nitric oxide synthase in hypertension. *J Clin Invest* **2003**;111:1201-1209

68. Wilcox CS. Reactive oxygen species: roles in blood pressure and kidney function. *Curr Hypertens Rep* **2002**;4:160-166

69. Babior BM. NADPH oxidase: an update. *Blood* **1999**;93:1464-1476

70. Babior BM, Lambeth JD, Nauseef W. The neutrophil NADPH oxidase. *Arch Biochem Biophys* **2002**;397:342-344

71. Kobayashi T, Tsunawaki S, Seguchi H. Evaluation of the process for superoxide production by NADPH oxidase in human neutrophils: evidence for cytoplasmic origin of superoxide. *Redox Rep* **2001**;6:27-36

72. Kuribayashi F, Nunoi H, Wakamatsu K, et al. The adaptor protein p40(phox) as a positive regulator of the superoxide-producing phagocyte oxidase. *Embo J* **2002**;21:6312-6320

73. Vergnaud S, Paclet MH, El Benna J, Pocidalo MA, Morel F. Complementation of NADPH oxidase in p67-phox-deficient CGD patients p67-phox/p40-phox interaction. *Eur J Biochem* **2000**;267:1059-1067

74. Griendling KK, Ushio-Fukai M. Redox control of vascular smooth muscle proliferation. *J Lab Clin Med* **1998**;132:9-15

75. Banfi B, Maturana A, Jaconi S, et al. A mammalian H^+ channel generated through alternative splicing of the NADPH oxidase homolog NOH-1. *Science* **2000**;287:138-142

76. Lambeth JD. Nox/Duox family of nicotinamide adenine dinucleotide (phosphate) oxidases. *Curr Opin Hematol* **2002**;9:11-17

77. Lambeth JD, Cheng G, Arnold RS, Edens WA. Novel homologs of gp91phox. *Trends Biochem Sci* **2000**;25:459-461

78. Suh YA, Arnold RS, Lassegue B, et al. Cell transformation by the superoxide-generating oxidase Mox1. *Nature* **1999**;401:79-82

79. Edens WA, Sharling L, Cheng G, et al. Tyrosine cross-linking of extracellular matrix is catalyzed by Duox, a multidomain oxidase/peroxidase with homology to the phagocyte oxidase subunit gp91phox. *J Cell Biol* **2001**;154:879-891

80. Dupuy C, Pomerance M, Ohayon R, et al. Thyroid oxidase (THOX2) gene expression in the rat thyroid cell line FRTL-5. *Biochem Biophys Res Commun* **2000**;277:287-292

81. Bengtsson SH, Gulluyan LM, Dusting GJ, Drummond GR. Novel isoforms of NADPH oxidase in vascular physiology and pathophysiology. *Clin Exp Pharmacol Physiol* **2003**;30:849-854

82. Kikuchi M, Ohnishi K, Harayama S. An effective family shuffling method using single-stranded DNA. *Gene* **2000**;243:133-137

83. Sorescu D, Weiss D, Lassegue B, et al. Superoxide production and expression of nox family proteins in human atherosclerosis. *Circulation* **2002**;105:1429-1435

84. Maly FE, Nakamura M, Gauchat JF, et al. Superoxide-dependent nitroblue tetrazolium reduction and expression of cytochrome b-245 components by human tonsillar B lymphocytes and B cell lines. *J Immunol* **1989**;142:1260-1267

85. Radeke HH, Cross AR, Hancock JT, et al. Functional expression of NADPH oxidase components (alpha- and beta-subunits of cytochrome b558 and 45-kDa flavoprotein) by intrinsic human glomerular mesangial cells. *J Biol Chem* **1991**;266:21025-21029

86. Geiszt M, Kopp JB, Varnai P, Leto TL. Identification of renox, an NAD(P)H oxidase in kidney. *Proc Natl Acad Sci U S A* **2000**;97:8010-8014

87. Wingler K, Wunsch S, Kreutz R, Rothermund L, Paul M, Schmidt HH. Upregulation of the vascular NAD(P)H-oxidase isoforms Nox1 and Nox4 by the renin-angiotensin system in vitro and in vivo. *Free Radic Biol Med* **2001**;31:1456-1464

88. Banfi B, Molnar G, Maturana A, et al. A Ca^{2+}-activated NADPH oxidase in testis, spleen, and lymph nodes. *J Biol Chem* **2001**;276:37594-37601

89. Griendling KK, Minieri CA, Ollerenshaw JD, Alexander RW. Angiotensin II stimulates NADH and NADPH oxidase activity in cultured vascular smooth muscle cells. *Circ Res* **1994**;74:1141-1148

90. Wang HD, Xu S, Johns DG, et al. Role of NADPH oxidase in the vascular hypertrophic and oxidative stress response to angiotensin II in mice. *Circ Res* **2001**;88:947-953

91. Mohazzab KM, Kaminski PM, Wolin MS. NADH oxidoreductase is a major source of superoxide anion in bovine coronary artery endothelium. *Am J Physiol* **1994**;266:H2568-2572

92. Mohazzab KM, Wolin MS. Sites of superoxide anion production detected by lucigenin in calf pulmonary artery smooth muscle. *Am J Physiol* **1994**;267:L815-822

93. Pagano PJ, Ito Y, Tornheim K, Gallop PM, Tauber AI, Cohen RA. An NADPH oxidase superoxide-generating system in the rabbit aorta. *Am J Physiol* **1995**;268:H2274-2280

94. Van Heerebeek L, Meischl C, Stooker W, Meijer CJ, Niessen HW, Roos D. NADPH oxidase(s): new source(s) of reactive oxygen species in the vascular system? *J Clin Pathol* **2002**;55:561-568

95. Guzik TJ, Mussa S, Gastaldi D, et al. Mechanisms of increased vascular superoxide production in human diabetes mellitus: role of NAD(P)H oxidase and endothelial nitric oxide synthase. *Circulation* **2002**;105:1656-1662

96. Meyer JW, Holland JA, Ziegler LM, Chang MM, Beebe G, Schmitt ME. Identification of a functional leukocyte-type NADPH oxidase in human endothelial cells :a potential atherogenic source of reactive oxygen species. *Endothelium* **1999**;7:11-22

97. Li JM, Shah AM. Intracellular localization and preassembly of the NADPH oxidase complex in cultured endothelial cells. *J Biol Chem* **2002**;277:19952-19960

98. Pagano PJ, Clark JK, Cifuentes-Pagano ME, Clark SM, Callis GM, Quinn MT. Localization of a constitutively active, phagocyte-like NADPH oxidase in rabbit aortic adventitia: enhancement by angiotensin II. *Proc Natl Acad Sci U S A* **1997**;94:14483-14488

99. Kalinina N, Agrotis A, Tararak E, et al. Cytochrome b558-dependent NAD(P)H oxidase-phox units in smooth muscle and macrophages of atherosclerotic lesions. *Arterioscler Thromb Vasc Biol* **2002**;22:2037-2043

100. Fukui T, Lassegue B, Kai H, Alexander RW, Griendling KK. Cytochrome b-558 alpha-subunit cloning and expression in rat aortic smooth muscle cells. *Biochim Biophys Acta* **1995**;1231:215-219

101. Lassegue B, Sorescu D, Szocs K, et al. Novel gp91(phox) homologues in vascular smooth muscle cells : Nox1 mediates angiotensin II-induced superoxide formation and redox-sensitive signaling pathways. *Circ Res* **2001**;88:888-894

102. Gu Y, Xu YC, Wu RF, Souza RF, Nwariaku FE, Terada LS. TNFalpha activates c-Jun amino terminal kinase through p47(phox). *Exp Cell Res* **2002**;272:62-74

103. Sorescu D, Somers MJ, Lassegue B, Grant S, Harrison DG, Griendling KK. Electron spin resonance characterization of the NAD(P)H oxidase in vascular smooth muscle cells. *Free Radic Biol Med* **2001**;30:603-612

104. Sundaresan M, Yu ZX, Ferrans VJ, Irani K, Finkel T. Requirement for generation of H2O2 for platelet-derived growth factor signal transduction. *Science* **1995**;270:296-299

105. Patterson C, Ruef J, Madamanchi NR, et al. Stimulation of a vascular smooth muscle cell NAD(P)H oxidase by thrombin. Evidence that p47(phox) may participate in forming this oxidase in vitro and in vivo. *J Biol Chem* **1999**;274:19814-19822

106. De Keulenaer GW, Alexander RW, Ushio-Fukai M, Ishizaka N, Griendling KK. Tumour necrosis factor alpha activates a p22phox-based NADH oxidase in vascular smooth muscle. *Biochem J* **1998**;329 (Pt 3):653-657

107. Marumo T, Schini-Kerth VB, Fisslthaler B, Busse R. Platelet-derived growth factor-stimulated superoxide anion production modulates activation of transcription factor NF-kappaB and expression of monocyte chemoattractant protein 1 in human aortic smooth muscle cells. *Circulation* **1997**;96:2361-2367

108. Seshiah PN, Weber DS, Rocic P, Valppu L, Taniyama Y, Griendling KK. Angiotensin II stimulation of NAD(P)H oxidase activity: upstream mediators. *Circ Res* **2002**;91:406-413

109. Frey RS, Rahman A, Kefer JC, Minshall RD, Malik AB. PKCzeta regulates TNF-alpha-induced activation of NADPH oxidase in endothelial cells. *Circ Res* **2002**;90:1012-1019

110. Griendling KK, Sorescu D, Lassegue B, Ushio-Fukai M. Modulation of protein kinase activity and gene expression by reactive oxygen species and their role in vascular physiology and pathophysiology. *Arterioscler Thromb Vasc Biol* **2000**;20:2175-2183

111. Touyz RM, Schiffrin EL. Ang II-stimulated superoxide production is mediated via phospholipase D in human vascular smooth muscle cells. *Hypertension* **1999**;34:976-982

112. Touyz RM, Schiffrin EL. Increased generation of superoxide by angiotensin II in smooth muscle cells from resistance arteries of hypertensive patients: role of phospholipase D-dependent NAD(P)H oxidase-sensitive pathways. *J Hypertens* **2001**;19:1245-1254

113. Zafari AM, Ushio-Fukai M, Minieri CA, Akers M, Lassegue B, Griendling KK. Arachidonic acid metabolites mediate angiotensin II-induced NADH/NADPH oxidase activity and hypertrophy in vascular smooth muscle cells. *Antioxid Redox Signal* **1999**;1:167-179

114. Hessler JR, Morel DW, Lewis LJ, Chisolm GM. Lipoprotein oxidation and lipoprotein-induced cytotoxicity. *Arteriosclerosis* **1983**;3:215-222

115. Cathcart MK, Morel DW, Chisolm GM, 3rd. Monocytes and neutrophils oxidize low density lipoprotein making it cytotoxic. *J Leukoc Biol* **1985**;38:341-350

116. Cathcart MK, Chisolm GM, 3rd, McNally AK, Morel DW. Oxidative modification of low density lipoprotein (LDL) by activated human monocytes and the cell lines U937 and HL60. *In Vitro Cell Dev Biol* **1988**;24:1001-1008

117. Chisolm GM, 3rd, Hazen SL, Fox PL, Cathcart MK. The oxidation of lipoproteins by monocytes-macrophages. Biochemical and biological mechanisms. *J Biol Chem* **1999**;274:25959-25962

118. Cathcart MK, McNally AK, Morel DW, Chisolm GM, 3rd. Superoxide anion participation in human monocyte-mediated oxidation of low-density lipoprotein and conversion of low-density lipoprotein to a cytotoxin. *J Immunol* **1989**;142:1963-1969

119. Paravicini TM, Gulluyan LM, Dusting GJ, Drummond GR. Increased NADPH oxidase activity, gp91phox expression, and endothelium-dependent vasorelaxation during neointima formation in rabbits. *Circ Res* **2002**;91:54-61

120. Warnholtz A, Nickenig G, Schulz E, et al. Increased NADH-oxidase-mediated superoxide production in the early stages of atherosclerosis: evidence for involvement of the renin-angiotensin system. *Circulation* **1999**;99:2027-2033

121. Guzik TJ, West NE, Black E, et al. Vascular superoxide production by NAD(P)H oxidase: association with endothelial dysfunction and clinical risk factors. *Circ Res* **2000**;86:E85-90

122. Barry-Lane PA, Patterson C, van der Merwe M, et al. p47phox is required for atherosclerotic lesion progression in ApoE$^{(-/-)}$ mice. *J Clin Invest* **2001**;108:1513-1522

123. Kirk EA, Dinauer MC, Rosen H, Chait A, Heinecke JW, LeBoeuf RC. Impaired superoxide production due to a deficiency in phagocyte NADPH oxidase fails to inhibit atherosclerosis in mice. *Arterioscler Thromb Vasc Biol* **2000**;20:1529-1535

124. Hsich E, Segal BH, Pagano PJ, et al. Vascular effects following homozygous disruption of p47(phox) : An essential component of NADPH oxidase. *Circulation* **2000**;101:1234-1236

125. Somers MJ, Mavromatis K, Galis ZS, Harrison DG. Vascular superoxide production and vasomotor function in hypertension induced by deoxycorticosterone acetate-salt. *Circulation* **2000**;101:1722-1728

126. Wu R, Millette E, Wu L, de Champlain J. Enhanced superoxide anion formation in vascular tissues from spontaneously hypertensive and desoxycorticosterone acetate-salt hypertensive rats. *J Hypertens* **2001**;19:741-748

127. Zalba G, Beaumont J, San Jose G, Fortuno A, Fortuno MA, Diez J. Vascular oxidant stress: molecular mechanisms and pathophysiological implications. *J Physiol Biochem* **2000**;56:57-64

128. Rajagopalan S, Harrison DG. Reversing endothelial dysfunction with ACE inhibitors. A new trend. *Circulation* **1996**;94:240-243

129. Otsuka S, Sugano M, Makino N, Sawada S, Hata T, Niho Y. Interaction of mRNAs for angiotensin II type 1 and type 2 receptors to vascular remodeling in spontaneously hypertensive rats. *Hypertension* **1998**;32:467-472

130. Hamilton CA, Brosnan MJ, McIntyre M, Graham D, Dominiczak AF. Superoxide excess in hypertension and aging: a common cause of endothelial dysfunction. *Hypertension* **2001**;37:529-534

131. Thannickal VJ, Fanburg BL. Reactive oxygen species in cell signaling. *Am J Physiol Lung Cell Mol Physiol* **2000**;279:L1005-1028

132. Anderson L, Henderson C, Adachi Y. Phosphorylation and rapid relocalization of 53BP1 to nuclear foci upon DNA damage. *Mol Cell Biol* **2001**;21:1719-1729

133. Lounsbury KM, Hu Q, Ziegelstein RC. Calcium signaling and oxidant stress in the vasculature. *Free Radic Biol Med* **2000**;28:1362-1369

134. Touyz RM, Yao G, Schiffrin EL. c-Src induces phosphorylation and translocation of p47phox: role in superoxide generation by angiotensin II in human vascular smooth muscle cells. *Arterioscler Thromb Vasc Biol* **2003**;23:981-987

135. Di Wang H, Hope S, Du Y, et al. Paracrine role of adventitial superoxide anion in mediating spontaneous tone of the isolated rat aorta in angiotensin II-induced hypertension. *Hypertension* **1999**;33:1225-1232

136. Rajagopalan S, Kurz S, Munzel T, et al. Angiotensin II-mediated hypertension in the rat increases vascular superoxide production via membrane NADH/NADPH oxidase activation. Contribution to alterations of vasomotor tone. *J Clin Invest* **1996**;97:1916-1923

137. Zafari AM, Ushio-Fukai M, Akers M, et al. Role of NADH/NADPH oxidase-derived H_2O_2 in angiotensin II-induced vascular hypertrophy. *Hypertension* **1998**;32:488-495

138. Nakamura K, Fushimi K, Kouchi H, et al. Inhibitory effects of antioxidants on neonatal rat cardiac myocyte hypertrophy induced by tumor necrosis factor-alpha and angiotensin II. *Circulation* **1998**;98:794-799

139. Zalba G, San Jose G, Moreno MU, et al. Oxidative stress in arterial hypertension: role of NAD(P)H oxidase. *Hypertension* **2001**;38:1395-1399

140. Touyz RM, Tabet F, Schiffrin EL. Redox-dependent signalling by angiotensin II and vascular remodelling in hypertension. *Clin Exp Pharmacol Physiol* **2003**;30:860-866

141. Rueckschloss U, Quinn MT, Holtz J, Morawietz H. Dose-dependent regulation of NAD(P)H oxidase expression by angiotensin II in human endothelial cells: protective effect of angiotensin II type 1 receptor blockade in patients with coronary artery disease. *Arterioscler Thromb Vasc Biol* **2002**;22:1845-1851

142. Ushio-Fukai M, Zafari AM, Fukui T, Ishizaka N, Griendling KK. p22phox is a critical component of the superoxide-generating NADH/NADPH oxidase system and regulates angiotensin II-induced hypertrophy in vascular smooth muscle cells. *J Biol Chem* **1996**;271:23317-23321

143. Fukui T, Ishizaka N, Rajagopalan S, et al. p22phox mRNA expression and NADPH oxidase activity are increased in aortas from hypertensive rats. *Circ Res* **1997**;80:45-51

144. Zalba G, Beaumont FJ, San Jose G, et al. Vascular NADH/NADPH oxidase is involved in enhanced superoxide production in spontaneously hypertensive rats. *Hypertension* **2000**;35:1055-1061

145. Pagano PJ, Chanock SJ, Siwik DA, Colucci WS, Clark JK. Angiotensin II induces p67phox mRNA expression and NADPH oxidase superoxide generation in rabbit aortic adventitial fibroblasts. *Hypertension* **1998**;32:331-337

146. Landmesser U, Cai H, Dikalov S, et al. Role of p47(phox) in vascular oxidative stress and hypertension caused by angiotensin II. *Hypertension* **2002**;40:511-515

147. Schieffer B, Luchtefeld M, Braun S, Hilfiker A, Hilfiker-Kleiner D, Drexler H. Role of NAD(P)H oxidase in angiotensin II-induced JAK/STAT signaling and cytokine induction. *Circ Res* **2000**;87:1195-1201

148. Rey FE, Cifuentes ME, Kiarash A, Quinn MT, Pagano PJ. Novel competitive inhibitor of NAD(P)H oxidase assembly attenuates vascular O_2^- and systolic blood pressure in mice. *Circ Res* **2001**;89:408-414

149. Duerrschmidt N, Wippich N, Goettsch W, Broemme HJ, Morawietz H. Endothelin-1 induces NAD(P)H oxidase in human endothelial cells. *Biochem Biophys Res Commun* **2000**;269:713-717

150. Rueckschloss U, Galle J, Holtz J, Zerkowski HR, Morawietz H. Induction of NAD(P)H oxidase by oxidized low-density lipoprotein in human endothelial cells: antioxidative potential of hydroxymethylglutaryl coenzyme A reductase inhibitor therapy. *Circulation* **2001**;104:1767-1772

151. Rey FE, Li XC, Carretero OA, Garvin JL, Pagano PJ. Perivascular superoxide anion contributes to impairment of endothelium-dependent relaxation: role of gp91(phox). *Circulation* **2002**;106:2497-2502

152. Bendall JK, Cave AC, Heymes C, Gall N, Shah AM. Pivotal role of a gp91(phox)-containing NADPH oxidase in angiotensin II-induced cardiac hypertrophy in mice. *Circulation* **2002**;105:293-296

153. Byrne JA, Grieve DJ, Bendall JK, et al. Contrasting roles of NADPH oxidase isoforms in pressure-overload versus angiotensin II-induced cardiac hypertrophy. *Circ Res* **2003**;93:802-805

154. Wassmann S, Laufs U, Muller K, et al. Cellular antioxidant effects of atorvastatin in vitro and in vivo. *Arterioscler Thromb Vasc Biol* **2002**;22:300-305

155. Ago T, Kitazono T, Ooboshi H, et al. Nox4 as the major catalytic component of an endothelial NAD(P)H oxidase. *Circulation* **2004**;109:227-233

156. Wilfinger WW, Mackey K, Chomczynski P. Effect of pH and ionic strength on the spectrophotometric assessment of nucleic acid purity. *Biotechniques* **1997**;22:474-476, 478-481

157. Hein L, Barsh GS, Pratt RE, Dzau VJ, Kobilka BK. Behavioural and cardiovascular effects of disrupting the angiotensin II type-2 receptor in mice. *Nature* **1995**;377:744-747

158. Peterson GL. A simplification of the protein assay method of Lowry et al. which is more generally applicable. *Anal Biochem* **1977**;83:346-356

159. Laemmli UK. Cleavage of structural proteins during the assembly of the head of bacteriophage T4. *Nature* **1970**;227:680-685

160. Darley-Usmar VM, Hogg N, O'Leary VJ, Wilson MT, Moncada S. The simultaneous generation of superoxide and nitric oxide can initiate lipid peroxidation in human low density lipoprotein. *Free Radic Res Commun* **1992**;17:9-20

161. Uttenthal LO, Alonso D, Fernandez AP, et al. Neuronal and inducible nitric oxide synthase and nitrotyrosine immunoreactivities in the cerebral cortex of the aging rat. *Microsc Res Tech* **1998**;43:75-88

162. Nedvetsky PI, Kleinschnitz C, Schmidt HH. Regional distribution of protein and activity of the nitric oxide receptor, soluble guanylyl cyclase, in rat brain suggests multiple mechanisms of regulation. *Brain Res* **2002**;950:148-154

163. Zabel U, Weeger M, La M, Schmidt HH. Human soluble guanylate cyclase: functional expression and revised isoenzyme family. *Biochem J* **1998**;335 (Pt 1):51-57

164. Fike CD, Kaplowitz MR. Nifedipine inhibits pulmonary hypertension but does not prevent decreased lung eNOS in hypoxic newborn pigs. *Am J Physiol* **1999**;277:L449-456

165. Vaziri ND, Ding Y, Ni Z. Compensatory up-regulation of nitric-oxide synthase isoforms in lead-induced hypertension; reversal by a superoxide dismutase-mimetic drug. *J Pharmacol Exp Ther* **2001**;298:679-685

166. Li Y, Zhu H, Kuppusamy P, Roubaud V, Zweier JL, Trush MA. Validation of lucigenin (bis-N-methylacridinium) as a chemilumigenic probe for detecting superoxide anion radical production by enzymatic and cellular systems. *J Biol Chem* **1998**;273:2015-2023

167. Russell A, Watts S. Vascular reactivity of isolated thoracic aorta of the C57BL/6J mouse. *J Pharmacol Exp Ther* **2000**;294:598-604

168. Weissmann N, Akkayagil E, Quanz K, et al. Basic features of hypoxic pulmonary vasoconstriction in mice. *Respir Physiol Neurobiol* **2004**;139:191-202

169. Marshall C, Mamary AJ, Verhoeven AJ, Marshall BE. Pulmonary artery NADPH-oxidase is activated in hypoxic pulmonary vasoconstriction. *Am J Respir Cell Mol Biol* **1996**;15:633-644

170. Sohn HY, Keller M, Gloe T, Morawietz H, Rueckschloss U, Pohl U. The small G-protein Rac mediates depolarization-induced superoxide formation in human endothelial cells. *J Biol Chem* **2000**;275:18745-18750

171. Beckman JS, Koppenol WH. Nitric oxide, superoxide, and peroxynitrite: the good, the bad, and ugly. *Am J Physiol* **1996**;271:C1424-1437

172. Hannan RE, Gaspari TA, Davis EA, Widdop RE. Differential regulation by AT(1) and AT(2) receptors of angiotensin II-stimulated cyclic GMP production in rat uterine artery and aorta. *Br J Pharmacol* **2004**;141:1024-1031

173. Munzenmaier DH, Greene AS. Opposing actions of angiotensin II on microvascular growth and arterial blood pressure. *Hypertension* **1996**;27:760-765

174. Nickenig G, Roling J, Strehlow K, Schnabel P, Bohm M. Insulin induces upregulation of vascular AT_1 receptor gene expression by posttranscriptional mechanisms. *Circulation* **1998**;98:2453-2460

175. Lassegue B, Alexander RW, Nickenig G, Clark M, Murphy TJ, Griendling KK. Angiotensin II down-regulates the vascular smooth muscle AT_1 receptor by transcriptional and post-transcriptional mechanisms: evidence for homologous and heterologous regulation. *Mol Pharmacol* **1995**;48:601-609

176. Nickenig G, Murphy TJ. Down-regulation by growth factors of vascular smooth muscle angiotensin receptor gene expression. *Mol Pharmacol* **1994**;46:653-659

177. Burson JM, Aguilera G, Gross KW, Sigmund CD. Differential expression of angiotensin receptor $_{1A}$ and $_{1B}$ in mouse. *Am J Physiol* **1994**;267:E260-267

178. Harada K, Komuro I, Shiojima I, et al. Pressure overload induces cardiac hypertrophy in angiotensin II type 1A receptor knockout mice. *Circulation* **1998**;97:1952-1959

179. Rahman M, Kimura S, Nishiyama A, Hitomi H, Zhang G, Abe Y. Angiotensin II stimulates superoxide production via both angiotensin AT_{1A} and AT_{1B} receptors in mouse aorta and heart. *Eur J Pharmacol* **2004**;485:243-249

180. Oliverio MI, Best CF, Smithies O, Coffman TM. Regulation of sodium balance and blood pressure by the AT_{1A} receptor for angiotensin II. *Hypertension* **2000**;35:550-554

181. Stocker R, Keaney JF, Jr. Role of oxidative modifications in atherosclerosis. *Physiol Rev* **2004**;84:1381-1478

182. Zhang H, Schmeisser A, Garlichs CD, et al. Angiotensin II-induced superoxide anion generation in human vascular endothelial cells: role of membrane-bound NADH-/NADPH-oxidases. *Cardiovasc Res* **1999**;44:215-222

183. Sohn HY, Raff U, Hoffmann A, et al. Differential role of angiotensin II receptor subtypes on endothelial superoxide formation. *Br J Pharmacol* **2000**;131:667-672

184. Chabrashvili T, Kitiyakara C, Blau J, et al. Effects of ANG II type 1 and 2 receptors on oxidative stress, renal NADPH oxidase, and SOD expression. *Am J Physiol Regul Integr Comp Physiol* **2003**;285:R117-124

185. Grimminger F, Weissmann N, Spriestersbach R, Becker E, Rosseau S, Seeger W. Effects of NADPH oxidase inhibitors on hypoxic vasoconstriction in buffer-perfused rabbit lungs. *Am J Physiol* **1995**;268:L747-752

186. Hoidal JR, Brar SS, Sturrock AB, et al. The role of endogenous NADPH oxidases in airway and pulmonary vascular smooth muscle function. *Antioxid Redox Signal* **2003**;5:751-758

187. Chassagne C, Eddahibi S, Adamy C, et al. Modulation of angiotensin II receptor expression during development and regression of hypoxic pulmonary hypertension. *Am J Respir Cell Mol Biol* **2000**;22:323-332

188. Li JM, Shah AM. Mechanism of endothelial cell NADPH oxidase activation by angiotensin II. Role of the p47phox subunit. *J Biol Chem* **2003**;278:12094-12100

189. Munzel T, Kurz S, Rajagopalan S, et al. Hydralazine prevents nitroglycerin tolerance by inhibiting activation of a membrane-bound NADH oxidase. A new action for an old drug. *J Clin Invest* **1996**;98:1465-1470

190. Liochev SI, Fridovich I. Lucigenin (bis-N-methylacridinium) as a mediator of superoxide anion production. *Arch Biochem Biophys* **1997**;337:115-120

191. Li JM, Shah AM. Differential NADPH- versus NADH-dependent superoxide production by phagocyte-type endothelial cell NADPH oxidase. *Cardiovasc Res* **2001**;52:477-486

192. Munzel T, Hink U, Heitzer T, Meinertz T. Role for NADPH/NADH oxidase in the modulation of vascular tone. *Ann N Y Acad Sci* **1999**;874:386-400

193. Lang D, Mosfer SI, Shakesby A, Donaldson F, Lewis MJ. Coronary microvascular endothelial cell redox state in left ventricular hypertrophy : the role of angiotensin II. *Circ Res* **2000**;86:463-469

194. Berry C, Hamilton CA, Brosnan MJ, et al. Investigation into the sources of superoxide in human blood vessels: angiotensin II increases superoxide production in human internal mammary arteries. *Circulation* **2000**;101:2206-2212

195. Freeman B. Free radical chemistry of nitric oxide. Looking at the dark side. *Chest* **1994**;105:79S-84S

196. Kissner R, Nauser T, Bugnon P, Lye PG, Koppenol WH. Formation and properties of peroxynitrite as studied by laser flash photolysis, high-pressure stopped-flow technique, and pulse radiolysis. *Chem Res Toxicol* **1997**;10:1285-1292

197. Beckman JS. Oxidative damage and tyrosine nitration from peroxynitrite. *Chem Res Toxicol* **1996**;9:836-844

198. Eiserich JP, Hristova M, Cross CE, et al. Formation of nitric oxide-derived inflammatory oxidants by myeloperoxidase in neutrophils. *Nature* **1998**;391:393-397

199. Crouser ED, Julian MW, Weinstein DM, Fahy RJ, Bauer JA. Endotoxin-induced ileal mucosal injury and nitric oxide dysregulation are temporally dissociated. *Am J Respir Crit Care Med* **2000**;161:1705-1712

200. MacMillan-Crow LA, Crow JP, Kerby JD, Beckman JS, Thompson JA. Nitration and inactivation of manganese superoxide dismutase in chronic rejection of human renal allografts. *Proc Natl Acad Sci U S A* **1996**;93:11853-11858

201. Wattanapitayakul SK, Weinstein DM, Holycross BJ, Bauer JA. Endothelial dysfunction and peroxynitrite formation are early events in angiotensin-induced cardiovascular disorders. *Faseb J* **2000**;14:271-278

202. Wang HD, Johns DG, Xu S, Cohen RA. Role of superoxide anion in regulating pressor and vascular hypertrophic response to angiotensin II. *Am J Physiol Heart Circ Physiol* **2002**;282:H1697-1702

203. Britten MB, Zeiher AM, Schachinger V. Clinical importance of coronary endothelial vasodilator dysfunction and therapeutic options. *J Intern Med* **1999**;245:315-327

204. Rubanyi GM, Vanhoutte PM. Superoxide anions and hyperoxia inactivate endothelium-derived relaxing factor. *Am J Physiol* **1986**;250:H822-827

205. Mancini GB, Henry GC, Macaya C, et al. Angiotensin-converting enzyme inhibition with quinapril improves endothelial vasomotor dysfunction in patients with coronary artery disease. The TREND (Trial on Reversing ENdothelial Dysfunction) Study. *Circulation* **1996**;94:258-265

206. Schlaifer JD, Wargovich TJ, O'Neill B, et al. Effects of quinapril on coronary blood flow in coronary artery disease patients with endothelial dysfunction. TREND Investigators. Trial on Reversing Endothelial Dysfunction. *Am J Cardiol* **1997**;80:1594-1597

207. Thai H, Wollmuth J, Goldman S, Gaballa M. Angiotensin subtype 1 rReceptor (AT1) blockade improves vasorelaxation in heart failure by up-regulation of endothelial nitric-oxide synthase via activation of the AT2 receptor. *J Pharmacol Exp Ther* **2003**;307:1171-1178

208. Wiemer G, Scholkens BA, Wagner A, Heitsch H, Linz W. The possible role of angiotensin II subtype AT2 receptors in endothelial cells and isolated ischemic rat hearts. *J Hypertens Suppl* **1993**;11 Suppl 5:S234-235

209. Saito S, Hirata Y, Emori T, Imai T, Marumo F. Angiotensin II activates endothelial constitutive nitric oxide synthase via AT_1 receptors. *Hypertens Res* **1996**;19:201-206

210. Zarahn ED, Ye X, Ades AM, Reagan LP, Fluharty SJ. Angiotensin-induced cyclic GMP production is mediated by multiple receptor subtypes and nitric oxide in N1E-115 neuroblastoma cells. *J Neurochem* **1992**;58:1960-1963

211. Caputo L, Benessiano J, Boulanger CM, Levy BI. Angiotensin II increases cGMP content via endothelial angiotensin II AT_1 subtype receptors in the rat carotid artery. *Arterioscler Thromb Vasc Biol* **1995**;15:1646-1651

212. Pueyo ME, Arnal JF, Rami J, Michel JB. Angiotensin II stimulates the production of NO and peroxynitrite in endothelial cells. *Am J Physiol* **1998**;274:C214-220

213. Tanaka N, Tanaka K, Nagashima Y, Kondo M, Sekihara H. Nitric oxide increases hepatic arterial blood flow in rats with carbon tetrachloride-induced acute hepatic injury. *Gastroenterology* **1999**;117:173-180

214. Siragy HM, Carey RM. The subtype-2 (AT2) angiotensin receptor regulates renal cyclic guanosine 3', 5'-monophosphate and AT_1 receptor-mediated prostaglandin E2 production in conscious rats. *J Clin Invest* **1996**;97:1978-1982

215. Siragy HM, Carey RM. The subtype 2 (AT_2) angiotensin receptor mediates renal production of nitric oxide in conscious rats. *J Clin Invest* **1997**;100:264-269

216. Siragy HM, de Gasparo M, Carey RM. Angiotensin type 2 receptor mediates valsartan-induced hypotension in conscious rats. *Hypertension* **2000**;35:1074-1077

217. Zhang C, Hein TW, Wang W, Kuo L. Divergent roles of angiotensin II AT_1 and AT2 receptors in modulating coronary microvascular function. *Circ Res* **2003**;92:322-329

218. Widdop RE, Jones ES, Hannan RE, Gaspari TA. Angiotensin AT_2 receptors: cardiovascular hope or hype? *Br J Pharmacol* **2003**;140:809-824

219. Schrammel A, Pfeiffer S, Schmidt K, Koesling D, Mayer B. Activation of soluble guanylyl cyclase by the nitrovasodilator 3-morpholinosydnonimine involves formation of S-nitrosoglutathione. *Mol Pharmacol* **1998**;54:207-212

220. Souza HP, Laurindo FR, Ziegelstein RC, Berlowitz CO, Zweier JL. Vascular NAD(P)H oxidase is distinct from the phagocytic enzyme and modulates vascular reactivity control. *Am J Physiol Heart Circ Physiol* **2001**;280:H658-667

221. Lassegue B, Clempus RE. Vascular NAD(P)H oxidases: specific features, expression, and regulation. *Am J Physiol Regul Integr Comp Physiol* **2003**;285:R277-297

222. Guzik TJ, Sadowski J, Kapelak B, et al. Systemic Regulation of Vascular NAD(P)H Oxidase Activity and Nox Isoform Expression in Human Arteries and Veins. *Arterioscler Thromb Vasc Biol* **2004**

223. Olson S, Oeckler R, Li X, et al. Angiotensin II stimulates nitric oxide production in pulmonary artery endothelium via the type 2 receptor. *Am J Physiol Lung Cell Mol Physiol* **2004**;287:L559-568

11. Curriculum vitae

Personal data

Name: Ashraf Mohamed Abouelwafa Taye

Date of Birth: Jan., 15,1970

Nationality: Egyptian

Profession: Teaching and Research Assistant, Minya University, Faculty of Pharmacy, Pharmacology Department, Egypt

Academic Qualification:

1) Pre-university Education

(a) Primary Education(1976-1982) Farshout primary school

(b) Prep Education(1982-1985)) Farshout prep school

(c) Secondary Education (1985-1988) Farshout secondary school

2) University Education

(i) B.Sc. Pharmaceutical Science, General grade:very good with degree of Honour, Faculty of Pharmacy, Assuit University.

The main subjects: Pharmacology, Toxicology, Clinical Toxicology, Pharmaceutics, Pharmacognosy, Biochemistry, Microbiology, Human Anatomy, Pathology, Parasitology, Histology, Analytical Chemistry, Organic and Inorganic Chemistry.

Special Post-graduate Courses: Instrumental Analysis, Physical Chemistry, Mathematics and Statistic, Advanced Pharmacology, Drug Pharmacokinetic, Bioassay and computer application, The pharmacological effects of medicinal plants.

(ii) M.Sc. in Pharmacology, Faculty of Pharmacy, Assuit University.

Title: (Evaluation of possible interactions between liquorice and some antidiabetic agents).

Professional experience

(1995-1999) Instructor in Faculty of Pharmacy, Al-Azher University, Assuit, Egypt.

(1999-2001) Assistant lecturer in Faculty of Pharmacy, Minya University, Egypt.

Professional Activities

Preparing the undergraduate laboratory for experimental pharmacology.

Fellowships: I have a scholarship (Channel system) from ministry of higher education of Egypt to Germany (2001-2002). Then, I got a scholarship (2003-2004) from Rudolf-Buchheim Institute for Pharmacology (Germany).

Publications and grants

A) Full papers to peer reviewed

1. **Ashraf Taye,** Swin Wind, Lutz Hein, Hemut Müller, Arun KSH and Harald H.H.W. Schmidt (**2004**). Countervailing effects of angiotensin type 1A and type 2 receptors on vascular function via Nox4-dependent oxidative stress and NO-dependent guanylyl cyclase. (submitted)

2. Pavel I. Nedvetsky, Peter M Schmidt, Tatiana Y. Nedvetskaya, **Ashraf Taye,** Helmut Müller, Johanes-Peter Stasch and Harald H.H.W. (**2005**)Beyond NO, beyond haem, Haem-free soluble guanylyl cyclase, a new peace in regulation puzzle. (submitted)

B) Abstracts and oral presentations (*)

Ashraf Taye, Gamal El-sherbeeny, Safwat Mangoura, Hasan Abou rahma, Alaa Elkoussi (**1998**). Adverse and drug interaction of drinking liquorice Naunyn-Schmiedeberg 's Archives of Pharmacology 358, R51 (München, Germany).

A.Taye, S.Wind, L.Hein, H H.H.W. Schmidt (**2004**). Differential effects of angiotensin II receptors (AT_{1A} and AT_2 on vasomotor activity and Nox expression in aorta from AT_{1A} or AT_2 receptor-deficient mice. Naunyn-Schmiedeberg's Archives of Pharmacology 369, R97 (Mainz, Germany).

Nedvetsky PI, Peter, TY. Nedvetskaya, **Taye A**, Müller M, Stasch J-F and Schmidt HHHW (**2004**). Regulation of soluble guanylyl cyclase by protoprophyrin agonists. Naunyn-Schmiedeberg 's Archives of Pharmacology 369, R39 (Mainz, Germany).

* **A.Taye,** S.Wind, L.Hein, H H.H.W. Schmidt (**2004**). Divergent effects of AT_1 and AT_2 receptors on vascular function involve Nox-dependent oxidative stress and NO-dependent guanylyl cyclase, 70th Annual Meeting of the German Cardiac Society (Mannheim, Germany).

A.Taye, S.Wind, L.Hein, H H.H.W. Schmidt (**2004**). Role of Nox1-dependent oxidative stress in the vascular function response to angiotensin II AT_{1A} or AT_2 receptor -deficient mice. 2nd international Nox2 meeting (Atlanta, USA).

*** A.Taye** (**2004**). "Divergent effects of AT_{1A} and AT_2 receptors on vascular functions" SFB 547 Retreat, Rauischholzhausen Castle,

*** A.Taye,** S.Wind, L.Hein, H H.H.W. Schmidt (**2004**) Divergent effects of AT_{1A} and AT_2 receptors on NO signaling. 9.NO-Forum of der deutschsprachigen Länder (Mainz,)